

OBSTRUCTED REGION EXPLOSION MODEL

DATE: December 2023

OREM is the vapour cloud explosion model developed for the SAFETI product Phast Risk v6.60. It includes the TNO Multi-energy and the Baker-Strehlow-Tang models and predicts the effects of vapour cloud explosions taking into account the interaction of obstructed regions and the flammable cloud. It is based on published literature and predicts explosion damage in the form of peak overpressures, positive phase duration and impulse in the region around vapour cloud explosions for use in consequence and risk assessments. This document presents the results of verification and validation of the explosion models.

Most recently a chapter based on 2-phase hydrogen tests was added.

Reference to part of this report which may lead to misinterpretation is not permissible.

| No. | Date | Reason for Issue | Prepared by | Verified by |
|-----|------|------------------|-------------|-------------|
|-----|------|------------------|-------------|-------------|





| | | | | |
|---|------------|------------------------|-------------------|----------------|
| 1 | March 2010 | For Phast Risk 6.6 | Y Xu | D. Worthington |
| 2 | May 2021 | Apply new template | D. Vazier | |
| 3 | April 2022 | Add 2-phase H2 chapter | David Worthington | Yongfu Xu |

Date: December 2023

Prepared by: Digital Solutions at DNV

© DNV AS. All rights reserved

This publication or parts thereof may not be reproduced or transmitted in any form or by any means, including copying or recording, without the prior written consent of DNV AS.



ABSTRACT

An explosion model has been developed for use in DNV's risk software Phast Risk v6.60. It is named the Obstructed Region Explosion Model and is referred to by the abbreviation OREM. OREM includes the TNO Multi-energy model^{1,2,3} and the Baker-Strehlow-Tang methodology^{4,5,6}, for the prediction of consequence and risk of vapour cloud explosions in process plants. Details of the explosion models implemented in OREM are given in the theory document⁷.

OREM predicts explosion damage in the form of peak over-pressures, positive phase duration and impulse in the region around vapour cloud explosions for use in consequence and risk assessment. Consequence predictions of the Multi-energy (ME) and the Baker - Strehlow-Tang (BST) models are validated against measurements and CFD predictions of peak overpressure and positive phase duration of explosions for a range of test cases, such as the test cases of BFETS3a, EMERGE & GAMES studies.

Most recently a chapter based on 2-phase hydrogen tests was added.

Table of contents

| | |
|---|----|
| ABSTRACT..... | I |
| 1 INTRODUCTION..... | 5 |
| 1.1 The Obstructed Region Explosion Model (OREM) | 5 |
| 1.2 Scope of the current document | 6 |
| 2 VERIFICATION & VALIDATION..... | 6 |
| 2.1 Verification of the ME blast curves | 6 |
| 2.2 Verification of the BST blast curves | 7 |
| 2.3 Validation against data of BFETS3a as reported by Fitzgerald | 7 |
| 2.4 Validation against EMERGE data | 8 |
| 2.5 Validation against the Shell Deer Park Ethylene case | 10 |
| 2.6 Validation against the cases reported in the GAMES report | 10 |
| 2.6.1 The Chemical Plant case | 11 |
| 2.6.2 The Gas Processing case | 13 |
| 2.6.3 The LNG Terminal case | 15 |
| 2.7 Overall assessment of ME& BST on consequence predictions | 17 |
| 3 2-PHASE HYDROGEN EXPLOSION VALIDATION..... | 19 |
| 3.1 INTRODUCTION | 19 |
| 3.2 The Preslhy explosion tests | 20 |
| 3.2.1 Test setup | 20 |
| 3.2.2 Test procedures | 22 |
| 3.2.3 Test programme | 23 |
| 3.2.4 Ambient conditions | 24 |
| 3.3 Discharge calculation | 26 |
| 3.4 Dispersion of the hydrogen releases | 28 |
| 3.4.1 UDM predictions | 28 |
| 3.4.2 KFX predictions | 29 |
| 3.5 Predictions of hydrogen explosions by the Multi-energy explosion model | 31 |
| 3.5.1 Setup of the cases in Safeti | 31 |
| 3.5.2 Grouping of the tests for validation | 32 |
| 3.5.3 Predictions by Phast/Safeti using UDM clouds by the Multi-Energy explosion model | 33 |
| 3.5.3.1 Tests with low congestion and low tank pressure (Groups 1-3) | 33 |
| 3.5.3.2 Tests with low congestion and high tank pressure (Groups 4-6) | 36 |
| 3.5.3.3 Tests with high congestion (tests in Groups 7 & 8) | 38 |
| 3.5.4 Predictions by ME model in Phast/Safeti using KFX clouds | 39 |
| 3.6 Predictions of hydrogen explosions by the Baker-Strehlow-Tang (BST) explosion model | 42 |
| 3.6.1 Setup of the cases in Safeti | 42 |
| 3.6.2 Flame speed selection for the PRESLHY tests | 43 |
| 3.6.3 Predictions by BST model in Phast/Safeti using UDM clouds | 44 |
| 3.6.3.1 Tests with low congestion and low tank pressure (Groups 1-3) | 44 |
| 3.6.3.2 Tests with low congestion and high tank pressure (Groups 4-6) | 47 |
| 3.6.3.3 Tests with high congestion (tests in Groups 7 & 8) | 49 |
| 3.7 Conclusions | 51 |
| 4 OBSERVATIONS..... | 52 |
| 5 RECOMMENDATIONS FOR FURTHER WORK..... | 53 |
| GLOSSARY..... | 72 |
| REFERENCES..... | 76 |

Table of figures

| | |
|--|----|
| Figure 1 The 2D and 2.5D geometries of the BFETS3a study (Source: Fitzgerald) | 7 |
| Figure 2 Typical geometry of the EMERGE tests | 9 |
| Figure 3 Plan view of the chemical plant illustrating the locations of the 6 obstructed regions, 9 ignition locations (IL-1 – IL-9) and 14 locations for pressure samples (Source: GAMES report) | 11 |
| Figure 4 Setup of the test rig for the Gas Processing case (Source: GAMES report) | 13 |
| Figure 5 Side view of the test rig (Source: GAMES report) | 14 |
| Figure 6 The LNG terminal case of the GAMES study (Source: GAMES report)..... | 15 |
| Figure 7 Plan view of the obstructed regions used to represent the LNG terminal by ME..... | 16 |
| Figure 8 Layout of the site for the PRESLHY tests | 20 |
| Figure 9 Setup of the explosion test | 21 |
| Figure 10 Photo image of the test rig with low level of congestion..... | 21 |
| Figure 11 Photo image of the test rig with high level of congestion | 22 |
| Figure 12 Layout of pressure transducers..... | 23 |
| Figure 13 Side view of the flammable clouds predicted by UDM (tank pressure 5bar, weather 1.5F)..... | 28 |
| Figure 14 Comparing the flammable cloud view predicted by UDM for impinged and free jet (tank pressure 5bar, nozzle diameter 12mm and weather 1.5F)..... | 28 |
| Figure 15 Flammable clouds of the test and hydrogen cloud predicted by KFX before the ignition (Test No12) | 29 |
| Figure 16 Flammable clouds of the test and hydrogen cloud predicted by KFX before the ignition (Test No14) | 29 |
| Figure 17 Flammable clouds of the test and hydrogen cloud predicted by KFX before the ignition (Test No15) | 30 |
| Figure 18 Flammable clouds of the test and hydrogen cloud predicted by KFX before the ignition (Test No17) | 30 |
| Figure 19 Setup of the case in Safeti..... | 32 |
| Figure 20 Cloud views predicted by UDM at three wind speeds for the tests in Group 3 (tank pressure 5bar, 12mm nozzle and low congestion) | 33 |
| Figure 21 Effect contours of 0.05bar overpressure of the tests with tank pressure of 1bar and low congestion..... | 34 |
| Figure 22 Comparing the measured and predicted overpressures for tests in Group 1 (1bar tank pressure, 6mm nozzle, low congestion) | 35 |
| Figure 23 Comparing the measured and predicted overpressures for tests in Group 2 (1 bar tank pressure, 12mm nozzle, low congestion)..... | 35 |
| Figure 24 Comparing the measured and predicted overpressures for tests in Group 3 (1 bar tank pressure, 25.4mm nozzle, low congestion)..... | 36 |
| Figure 25 Comparing the measured and predicted overpressures for tests in Group 4 (5 bar tank pressure, 6mm nozzle, low congestion) | 37 |
| Figure 26 Comparing the measured and predicted overpressures for tests in Group 5 (5 bar tank pressure, 12mm nozzle, low congestion)..... | 37 |
| Figure 27 Comparing the measured and predicted overpressures for tests in Group 6 (5 bar tank pressure, 24.5mm nozzle, low congestion)..... | 38 |
| Figure 28 Comparing the measured and predicted overpressures tests in Group 7 (1 bar tank pressure, 6mm nozzle, high congestion) | 39 |
| Figure 29 Comparing the measured and predicted overpressures tests in Group 8 (1 bar tank pressure, 12mm nozzle, high congestion) | 39 |
| Figure 30 Effect curves of 0.05 bar overpressure predicted by Safeti using UDM and KFX clouds for Tests 12, 14, 15 & 17 (5 bar tank pressure, 12mm nozzle, low congestion) | 40 |
| Figure 31 Comparing the measured and predicted overpressures using UDM and KFX clouds with calculated explosion strength using the Games correlations for the Multi-Energy explosion model for tests in Group 5 (5 bar tank pressure, 12mm nozzle, low congestion) | 41 |
| Figure 32 Comparing the measured and predicted overpressures for tests in Group 1 (1bar tank pressure, 6mm nozzle, low congestion) | 45 |
| Figure 33 Comparing the measured and predicted overpressures for tests in Group 2 (1 bar tank pressure, 12mm nozzle, low congestion)..... | 46 |
| Figure 34 Comparing the measured and predicted overpressures for tests in Group 3 (1 bar tank pressure, 25.4mm nozzle, low congestion)..... | 46 |
| Figure 35 Comparing the measured and predicted overpressures for tests in Group 4 (5 bar tank pressure, 6mm nozzle, low congestion) | 47 |
| Figure 36 Comparing the measured and predicted overpressures for tests in Group 5 (5 bar tank pressure, 12mm nozzle, low congestion)..... | 48 |
| Figure 37 Comparing the measured and predicted overpressures for tests in Group 6 (5 bar tank pressure, 24.5mm nozzle, low congestion)..... | 48 |
| Figure 38 Comparing the measured and predicted overpressures tests in Group 7 (1 bar tank pressure, 6mm nozzle, high congestion) | 50 |

| | |
|---|----|
| Figure 39 Comparing the measured and predicted overpressures tests in Group 8 (1 bar tank pressure, 12mm nozzle, high congestion) | 50 |
| Figure 40 Charts of side-on peak overpressure as reproduced by ME (black lines: original blast curve; symbols: reproduced by ME) | 54 |
| Figure 41 Charts of dynamic peak overpressure as reproduced by ME (black lines: original blast curve; colour lines: reproduced by ME) | 55 |
| Figure 42 Charts of positive phase duration as reproduced by ME (black lines: original blast curve; symbols: reproduced by ME) | 56 |
| Figure 43 Charts of side-on peak overpressure as reproduced by BST (black lines: original blast curve; colour lines: reproduced by BST) | 57 |
| Figure 44 Charts of impulse as reproduced by BT (black lines: original blast curve; colour lines: reproduced by BST) | 57 |
| Figure 45 Plot of BFETS3a_A, 2D, high congestion, methane tests: measured, ME and BST predicted overpressures as a function of distance | 58 |
| Figure 46 Plot of BFETS3a_B, 2.5D, high congestion, methane tests: measured, ME and BST predicted overpressures as a function of distance | 58 |
| Figure 47 Plot of BFETS3a_C, 2.5D, high congestion, methane tests: measured, ME and BST predicted overpressures as a function of distance | 59 |
| Figure 48 Plot of BFETS3a_D, 2.5D, high congestion, methane tests: measured, ME and BST predicted overpressures as a function of distance | 59 |
| Figure 49 Plot of BFETS3a_E, 2.5D, high congestion, methane tests: measured, ME and BST predicted overpressures as a function of distance | 60 |
| Figure 50 Plot of BFETS3a_A, 2D, high congestion, methane tests: ME and BST predicted positive duration as a function of distance | 60 |
| Figure 51 Plot of BFETS3a_B, 2.5D, high congestion, methane tests: ME and BST predicted positive duration as a function of distance | 61 |
| Figure 52 Plot of EMERGE_1, small scale, 3D, high congestion, methane tests: measured, ME and BST predicted overpressures as a function of distance | 62 |
| Figure 53 Plot of EMERGE_2, small scale, 3D, high congestion, propane tests: measured, ME and BST predicted overpressures as a function of distance | 62 |
| Figure 54 Plot of EMERGE_3, medium scale, 3D, high congestion, methane tests: measured, ME and BST predicted overpressures as a function of distance | 63 |
| Figure 55 Plot of EMERGE_4, medium scale, 3D, high congestion, propane tests: measured, ME and BST predicted overpressures as a function of distance | 63 |
| Figure 56 Plot of EMERGE_5, medium scale, 3D, medium congestion, methane tests: measured, ME and BST predicted overpressures as a function of distance | 64 |
| Figure 57 Plot of EMERGE_6, medium scale, 3D, medium congestion, propane tests: measured, ME and BST predicted overpressures as a function of distance | 64 |
| Figure 58 Plot of EMERGE_7, large scale, 3D, medium congestion, methane tests: measured, ME and BST predicted overpressures as a function of distance | 65 |
| Figure 59 Comparing the predicted positive phase durations by ME and BST as a function of distance: EMERGE_5, medium scale, 3D, medium congestion & methane | 65 |
| Figure 60 Comparing the predicted positive phase durations by ME and BST as a function of distance: EMERGE_6, medium scale, 3D, medium congestion & propane | 66 |
| Figure 61 Comparing the predicted positive phase durations by ME and BST as a function of distance: EMERGE_7, large scale, 3D, medium congestion & methane | 66 |
| Figure 62 Plot of the Shell Deer Park, large scale, 2.5D, High congestion, ethylene tests: measured, ME and BST predicted overpressures as a function of distance | 67 |
| Figure 63 Comparing the predicted overpressures of ME and BST with the predictions by AutoReaGas for the chemical plant case of the GAMES report | 68 |
| Figure 64 Comparing the predicted overpressures of ME and BST with measurements and predictions by AutoReaGas for the gas processing case of the GAMES report | 68 |
| Figure 65 Validating the "1/3 Rule" for the Gas Processing case of the GAMES study: fully filled obstructed regions | 69 |
| Figure 66 Comparing the predicted overpressures on a transect along OSR1, OSR2 & OSR-5 by ME and BST for Case 3 of the LNG Terminal of the GAMES report | 69 |
| Figure 67 Comparing overpressure predictions of ME and BST models in Phast Risk against measurements and CFD predictions (all cases) | 70 |
| Figure 68 Comparing the overpressure predictions of ME and BST models in Phast Risk against measurements (selected cases) | 71 |

1 INTRODUCTION

1.1 The Obstructed Region Explosion Model (OREM)

This document describes the verification and validation of the Obstructed Region Explosion model (OREM) as implemented in Phast and Phast Risk v6.6 of the SAFETI products for predicting the consequence and risk of vapour cloud explosions in obstructed regions of process plants. Details of the model can be found in the theory document⁷. OREM has included the TNO Multi-energy model as described in the Dutch Yellow Book for consequence modelling and other publications^{1,2,3}, and the Baker-Strehlow-Tang methodology as described in published papers^{4,5,6}. OREM is only available if you have a license for the [Extended Explosion Modelling](#) of Phast Risk v660.

For brevity sometimes the Multi-energy model of OREM will be referred to as 'ME' and the Baker-Strehlow-Tang Model as 'BST' in this document. The paragraphs marked with **ME** and **BST** are specific to the Multi-energy model and the Baker-Strehlow-Tang Model respectively.

The ME in OREM predicts the consequences of vapour cloud explosions in the form of peak overpressures and positive phase duration in the region around the explosion using the blast curves developed by TNO for an idealised hemispherical stoichiometric fuel-air charge. Distance from the explosion may be specified and then overpressure and duration are calculated using ME. Alternatively a target overpressure or duration may be input and ME will return the distance to this targeted effect from centre of the explosion.

The BST in OREM predicts the consequences of vapour cloud explosions in the form of peak overpressure and impulse in the region around the explosion using the flame speed table and the blast curves developed by Baker et al for an idealised stoichiometric fuel-air charge. Distance from the explosion may be specified and then overpressure and impulse can be calculated using BST. Alternatively a target overpressure or impulse may be input and BST will then return the distance to this targeted effect from centre of the explosion.

Used in this way OREM is a simple look-up function and it requires the user to describe the explosion source to work out two correlating parameters, i.e. total combustion energy and explosion strength (i.e. the blast curves) for consequence and risk assessments. There are two models to determine these parameters and their availability varies among products as given in Table 1. The two models are:

1. **Standard explosion model**

ME Using ME a list of obstructed volumes is given for each modelled case. Each volume must be given a ME curve number. The modelling considers each volume as a separate explosion source. The energy of each explosion is determined based on total flammable mass in the cloud and obstructed volume. approximately, and the explosion effects are calculated accordingly.

BST Using BST one obstructed volume can be given for each modelled case. This volume defines one confined explosion with the explosion energy determined based on total flammable mass in the cloud and the given volume approximately, and flame speed of the explosion can be given as an input or determined by BST using the flame speed table based on the characteristics of the obstructed volume.

2. **Obstructed region explosion model (OREM)**

ME The number of explosion sources from a case and their explosion energies are determined using the time-varying behaviour of the flammable clouds from the dispersion modelling and layout of the obstructed regions around the accident release. The strength of each explosion can be given as an input or determined by ME using the GAME correlations based on key characteristics of the obstructed regions.

BST BST calculates the explosion sources from a case and their explosion energies using the time-varying behaviour of the flammable clouds from the dispersion modelling and layout of the obstructed regions around the release. Flame speed of each explosion can be given as an input or determined by BST using the flame speed table based on the key characteristics the obstructed regions.

The model results may be used directly by the analyst to assess the explosion hazards or may be used as input to vulnerability models to calculate risk. In the first implementation of the model in Phast Risk 6.6 the use of the obstructed region explosion model is limited to use in the risk calculations as highlighted in the table below. In the product OREM is referred to as '3D Obstructed Region' while the previous method is '2D Damage Zone'.

| | Phast | Safeti Standard | Safeti with the option of Extended explosion modelling (from version 6.6) |
|---|-------|--|---|
| Standard explosion model – Standalone consequences only | Yes | Yes | Yes – NB standalone explosion models not used in the risk calculations except the BLEVE Blast model |
| Standard explosion model – Linked | Yes | No – instead it uses ‘3D Purple Book’ for explosion risk | No – instead ‘3D Purple Book’ is used for explosion risk |
| Obstructed region explosion model | No | No | Yes (i.e. ‘3D Obstructed Region’) |

Table 1 Model options in Phast and Safeti Products

1.2 Scope of the current document

This document contains the verification and validation results of ME and BST models.

2 VERIFICATION & VALIDATION

The predictions of ME and BST are compared with measurements and predictions of other models, such as AutoReaGas (a 3-dimensional CFD based software for modelling gas explosions by Century Dynamics and TNO). No detail is given for these reference models in this document and users should refer to the reference papers for details. Two sets of predictions are given by the BST model for the two methods correcting the ground effect for explosions on or near to the ground, i.e. one with a given ground reflection factor and the ground correction method, and please refer to the theory document of OREM for details of these methods⁷.

2.1 Verification of the ME blast curves

In the Multi-energy methodology, the severity of vapour cloud explosions is described by numeric values ranging from 1 to 10. The higher the numeric value the greater the explosion strength/severity. An explosion with a strength of curve 10 would produce an initial side-on overpressure over 20 bar, while the overpressure is only about 0.01 bar for an explosion with a strength of curve 1. Where a non-integer valued explosion strength is specified for an explosion, the explosion behaviour is determined by simple linear interpolation across the adjacent explosion strengths that bound the specified value.

The blast curves used by ME for side-on and dynamic overpressures and positive phase duration were digitised from the published curves in the Yellow Book¹ and represented by numerical formulae as:

Each overpressure curve is divided into three regions as:

- Region 1: the first region corresponds to the region of constant overpressure. Here, the overpressures are observed to be approximately uninfluenced by changes in distance from the explosion centre.
- Region 2: each log-log curve data is fitted to a sixth order polynomial.
- Region 3: the curves for blast strengths in this region are fitted to linear equations. The curves for blast strengths 6-9 are observed to merge with the curve for blast strength “10” in this region.

The blast curves for positive phase duration are represented by two regions for blast strengths 1-5 and three regions for strengths 6-10. Each region is generally expressed as a sixth order polynomial.

Figure 40 - Figure 42 compare the predicted side-on overpressure, dynamic overpressure and the positive duration against the published curves for the Multi-energy model in the Yellow Book¹ for explosions with

specified strengths. The shape of each curve has been represented well by the model. This also verifies the performance of OREM in predicting overpressures and positive phase duration at given distances when blast curve is specified for explosions defined by 'Defined Strength' obstructions.

2.2 Verification of the BST blast curves

In the BST methodology, the severity of an explosion is indicated by the flame speed. Nine blast curves have been provided for explosions with flame speeds between Mach numbers 0.2 and 5.2. The higher the flame Mach number the greater the explosion strength/severity. An explosion with a flame speed of Mach number 5.2 would generate an initial peak side-on overpressure over 20 bar, while the overpressure would be only about 0.07 bar if the Mach number is 0.02. Where a value between the nine Mach numbers is specified, the explosion behaviour is determined by simple linear interpolation across adjacent Mach numbers bounding the specified value.

The blast curves for side-on overpressure and impulse for BST were digitised from the published curves⁵. Each curve is made of three parts which are represented by numerical formulae as:

- Region 1: the first region corresponds to the region of constant overpressure. Here, the overpressure and impulse are observed to be approximately uninfluenced by changes in distance from the explosion centre.
- Region 2: each log-log curve is fitted to a sixth order polynomial between Regions 1 & 3.
- Region 3: the curves are fitted to linear equations in the far field.

Figure 43 - Figure 44 compare the predicted side-on overpressure and impulse against the published blast curves⁵ for explosions with the same specified flame speeds as the original BST blast curves. The agreement is very good. This also verifies the performance of OREM in predicting overpressures or impulse at given distances when the blast curve is specified for explosions generated by 'Defined Flame Speed' obstructions.

2.3 Validation against data of BFETS3a as reported by Fitzgerald⁸

BFETS2 was conducted by the Steel Construction Institute for 1D vapour cloud explosions and BFETS3a was a follow-on project carried out by British Gas to investigate gas explosions with the degree of confinement of 2D and 2.5D as illustrated in

Figure 1. Forty-five experiments were performed in BFETS3a and 21 of them were used as reported by Fitzgerald⁸. Table 2 below lists the parameters used as given in the Fitzgerald paper.

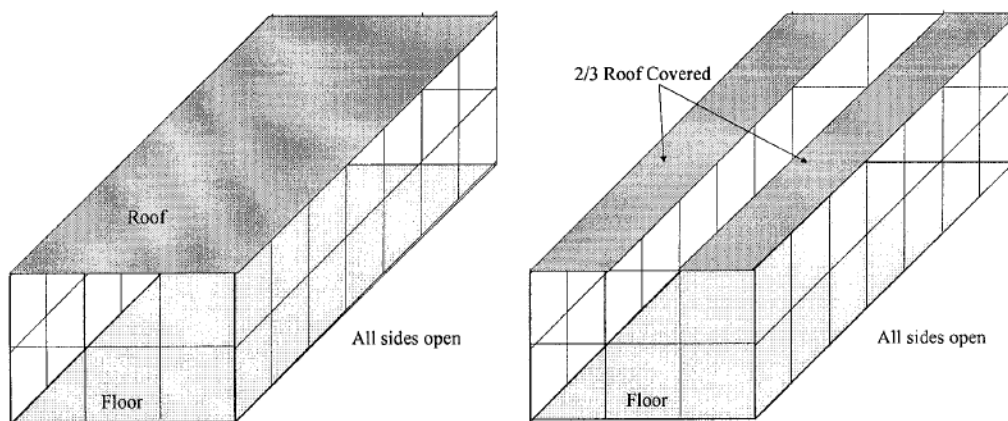


Figure 1 The 2D and 2.5D geometries of the BFETS3a study (Source: Fitzgerald⁸)

| Case | Geometry | | | | Material | | BST parameter | | | ME parameter |
|-----------|------------|-----------|------------|---------|----------|-------------------------|-----------------------|------------------|-----------------------|----------------|
| | Length (m) | Width (m) | Height (m) | VBR (%) | Fuel | Energy ¹ (J) | Degree of Confinement | Congestion level | Fuel reactivity level | Blast strength |
| BFETS3a_A | 28 | 12 | 8 | 8.46 | Methane | 8.5E+09 | 2D | High | Low | 6.908 |
| BFETS3a_B | 28 | 12 | 8 | 8.46 | Methane | 8.5E+09 | 2.5D | High | Low | 6.908 |
| BFETS3a_C | 28 | 12 | 8 | 9.62 | Methane | 8.5E+09 | 2.5D | High | Low | 7.452 |
| BFETS3a_D | 28 | 12 | 8 | 9.67 | Methane | 8.5E+09 | 2.5D | High | Low | 7.557 |
| BFETS3a_E | 28 | 12 | 8 | 8.27 | Methane | 8.5E+09 | 2.5D | High | Low | 6.976 |

Table 2 Input data used for the BFETS3a test cases (Source: Fitzgerald⁸)

Figure 45 - Figure 49 compare the predicted side-on overpressures by ME and BST against the measurements. ME has predicted the side-one overpressures well for the two cases of strong explosions, i.e. cases BFETS3a_C & BFETS3a_D where the initial peak overpressure is over 1 bar and the explosion efficiency is 100%, but has under-predicted the overpressures for the other three cases which have the initial peak overpressure just below 1bar and the explosion efficiency would be 50% using the GAME recommendation for explosion efficiency as given in the theory document⁷.

The BST model with a given ground correction factor of 2 has significantly under-predicted when compared with the measurements and the ME predictions in all cases, particularly in the near field of the explosions. However the predictions in the far field, i.e. 50m from the edge of the obstructed region, agree well with the measurements. This maybe is due to the fact that the updated flame speed table of BST was developed with emphasis on good predictions outside the congested regions⁴.

The BST model with the ground correction method has improved predictions both inside and outside the obstructed region in all cases, particularly for BFETS3a_A & BFETS3a_B where the predictions are within the ranges of measurements.

There were no measurements of positive phase duration reported in these tests, so only model predictions are compared in Figure 50 and Figure 51 for BFETS3a_A & BFETS3a_B. The positive phase duration of the BST models is calculated by assuming the impulse is half of the product of peak side-on overpressure and duration.

2.4 Validation against EMERGE data

The EMERGE tests were carried out by TNO, BG and CMR to investigate the effect of size, fuel reactivity and congestion level on vapour cloud explosions.

Figure 2 shows a typical geometry of the EMERGE tests and Table 3 summaries the parameters of the tests (Fitzgerald⁸). The test cases are different in scale as

- EMERGE 1 – EMERGE 2: small-scale
- EMERGE 3 – EMERGE 6: medium-scale
- EMERGE 7 - EMERGE 8: large-scale

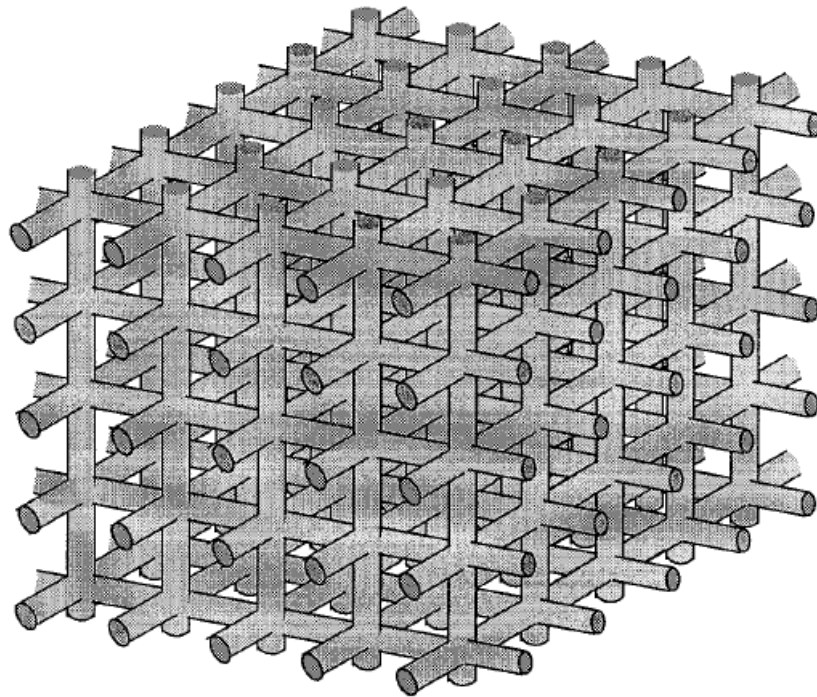


Figure 2 Typical geometry of the EMERGE tests

| Case | Geometry | | | | Material | | BST parameter | | | ME parameter |
|---------|------------|-----------|------------|---------|----------|-------------------------|-----------------------|------------------|-----------------------|----------------|
| | Length (m) | Width (m) | Height (m) | VBR (%) | Fuel | Energy ¹ (J) | Degree of Confinement | Congestion level | Fuel reactivity level | Blast strength |
| EMERGE1 | 2 | 2 | 2 | 10 | Methane | 1.2E+07 | 3D | High | Low | 7.051 |
| EMERGE2 | 2 | 2 | 2 | 10 | Propane | 1.4E+07 | 3D | High | Medium | 7.577 |
| EMERGE3 | 4 | 4 | 2 | 10 | Methane | 1.0E+08 | 3D | High | Low | 7.378 |
| EMERGE4 | 4 | 4 | 2 | 10 | Propane | 1.1E+08 | 3D | High | Medium | 7.904 |
| EMERGE5 | 4 | 4 | 2 | 4.8 | Methane | 1.0E+08 | 3D | Medium | Low | 4.815 |
| EMERGE6 | 4 | 4 | 2 | 4.8 | Propane | 1.1E+08 | 3D | Medium | Medium | 5.285 |
| EMERGE7 | 8 | 8 | 4 | 10 | Methane | 7.9E+08 | 3D | High | Low | 8.139 |
| EMERGE8 | 8 | 8 | 4 | 10 | Propane | 8.5E+08 | 3D | High | Medium | 8.586 |

Table 3 Input data used for the EMERGE cases (Fitzgerald⁸)

Results and discussions

Figure 52 - Figure 58 compare the predicted overpressures by ME against measurements and the predictions of BST. The predictions by ME are generally conservative and agree well with the measurements of the medium- and large-scale tests, i.e. EMERGE 3 – EMERGE 6 and EMERGE 7 (no measurements were available for EMERGE 8). Over-predictions are produced for the two small-scale cases.

As for the BFETS3a cases, BST has consistently under-predicted the side-on overpressure, particularly in the near field, for the medium- and large-scale cases. The predictions in the far field are satisfactory. However, the overpressures in the far field are generally very low in these EMERGE cases.

No measurements were available to validate the predictions of the positive phase duration for these cases. Figure 59- Figure 61 compare the predictions between ME and BST.

¹ This is the combustion energy of the flammable material contained inside the obstructed region. The explosion energy given in the Fitzgerald paper has applied the overpressure dependent explosion efficiency for the Multi-energy model and a ground reflection factor of 2 for the BST model.

2.5 Validation against the Shell Deer Park Ethylene case

A large vapour cloud explosion occurred at the Shell Chemical Company plant at Deer Park, Texas in 1997. An investigation into the incident had estimated explosion overpressures at various locations from the explosion based on observed window breakages. A 100% window breakage indicates an overpressure higher than 1 psi, 50% breakage for an overpressure between 0.3-0.5psi and any window breakage for a minimum overpressure of 0.15psi, based on the window thickness in the Deer Park area. The estimated overpressures have been used to validate the predictions here. This case was included in the Fitzgerald study and Table 4 summarises the input data.

| Case | Geometry | | | | Material | | BST parameter | | | ME parameter |
|-------------------------------|------------|-----------|------------|---------|------------------------------|-------------------------|-----------------------|------------------|-----------------------|----------------|
| | Length (m) | Width (m) | Height (m) | VBR (%) | Fuel | Energy ² (J) | Degree of Confinement | Congestion level | Fuel reactivity level | Blast strength |
| Shell Deer Park Ethylene Case | 50.6 | 25.3 | 15.2 | 10 | 19% Hydrogen 81% Ethylene | 6.8x10 ¹⁰ | 2.5D | High | High | 10 |

Table 4 Input data used for the ME and BST predictions of Shell Deer Park Ethylene case (Fitzgerald⁸)

The explosion of this case was strong and the blast curve selected for it was curve 10 for the Multi-energy model and flame Mach number 5.2 for the BST model. Figure 62 compares the predictions by ME against the estimated overpressures from accident investigation and BST predictions. For this case, the ME predictions are higher than the estimations at the locations of 100% and minimum breakages and are within the estimated pressure range at the location of 50% window breakage.

Even though the BST model has consistently under-predicted the overpressures near to explosions in the BFETS3a & EMERGE cases, its predictions for this case have compared very well with the observations and are higher than those of the Multi-energy model. Unlike the test cases of BFETS3a & EMERGE, this is an explosion in a real process plant with overpressure data over 150m away from the explosion, the results has again demonstrated the capabilities of both ME and BST models for predicting explosion consequences in the far field.

The flame Mach number of the case is 5.2 which is the highest flame speed in the BST flame speed table, therefore no correction was made to the initial peak overpressure by the ground correction method (see the theory manual for details) and so the same results are predicted by BST with a ground reflection factor of 2 and the ground correction method.

2.6 Validation against the cases reported in the GAMES report

To guide the application of the TNO Multi-energy model, the GAME project derived two corrections to estimate the initial overpressure produced by a vapour cloud explosion and this pressure is then used to select blast curves for consequence and risk calculations. The correlations were developed based on tests with well-defined parameters and geometries and were found difficult to apply for real process plants. A follow-on project, i.e. the GAMES project, applied the correlations to four process units to investigate the difficulties and problems of using the correlations. Measurements and predictions using AutoReaGas and the Multi-energy model as found in the GAMES report for the test cases were used to validate the predictions of ME and BST of OREM.

Ignition location is important for flame propagation in obstructed regions and this can only be simulated accurately by advanced CFD models, such as AutoReaGas. Its effect on the predicted consequences has been illustrated in the GAMES report. However, simple models, such as the Multi-energy and Baker-Strehlow-Tang models, have no features to handle ignition location accurately, so they are often used to predict the worst-case scenarios. For VCEs in obstructed regions, central ignition is usually considered to be the worst-case scenario and this is the case for the ME and BST predictions given here. So the predictions of ME and BST are only compared with the AutoReaGas results with central ignitions as reported in the GAMES report.

² The energy reported in the Fitzgerald study for the BST model has included the correction for the ground reflection

Only the data used by BST and ME are included here for the test cases and please refer to the GAMES report for their details if required.

2.6.1 The Chemical Plant case

Figure 3 shows the plan view of the chemical plant investigated by the GAMES study. To apply the ME model, the plant is divided into 6 obstructed regions with obstructed region 1 consisting of two sub-regions, i.e. 1A & 1B. The obstructed regions are defined as 'Calculated Strength' obstructions with input data as shown in Table 5. Table 6 summarises the parameters calculated by ME & BST to select blast curves. The results are compared with the AutoReaGas case with ignition at location iL8.

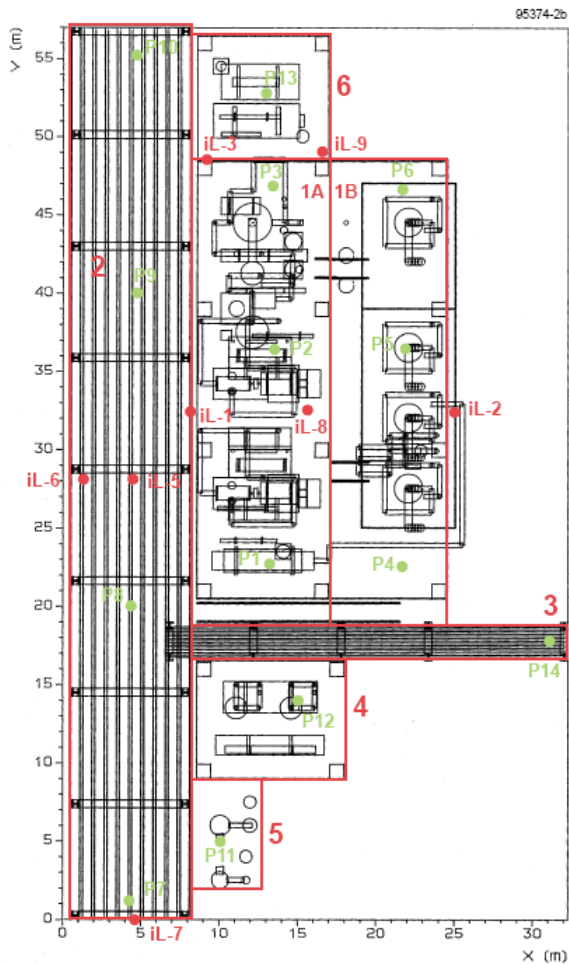


Figure 3 Plan view of the chemical plant illustrating the locations of the 6 obstructed regions, 9 ignition locations (iL-1 – iL-9) and 14 locations for pressure samples (Source: GAMES report³)

| Obstructed subregion | x (m) | y (m) | z (m) | VBR | D _{arm} (m) | D _{ham} (m) | D _{hym} (m) |
|---------------------------|----------|-----------|-------|------|----------------------|----------------------|----------------------|
| OSR-1a ^{7.5} | 8.5-17 | 18.5-48.5 | 0-7.5 | 0.12 | 0.32 | 0.11 | 0.56 |
| OSR-1b ^{7.5} | 17-25 | 18.5-48.5 | 0-7.5 | 0.07 | 0.17 | 0.07 | 0.41 |
| OSR-2 | 0.5-8.5 | 0-57 | 0-7.5 | 0.15 | 0.50 | 0.40 | 0.52 |
| OSR-3 ^{7.5} | 8.5-32.5 | 16.5-18.5 | 0-5 | 0.03 | 0.16 | 0.15 | 0.16 |
| OSR-4 ^{7.5} | 8.5-18 | 9-16.5 | 0-7.5 | 0.20 | 0.95 | 0.51 | 1.29 |
| OSR-5 | 8.5-12.5 | 2-9 | 0-7.5 | 0.11 | 0.91 | 0.75 | 1.03 |
| OSR-6 ^{7.5} | 8.5-17 | 48.5-56.5 | 0-7.5 | 0.11 | 1.01 | 0.09 | 0.87 |
| SR ^{7.5} (total) | | | | 0.13 | 0.37 | 0.14 | 0.55 |

Table 5 Parameters of the obstructed regions (Source: GAMES report³)

| Parameter | BST | ME |
|-------------------------------|---------|--|
| Degree of confinement | 3D | 3D |
| Overall VBR | 12.4% | 12.4% |
| Overall congestion level | High | -- |
| Flammable material | Methane | Methane |
| Material reactivity level | Low | -- |
| Laminar Burning Speed (m/s) | 0.45 | 0.45 (Laminar burning speed as give in the GAMES report) |
| Overall typical diameter (m) | -- | 0.556 |
| Overall Flame path length (m) | -- | 15.9 |

Table 6 Summary of parameters used by ME and BST

Results and discussions

Figure 63 compares the side-on overpressures predicted by ME & BST with the overpressures predicted by AutoReaGas within the obstructed region (no overpressure was reported outside the obstructed regions in the report). The differences in the predicted peak overpressures inside the obstructed region are given in Table 7. The prediction of ME agrees well the CFD prediction with an over-prediction of 17.7%. However the ME prediction is lower than the prediction of the Multi-energy model from the GAMES study and it was mainly caused the difference in VBR used, which is 13% for the GAMES study as shown in Table 5 and 12.4% for ME as shown in Table 6 (The VBR used by ME was calculated using the method given in the OREM theory⁷ using the data in Table 5). Even though the difference in VBR seems small, but the difference in the predicted initial peak overpressure is significant and this has demonstrated the importance of accurate estimation of VBR for ME applications.

The ME predictions are much better than the BST predictions. It is known that the BST model with ground reflection significantly underestimates the overpressures in and near to the explosion source as shown in previous test cases.

Even though the BST model has under-predicted the overpressures in the near field when compared with ME, their predictions in the far field are close. The BST model with the ground correction method becomes even more conservative than the ME model in the far field.

| Model | Predicted peak overpressure Inside the obstructed regions | Diff (%) |
|---|--|-------------|
| AutoReaGas (as reported in the GAMES report) | 182 | - |
| ME or OREM | 208.9 | 14.7 |
| The Multi-energy model (GAMES study) | 248.0 | 36.2 |
| BST (Reflection factor of 2) | 33.3 | -81.7 |
| BST (Ground correction method) | 69.2 | -62.0 |

Table 7 Comparing the predicted peak side-on overpressures inside the obstructed regions by ME, BST and CFD models

2.6.2 The Gas Processing case

Figure 4 illustrates the gas processing case investigated in the GAMES project. This is an experimental rig constructed by British Gas plc and the result was made available for a EU sponsored Explosion Modelling Evaluation (EME) project. The test rig consists of a mixture of pipework, cylindrical vessels and supporting structures with parameters as illustrated in Figure 5 and Table 8 gives the parameters used by ME and BST models. Measurements were made in- and outside the obstructed region and they were used to validate the predictions.

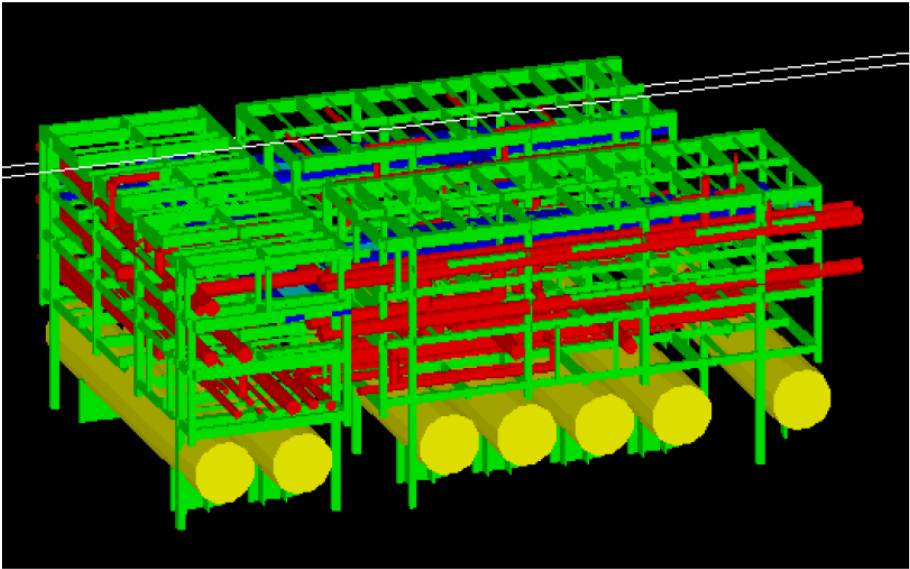


Figure 4 Setup of the test rig for the Gas Processing case (Source: GAMES report³)

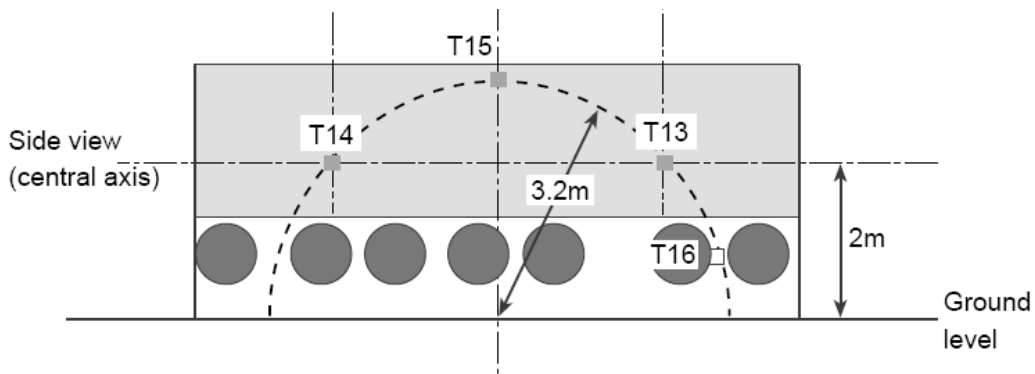


Figure 5 Side view of the test rig (Source: GAMES report³)

| Parameter | BST | ME |
|-------------------------------|---------|---------------------------------------|
| Degree of confinement | 3D | 3D |
| Overall VBR | 14% | 14% |
| Overall congestion level | High | -- |
| Flammable material | Propane | Propane |
| Material reactivity level | Medium | -- |
| Laminar Burning Speed (m/s) | 0.52 | 0.52 (as reported in the GAMES study) |
| Overall typical diameter (m) | -- | 0.25 |
| Overall Flame path length (m) | -- | 4.19 |

Table 8 Summary of parameters used by ME and BST

Results & assessment

The predicted peak overpressure inside the obstructed region by ME is 56.8kPa, which agrees with the prediction of 57kPa by the same model in the GAMES study for the case with the hydraulic diameter as the typical diameter and central ignition. Table 9 compares the predictions of the two studies outside the explosion sources with different explosion efficiencies as explained in the OREM theory⁷. They agree each other well with small differences which are caused by a slight difference in the explosion strength selected for the case. The explosion strength used is 6.3 in the GAMES study and 6.2 for ME.

| | Model | Overpressure at distance to the centre (kPa) | | |
|---|--------------------------------------|--|------|------|
| | | 8m | 16m | 24m |
| 100% explosion efficiency | The Multi-energy model (GAMES study) | 56 | 37 | 24 |
| | The ME in OREM | 55.7 | 36.4 | 22.8 |
| Overpressure dependent explosion efficiency | The Multi-energy model (GAMES study) | 51 | 29 | 18 |
| | The ME in OREM | 51.2 | 28.2 | 17.1 |
| '1/3 Rule' | The Multi-energy model (GAMES study) | NA | NA | NA |
| | The ME in OREM | 47.4 | 23.8 | 14.3 |

Table 9 Comparing ME predictions against the Multi-energy predictions from the GAMES study

There were 16 pressure transducers mounted inside the obstructed region and 3 transducers outside the test rig. The overpressures measured inside the rig varied between 14 and 36 kPa with an average of 24 kPa. Because a vapour cloud explosion tends to build up overpressure on the way while propagating through the obstructed region, so higher overpressure would normally be measured near to the edge of the test rig. Without the complexity to model the build-up of overpressure inside the explosion source, both ME and BST assume constant overpressure within the explosion source and they have over-predicted the peak overpressure inside the obstructed region as shown in Figure 64.

Both ME and BST have produced over-predictions in this case. The GAMES study has attributed the over-prediction by the Multi-energy model to obstacle configuration which could cause the GAME correlations to overestimate the initial peak overpressure and consequently select a higher explosion strength.

The setup of this case is considered to be suitable to apply the “1/3 Rule” developed for ME (please refer to the theory document for details). At the start of test, the rig was fully filled with propane and it was ignited at the centre of the rig near to the ground. While flame was propagating through the obstructed region, most of the propane inside the obstructed region would have been expelled from the region by expanding gas and did not contribute to the confined explosion. According to the “1/3 Rule”, only one third of it has contributed to the explosion and it has produced improved predictions as shown in Figure 65.

2.6.3 The LNG Terminal case

Figure 6 shows the 3D overview of the LNG terminal investigated in the GAMES project and Figure 7 illustrates obstructed regions constructed to represent it to apply ME. This case consists of a number of long pipebridges which connect the largest obstructed region OSR-1 with smaller regions OSR-2 and OSR-3. OSR-5 and OSR-7 were divided into sub-regions to avoid overlap between obstructed regions. The pipebridges have enclosed a large volume of open space without any obstacles. OSR-4 is isolated from the others. Detailed description of the case and data for the obstructed regions can be found in the GAMES report³. VBRs of the obstructed regions are generally low between 4% and 6% in this case.

In the GAMES study, four reduced cases (each reduced case includes only part of the terminal) were investigated by comparing the predictions of AutoReaGas and the Multi-energy models and Table 10 gives the parameters of these cases.

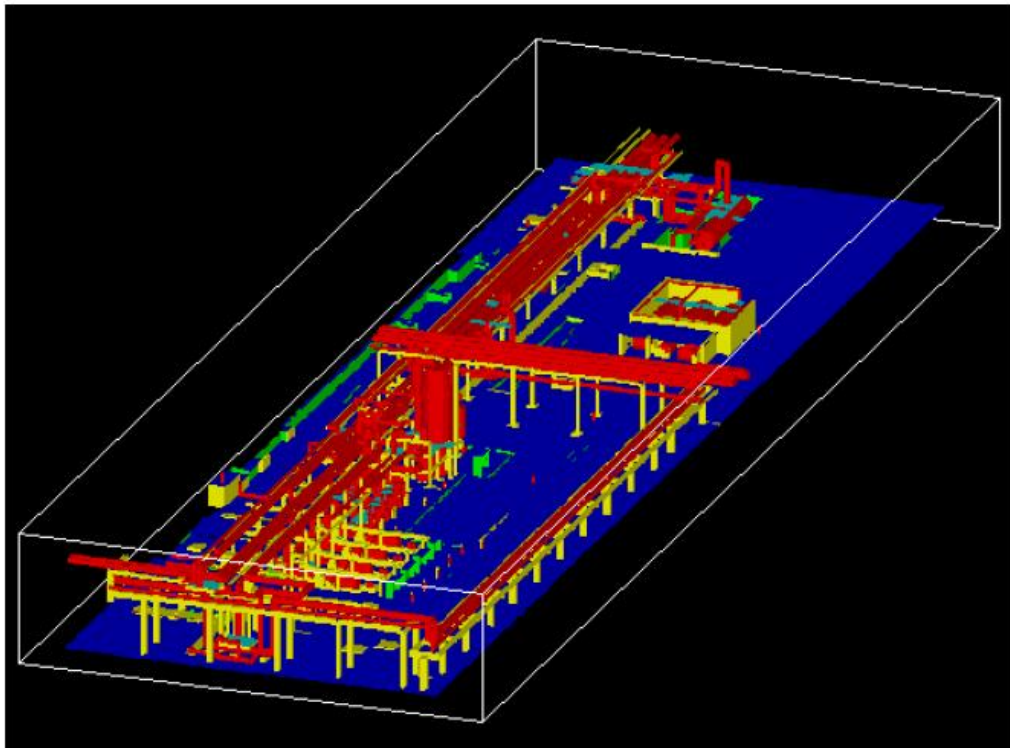


Figure 6 The LNG terminal case of the GAMES study (Source: GAMES report³)

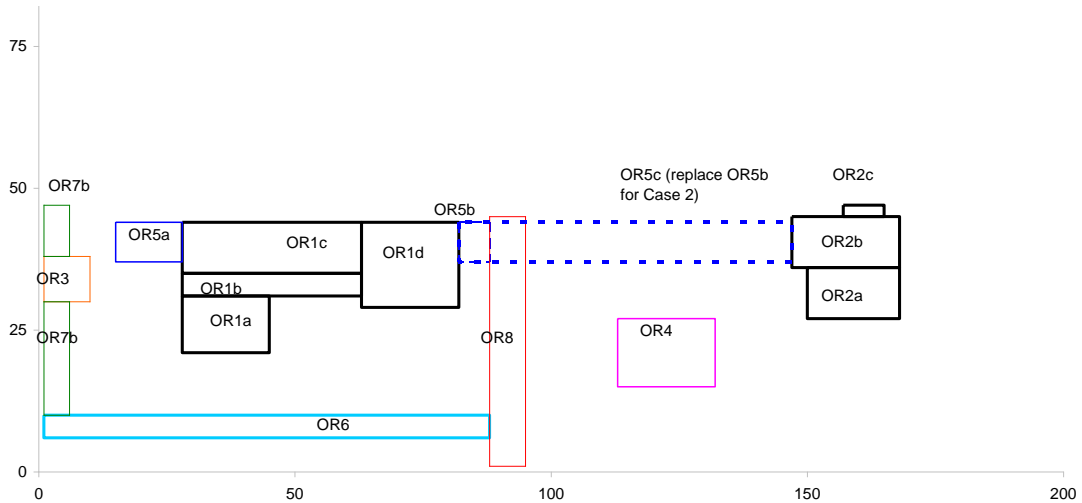


Figure 7 Plan view of the obstructed regions used to represent the LNG terminal by ME

| | Case1 &Case2 | | Case3 | Case4 |
|--|--------------|--------|-------------|-------------------|
| Obstructed regions included | OSR-1 | OSR-2 | OSR-1, 2, 5 | OSR-1, 3, 6, 7, 8 |
| Degree of confinement | 3D | 3D | 3D | 3D |
| Overall VBR | 6.0% | 4.0% | 5.1% | 4.8% |
| Overall congestion level | Medium | Medium | Medium | Medium |
| Flammable material | LNG | LNG | LNG | LNG |
| Laminar Burning speed (m/s) (as given in the GAMES report) | 0.45 | 0.45 | 0.45 | 0.45 |
| Flammable material reactivity level for BST | Low | Low | Low | Low |
| Ignition positions (as indicated in the GAMES report) | IL-2 | IL-5 | IL-2 | IL-3 |
| Flame Path Length (m) | 0.48 | 0.46 | 0.48 | 0.48 |
| Typical diameter (m) | 12.1 | 8.9 | 14.5 | 15.9 |

Table 10 Input data of the obstructed regions of the four reduced cases investigated

Results & assessments

Table 11 compares the predicted peak overpressures inside the obstructed regions of the four reduced cases by ME and BST against predictions of AutoReaGas and the Multi-energy model as reported in the GAMES report (1998). Both ME and BST models have under-predicted the overpressures in this case.

| Models | Case 1 | | Case 2 | | Case 3 | | Case 4 | |
|---|-----------------------------|--------|-----------------------------|--------|-----------------------------|--------|-----------------------------|--------|
| | Predicted peak overpressure | Diff % | Predicted peak overpressure | Diff % | Predicted peak overpressure | Diff % | Predicted peak overpressure | Diff % |
| AutoReaGas (reported in the GAMES report) | 65 | - | 22 | - | 63 | - | 23.4 | - |
| ME of OREM | 19 | -70.8 | 3 | -86.4 | 20.2 | -68.0 | 22.1 | -5.6 |
| Multi-energy model (The GAMES study) | 19 | -70.8 | 3 | -86.4 | NA | -- | 24 | 2.6 |
| BST (reflection factor) | 18.0 | -75.3 | 18.0 | -18.2 | 18.0 | -71.4 | 18.0 | -23.1 |
| BST (Ground correction method) | 32.6 | -49.8 | 32.6 | 48.2 | 32.6 | -48.3 | 32.6 | 39.3 |

Table 11 Comparing the predicted side-on overpressures inside the obstructed regions

In cases 3 & 4, the obstructed regions are linked by a pipe-bridge with no separation, therefore only one explosion source would be set up by BST and ME for each case and this is reflected in the predicted overpressures shown in Figure 66 for case 3. In the GAMES study, two peaks were predicted by AutoReaGas for Case 3 and this was attributed to the slowdown of the flame along the long pipe-bridge of OSR-5 before reaching OSR-2.

2.7 Overall assessment of ME& BST on consequence predictions

The Multi-energy and the Baker-Strehlow-Tang models are simple vapor cloud explosion models using blast curves derived from modeling data of idealized cases and they are best suited for VCEs in obstructed regions with obstacles distributed uniformly in all directions with well-defined parameters required by the models. In reality, great variations always exist in obstacle size and distribution in process plants, so effectiveness of the models for real scenarios would vary between cases as shown by the test cases given in previous sections and their capabilities are better evaluated over a wide range of cases in a systematic way.

Figure 67 compares the predictions of ME and BST against the measurements and CFD predictions of all the test cases listed above. The average errors are -30% and -63% for the ME and BST with a ground reflection factor of 2. The study by Fitzgerald (2001) reported an average error of -23% and -75% respectively for the two models. The small difference in ME predictions between the two studies is because Figure 67 has included the GAMES test cases and has excluded the BFETS2 cases, which are 1D gas explosions and are included in the Fitzgerald study. The difference in BST predictions is due to two reasons: (1) difference in cases as for the ME model, (2) the updated flame speed table was used by BST but the Fitzgerald study was carried out before the flame speed table was updated. The updated flame speed table is based on measurements from tests close to full-scale process plants and does produce improved predictions.

The ground correction method applied to the BST model has improved the overpressure predictions. The error of all cases has reduced to -42%, as shown in Figure 67, from -63% for the BST model with a ground reflection factor of 2. However, the under-predictions are still quite significant.

As illustrated by Figure 67, the correlations between the measurements (including CFD predictions) and the predictions of ME and BST of OREM are dominated by a few cases of very strong explosions. In the Fitzgerald study, the BST model was found to produce better predictions for more realistic scenarios. To reach this conclusion, test cases with small obstructed regions (i.e. EMERGE cases 1-6) and explosions with overpressures higher than 10psi were excluded and only test cases having measurements both in- and outside the obstructed regions were included. Applying similar selection criteria, Figure 68 shows comparison of the results by ME and BST against measurements. Improved predictions have achieved by all models. The results



by ME agree very well with the measurements with slight over-predictions. Underprediction by the BST model with the ground correction method has reduced to below -19%, and this is significantly better than -48% achieved by BST with a ground reflection factor of 2.

3 2-PHASE HYDROGEN EXPLOSION VALIDATION

3.1 INTRODUCTION

PRESLHY, the European sponsored research project on safe use of liquid hydrogen, has carried out 23 tests on explosions from the releases of liquid hydrogen into congested regions by HSE at HSE Science and Research Centre⁹. Conclusions from the test results by PRESLHY are:

- Wind plays a dominant role in the dispersion and development of hydrogen cloud from a release of liquid hydrogen. This includes transient and localised gusts which are difficult to measure and predict.
- Results show that an increasing hydrogen inventory, either through an increased tank pressure or larger nozzle, can result in a larger event upon ignition. However, significant variability was observed when tests were repeated.
- For explosions in low congested regions (volume blockage ratio < 1.5% and area blockage ratio < 1m²/m³ and congestion length scale between 20-25mm), it is conservative to use ME blast curve 5 for predicting explosions.
- For explosions in high congestion regions (volume blockage ratio > 4% and congestion length scale between 25-50mm), high level explosion and possible DDT could occur, the explosion could involve all of the cloud.

Objectives of this study are:

- Validate predictions of the Multi-Energy model in Phast/Safeti for hydrogen explosions in congested regions
- Develop a guidance for users to apply Phast/Safeti for hydrogen explosions in congested regions

This validation was carried out in five steps as:

- Discharge modelling. This ensures the modelled hydrogen releases are close to the tests.
- Predicting overpressures using the Multi-Energy explosion model in Phast/Safeti with dispersion predicted using methods implemented in Phast/Safeti, i.e. UDM (the default dispersion model), Cylinder cloud and Fill obstructed region first (two simple dispersion methods for improved explosion predictions inside congested regions).
- Predicting overpressure using the Multi-Energy explosion model in Phast/Safeti with hydrogen dispersion predicted using KFX (A CFD modelling tool from DNV)
- Analysing the results
- Conclusions and recommendations to apply Phast/Safeti for hydrogen explosions

3.2 The Preslhy explosion tests

3.2.1 Test setup

In all 23 tests, liquid hydrogen was supplied by Air Liquide in a vacuum insulated tanker with a content up to 2.5 tonnes. The tanker was connected directly to the release pipework and the release height was approximately 0.8m as shown in Figure 8.

The test rig is a steel frame consisting 18 1m³ sections configured as a 3m square base with a height of 2m as shown in Figure 9 & Figure 10. Congestion of the rig is added in the form of ladder-like structures, referred to as congestion frames. Each of these is made up of made up of 26 +/- 1 mm (nominal 1") cylindrical bars spaced 125 mm apart between two 5 mm x 50 mm bars. These have varying lengths dependant on the position in the rig. In the top half, the congestion frames were inserted horizontally and spanned the entire length of the congestion rig (3 m). Three congestion frames were used in each layer, and four layers were used.

Scaffold poles were inserted vertically in the rig to achieve a higher level of congestion as shown in Figure 11. Two congestion levels are tested as listed in Table 12 and they are referred as low and high congestions in this report.

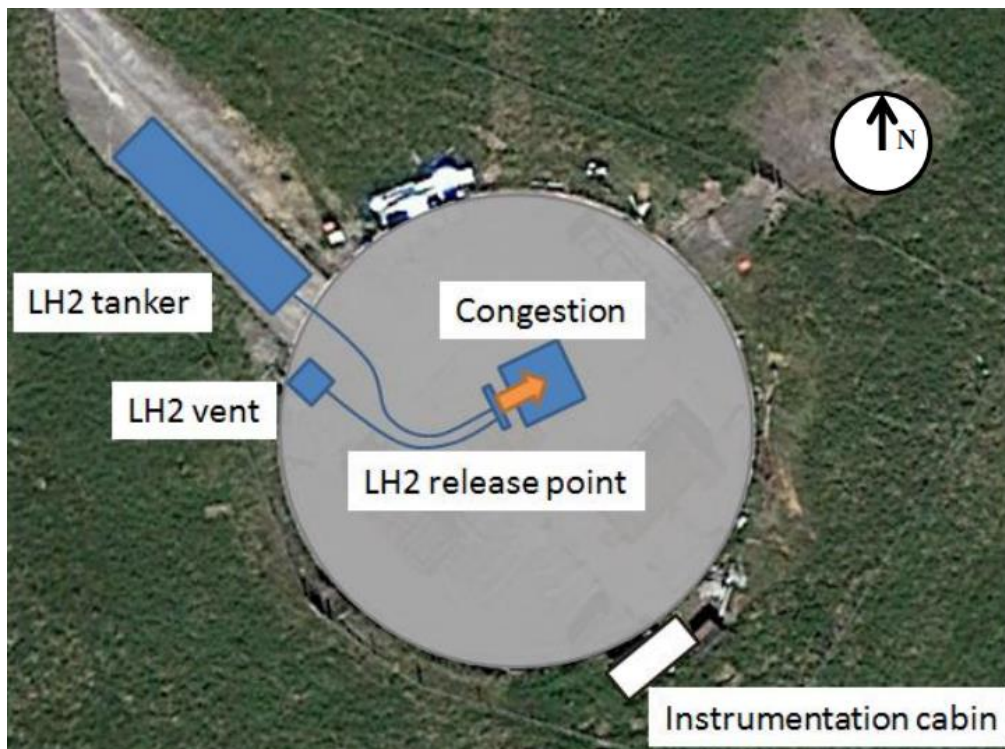


Figure 8 Layout of the site for the PRESLHY tests

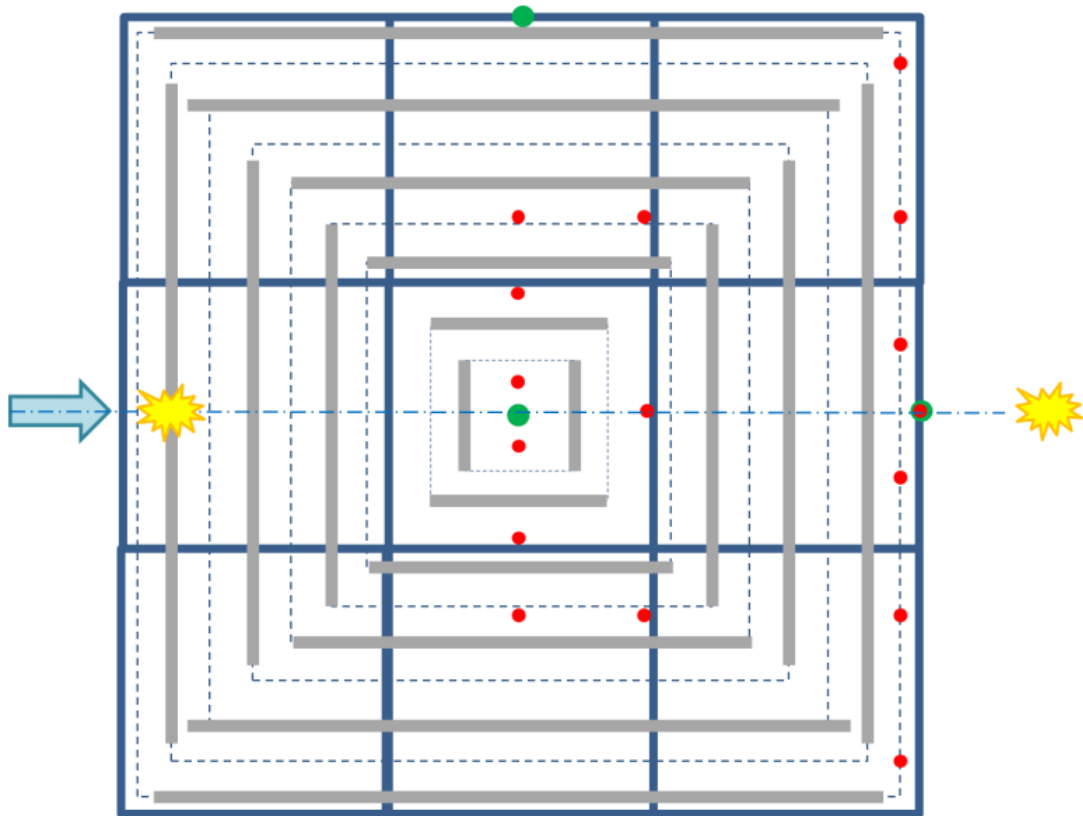


Figure 9 Setup of the explosion test



Figure 10 Photo image of the test rig with low level of congestion



Figure 11 Photo image of the test rig with high level of congestion

| | | Low level of congestion | High level of congestion |
|---|-------------|-------------------------|--------------------------|
| Area blockage ratio (m ² /m ³) | Bottom half | 0.8 | 1.33 |
| | Top half | 1.0 | 1.53 |
| Volume blockage ratio (%) | Bottom half | 1.54 | 4.20 |
| | Top half | 1.93 | 4.60 |

Table 12 Characteristics of the congested regions of the PRESLEY tests

3.2.2 Test procedures

Before the release of liquid hydrogen in a test, the pipework was purged first with nitrogen and then with ambient hydrogen gas. Hydrogen release before ignition was not a set time in these tests, but the test rig was saturated by the time of ignition to achieve a steady state output from the tests.

Pressure transducers were arranged in and around the test rig as shown in Figure 12. The transducers are located 0.5m above the ground at 90 degrees from the expected blast wave to measure incident blast pressures. The maximum pressures detected by the transducers are used to validate the predictions.

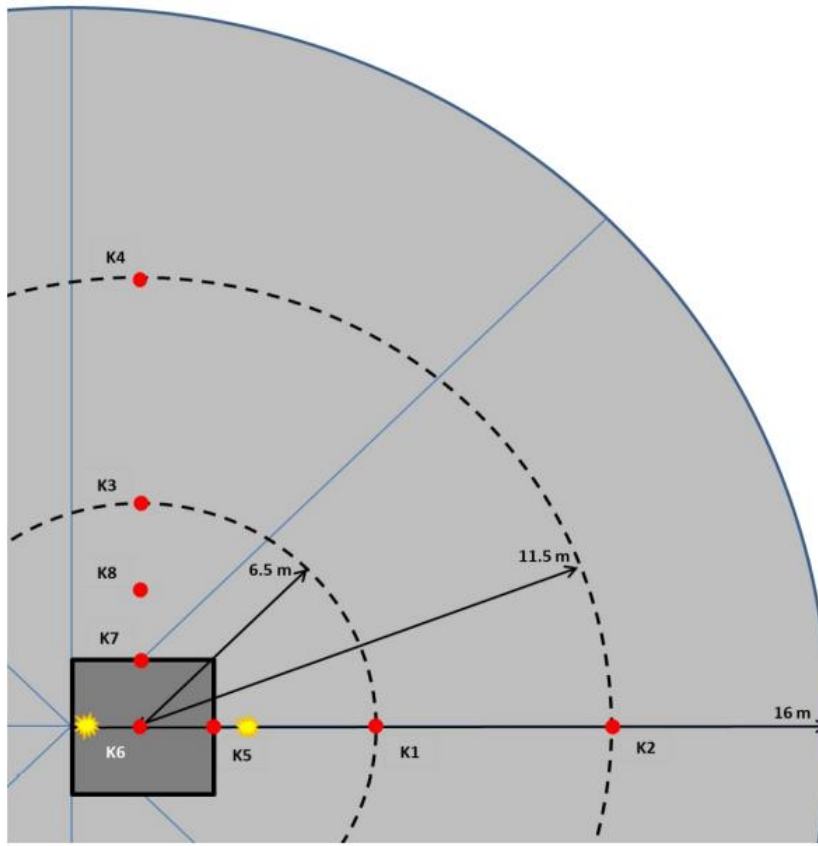


Figure 12 Layout of pressure transducers

3.2.3 Test programme

23 ignited tests were carried out as listed in Table 13. The table also includes measured peak overpressures within the congested regions and at the range of 6.5m and 11.5m from centre of the test rig.

Table 13 Test settings and result overview of the PRESLHY tests⁹

| Test No. | Orifice Diameter (mm) | Tanker pressure (barg) | Ignition point | Congestion level | P max (bar) | At | Noise (dB) | Pmax 6.5m (mbar) | Pmax 11.5m (mbar) |
|----------|-----------------------|------------------------|----------------|------------------|-------------|----|----------------|------------------|-------------------|
| 1 | 6 | 1 | Front | Low | 0.01 | K6 | * ¹ | 2 | 1 |
| 2 | 12 | 1 | Front | Low | 0.52 | K7 | * ¹ | 40 | 23 |
| 3 | 25.4 | 1 | Front | Low | 0.16 | K5 | * ¹ | 5 | 4 |
| 4 | 12 | 1 | Front | Low | 0.03 | K5 | 123 | 12 | 7 |
| 5 | 25.4 | 1 | Front | Low | 0.02 | K5 | 117 | 11 | 5 |
| 6 | 12 | 1 | Front | Low | 0.04 | K5 | 125 | 12 | 7 |
| 7 | 25.4 | 1 | Front | Low | 0.38 | K5 | 114 | 7 | 4 |
| 8 | 12 | 1 | Rear | Low | 0.07 | K6 | * ² | 14 | 8 |
| 9 | 12 | 1 | Rear | Low | 0.04 | K6 | 123 | 10 | 5 |
| 10 | 25.4 | 1 | Rear | Low | 0.01 | K6 | 108 | 4 | 2 |
| 11 | 6 | 5 | Front | Low | 0.14 | K5 | 122 | 13 | 7 |
| 12 | 12 | 5 | Rear | Low | 0.39 | K5 | 132 | 40 | 25 |
| 13 | 12 | 5 | Front | Low | 0.13 | K5 | 131 | 50 | 30 |
| 14 | 12 | 5 | Rear | Low | 0.53 | K5 | 127 | 20 | 12 |
| 15 | 12 | 5 | Front | Low | 0.10 | K5 | 132 | 40 | 20 |
| 16 | 12 | 5 | Rear | Low | 0.55 | K6 | 134 | 40 | 20 |
| 17 | 12 | 5 | Front | Low | 0.67 | K5 | 129 | 30 | 15 |
| 18 | 25.4 | 5 | Front | Low | 0.04 | K5 | 120 | 15 | 7 |
| 19 | 25.4 | 5 | Rear | Low | 0.15 | K5 | 137 | 70 | 40 |
| 20 | 6 | 1 | Front | High | 0.01 | K6 | * ² | 3 | 2 |
| 21 | 12 | 1 | Front | High | 0.15 | K5 | 134 | 40 | 25 |
| 22 | 12 | 1 | Front | High | 0.13 | K5 | 132 | 65 | 40 |
| 23 | 12 | 1 | Front | High | 1.28 | K5 | 145 | 470 | 205 |

3.2.4 Ambient conditions

Ambient conditions were measured at two locations in the tests as:

- 3m height at a downwind distance of 20m from the release.
- 1.5m height next to the release point.

Ambient conditions of the tests are shown in Table 14. Weather conditions at the two locations of a test are not always in agreement as shown in the table. Because no exact wind direction is reported for measurements near to the release point and ambient conditions at the downwind distance of 3m height

seems reasonable for dispersion calculation, so weather condition at the downwind position is used in this validation.

Table 14 Wind conditions of the PRESLHY tests⁹

| Trial No. | Local 5 min average wind speed (m/s) | Local 5 min average wind direction | Far-field wind speed (m/s) | Far-field wind direction (°) |
|-----------|--------------------------------------|------------------------------------|----------------------------|------------------------------|
| 1 | 1.0 | W | 2.03 | 172 |
| 2 | 3.4 | S | 2.00 | 136 |
| 3 | 2.0 | SW | 0.52 | 224 |
| 4 | 2.7 | SE | 1.09 | 123 |
| 5 | 2.4 | W | 1.38 | 189 |
| 6 | 0.7 | SE | 1.44 | 107 |
| 7 | 1.7 | SSE | 1.62 | 112 |
| 8 | 2.0 | W | 2.58 | 266 |
| 9 | 2.0 | W | 3.74 | 243 |
| 10 | 2.0 | N | 2.62 | 250 |
| 11 | 1.0 | NE | 1.01 | 127 |
| 12 | 0.7 | SE | 1.44 | 45 |
| 13 | 1.0 | NW | 1.01 | 139 |
| 14 | 1.0 | NE | 2.48 | 79 |
| 15 | 2.4 | NE | 2.14 | 42 |
| 16 | 2.7 | N | 1.24 | 299 |
| 17 | 0.7 | N | 0.69 | 312 |
| 18 | 0.7 | SE | 0.60 | 70 |
| 19 | 0.7 | E | 1.21 | 179 |
| 20 | 2.0 | E | 1.37 | 94 |
| 21 | 1.4 | SE | 2.70 | 85 |
| 22 | 2.4 | E | 2.14 | 50 |
| 23 | 2.0 | E | 3.22 | 71 |

3.3 Discharge calculation

Test setup for all the PRESLHY tests is similar. Tank pressure and size of the release nozzle are the two release conditions having dominant effects on discharge and flammable clouds. Pipe sections connecting the tank and the release station consist of several components as shown in Table 15.

Because of difficulties and uncertainty in direct modelling the pipe sections between the tank and the release point and the importance of accurately discharge calculation for predicting explosion, different discharge scenarios in Phast/Safeti were selected to ensure a reasonable match of the release rates between tests and predictions. Scenarios used to model the tests and the release rates predicted are listed in Table 16.

Observations of the discharge results are:

- The predicted release rate is about 20% below the measured flow rate for the releases of 6mm nozzle. Even so, predicted explosions for the tests of 6mm nozzle have not shown any underprediction, therefore the discharge model has not adjusted to match the measured release rate.
- Releases rates of the 12mm and 25.4mm nozzles are controlled at the measured release rates, so simulations of these cases have the same release rate as the tests.

Table 15 Dimensions of the pipe sections between tank and release station⁹

| Description | Length (m) | Thermal conductivity (W/m.K)* |
|----------------------------|------------|-------------------------------|
| Vacuum insulated hose | 20 | 2.5 W/m |
| Electrically isolated pipe | 0.5 | 0.021 |
| Mass flow meter | 0.4 | n/a |
| Valve section | 0.6 | 13-17 |
| Flexible hose | 1.75 | 0.034 |

Table 16 Release rates of the PRESLHY tests

| Tank pressure (barg) | Nozzle diameter (mm) | Measured release rate (g/s) | Phast scenario type | Predicted release rate (g/s) |
|----------------------|----------------------|-----------------------------|--|------------------------------|
| 5 | 6 | 90-100 | Leak (discharge coefficient at 1.0) | 75.1 |
| 5 | 12 | 265 | Short pipe (impinged jet release & flow control) | 265 |
| 5 | 25.4 | 298 | Short pipe (impinged jet release & flow control) | 298 |
| 1 | 6 | NA | Leak (discharge coefficient at 1.0) | 35.5 |
| 1 | 12 | 104-107 | Short pipe (impinged jet release & flow control) | 105.5 |
| 1 | 25.4 | 135-144 | Short pipe (impinged jet release & flow control) | 139.5 |

3.4 Dispersion of the hydrogen releases

3.4.1 UDM predictions

Figure 13 shows the predicted cloud views by UDM for releases of 5bar tank pressures. Cloud views of the 12mm and 24.5mm releases are similar and this is because release rates of them are controlled at 265 and 298 g/s respectively as the measured release rates. Even though UDM has no consideration of effect of the congested region on dispersion, the effect is partly included in the modelling by applying the releases as impinging jet releases in Phast/Safeti. Jet impingement has caused the hydrogen clouds to slow down and to rise quicker, as shown by the UDM results in Figure 14.

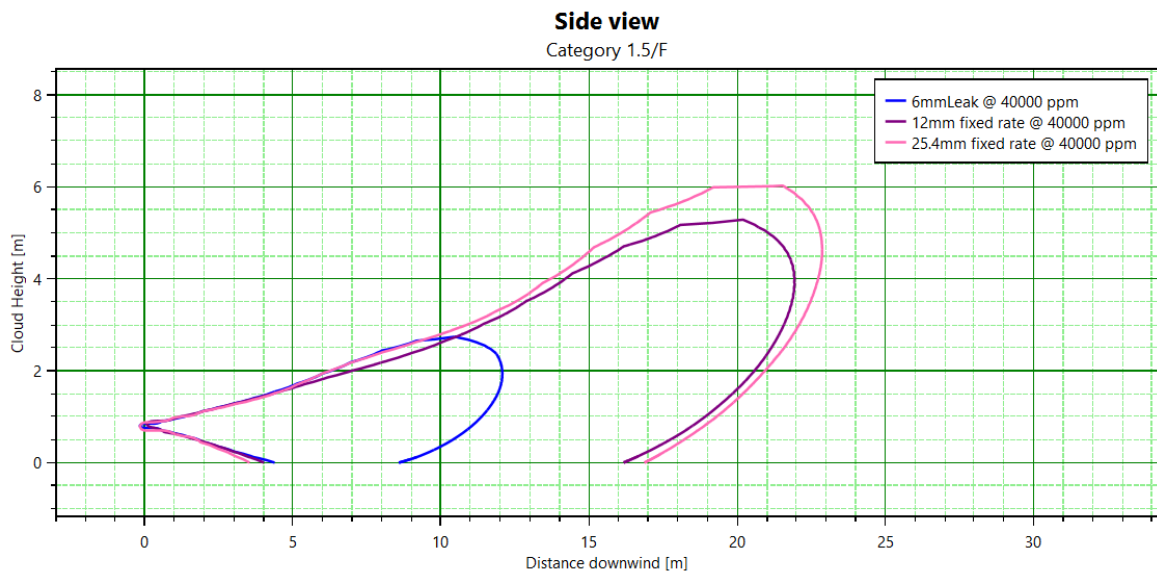


Figure 13 Side view of the flammable clouds predicted by UDM (tank pressure 5bar, weather 1.5F)

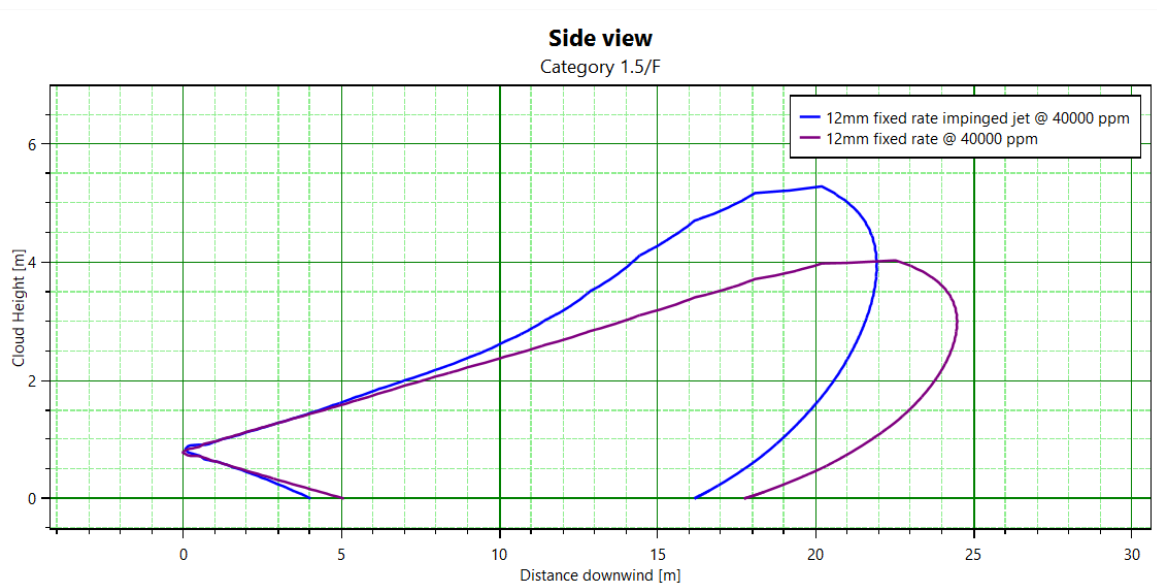


Figure 14 Comparing the flammable cloud view predicted by UDM for impinged and free jet (tank pressure 5bar, nozzle diameter 12mm and weather 1.5F)

3.4.2 KFX predictions

Figure 15- Figure 18 show photo images of hydrogen clouds prior to ignition in tests and iso-surfaces of cloud temperature at 273.15K predicted by KFX for tests of No 12, 14,15,17. Perspectives of the photo images are similar as the KFX predictions, the highlighted black regions in KFX results is the congested region.

Observations of the results are:

- Visible clouds in the photo images of the tests show condensed water vapour caused by the releases of liquid hydrogen at about -253 °C. Without direct modelling water vapours in the KFX simulations, the photo images are compared qualitatively with the predicted temperature iso-surfaces at 0 °C. At this temperature, water vapour in the air condenses to droplets to becoming visible. The predicted clouds are similar as the image qualitatively.
- Hydrogen clouds from a release are sensitive to weather conditions as observed in the tests.. Wind conditions are measured at two locations in the tests as shown in Table 14. But wind directions at the two stations are not always the same, this indicates strong turbulence or fluctuation of wind in the local area and would cause uncertainties in the predicted hydrogen clouds by KFX.
- A capability has been developed for Safeti to use KFX dispersion results for risk calculations. Predicted overpressures using the KFX clouds for these 4 tests are given in section 3.5.4.

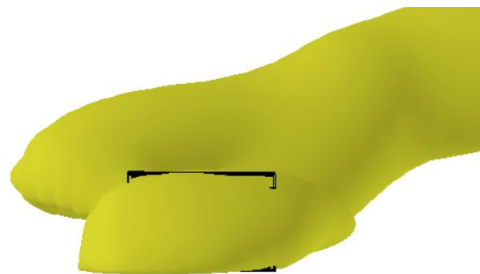


Figure 15 Flammable clouds of the test and hydrogen cloud predicted by KFX before the ignition (Test No12)

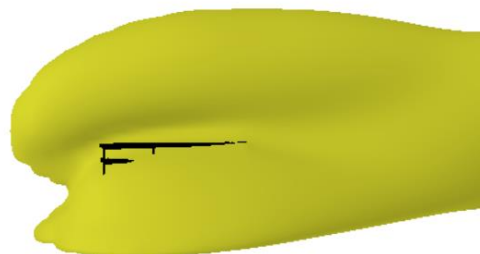


Figure 16 Flammable clouds of the test and hydrogen cloud predicted by KFX before the ignition (Test No14)

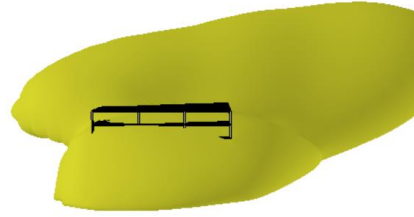


Figure 17 Flammable clouds of the test and hydrogen cloud predicted by KFX before the ignition (Test No15)

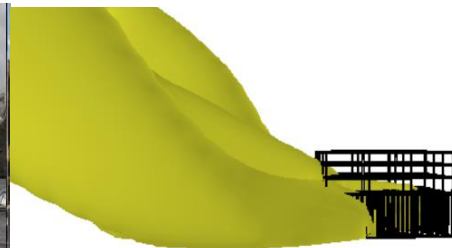


Figure 18 Flammable clouds of the test and hydrogen cloud predicted by KFX before the ignition (Test No17)

3.5 Predictions of hydrogen explosions by the Multi-energy explosion model

3.5.1 Setup of the cases in Safeti

Explosion models available in Phast and Safeti are the same. Safeti is used in this study because of its capability in ignition modelling and the convenience of extracting explosion results using risk ranking points. Figure 19 shows setup of the PRES-LHY cases in Safeti. The main features include:

- The congested region is defined as a ME congestion of either defined explosion strength or calculated explosion strength, i.e. the pink shaded area in Figure 19. A Multi-Energy blast curve is selected for each ME congestion of defined strength and GAMES correlations are used for ME congestions of calculated explosion strength. The calculated strength of an explosion depends on characteristics of the congested region, flammable mass within the region and properties of the vapour cloud.
- Locations of the pressure transducers are specified as risk ranking points, i.e. the blue dots in Figure 19.
- Ignition. Release before ignition was not a set time in the tests, but a steady state was required and the congestion rig was steady by the time of ignition. The clouds were ignited at one of two locations as illustrated in Figure 9. The free field ignition method in Safeti has similar principles as the tests and is selected for this work. Plant boundary for free field ignition of the tests is shown by the blue square in Figure 19.

Explosions predicted by the Multi-Energy model in Phast/Safeti are highly dependent on methods used to estimate explosion strength and flammable mass participating an explosion. There are quite a few methods for selection in Phast/Safeti and each could produce different results from the others.

Methods for explosion strength, i.e. peak overpressure of an explosion

The peak overpressure of an explosion is the result of accelerated burning of a vapour cloud and it can be determined in two ways in Phast/Safeti. The two ways are:

- Defined explosion strength: A ME blast curve is specified for an explosion by specifying a ME blast curve. The PRES-LHY study on hydrogen explosions has recommended ME blast curve 5 for explosions within congestions having VBR less than 1.5% and no specific blast curve is recommended for explosions having higher VBR.
- Calculated explosion strength: The peak overpressure of an explosion is calculated using correlations based on tests or numerical simulations. There is no published correlation for hydrogen explosions so far and so the GAMES correlations developed for vapour cloud explosion of hydrocarbons is tested here. Peak overpressure predicted by Games correlations depends on congestion, flammable cloud within the congestion and laminar burning velocity of the fuel.

Methods for predicting flammable clouds within a congested region

- Normal dispersion. Dispersion cloud predicted by UDM is used to decide flammable mass of an explosion.
- Fill obstructed region first. Dispersion cloud predicted by UDM is redistributed into the congested region where it is released, flammable cloud comes out the congested region after the region is fully occupied. This is a simple dispersion method implemented in Phast/Safeti and gives the most conservative estimation of flammable mass for explosions. Details of this and the Cylinder cloud methods can be found in the theory manual for the explosion models in Phast/Safeti10.

-- Cylinder cloud. A cylinder cloud around the release point is assumed for a release. This is another simple dispersion method available in Phast/Safeti and is good for releases inside densely congested regions.

-- KFX cloud. KFX is used to predict vapour dispersion from a release and the predicted clouds are then used for explosion calculation by Safeti. This method should give more accurate predictions of flammable clouds by considering the effects of crosswind and obstacles.

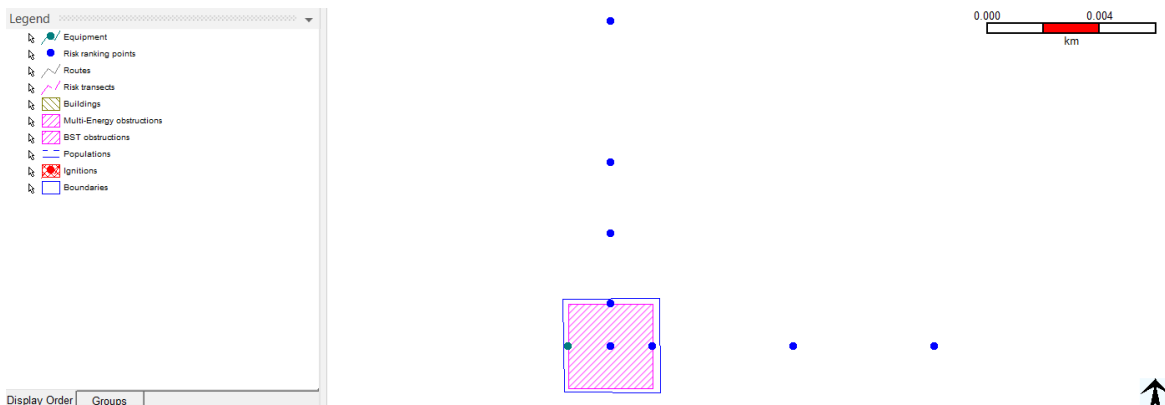


Figure 19 Setup of the case in Safeti

3.5.2 Grouping of the tests for validation

Instead of looking into the predictions for individual cases, the 23 PRESLEY tests listed in Table 13 are divided into 8 groups as shown in Table 17 and predicted explosions are assessed in groups because of the following reasons:

- Tests in a group have the same tank pressure, nozzle diameter and congestions, so the tests in a group should have very similar discharge results.
- The tests in a group differ in wind speed. Wind speeds of the PRESLEY tests are in a range between 0.5 and 3.74m/s, the differences among the cases in a group are smaller as shown in Table 17. The differences in wind speed do cause some differences in cloud dispersion between tests in a group, particularly at far field as illustrated in Figure 20, but the differences in the near field are quite small within the speed range of the tests. In the PRESLEY tests, the congestion rig is within 3m from the release point as illustrated in Figure 19 and the predicted flammable clouds by UDM within the congested region would be very similar among the cases within the group.
- Apart from differences in wind speed, wind direction also varies among tests in a group. However, crosswind effect is not modelled in Phast/Safeti and wind is assumed in the same direction of the release.
- Because of these reasons, explosions predicted by Phast/Safeti for the tests in a group would be very similar and it seem reasonable to group them together.
- The grouping may also help to understand the impact of ignoring crosswind on explosion results.

Table 17 Grouping of the PRESLHY tests

| Group No | Tank Pressure (barg) | congestion level | Nozzle diameter (mm) | No of tests in the group | Average wind speed | Range of wind speed (m/s) |
|----------|----------------------|------------------|----------------------|--------------------------|--------------------|---------------------------|
| 1 | 1 | Low | 6 | 1 | 2.03 | 2.03 |
| 2 | 1 | Low | 12 | 5 | 2.18 | 1.07--3.74 |
| 3 | 1 | Low | 25.4 | 4 | 1.54 | 0.52--2.62 |
| 4 | 5 | Low | 6 | 1 | 1.01 | 1.01 |
| 5 | 5 | Low | 12 | 6 | 1.50 | 0.69--2.48 |
| 6 | 5 | Low | 25.4 | 2 | 0.65 | 0.60--1.21 |
| 7 | 1 | High | 6 | 1 | 1.37 | 1.37 |
| 8 | 1 | High | 12 | 3 | 2.69 | 2.14--3.22 |

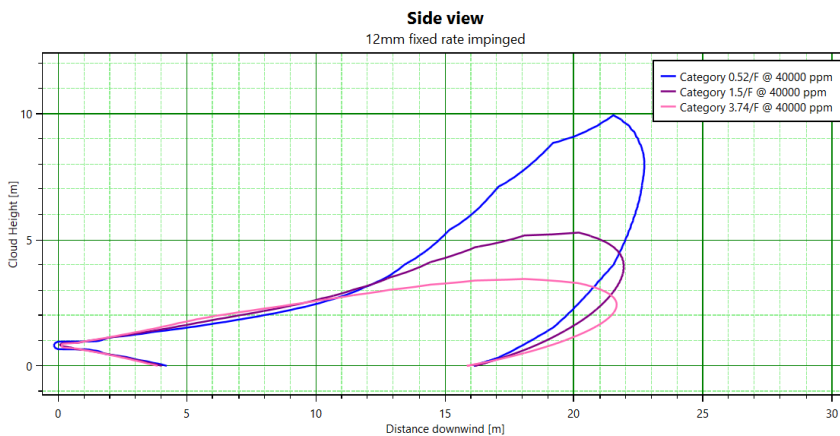


Figure 20 Cloud views predicted by UDM at three wind speeds for the tests in Group 3 (tank pressure 5bar, 12mm nozzle and low congestion)

3.5.3 Predictions by Phast/Safeti using UDM clouds by the Multi-Energy explosion model

3.5.3.1 Tests with low congestion and low tank pressure (Groups 1-3)

UDM is the default method for cloud dispersion and all results presented in this section are predicted using cloud views predicted by UDM. The PRESLHY report has recommended ME blast curve 5 for hydrogen explosions in low congested regions (volume blockage ratio < 1.5% and area blockage ratio < 1m²/m³ and congestion length scale between 20-25mm). VBR (volume blockage ratio) of the low congestion rig of the PRESLHY tests is 1.74% which is slightly higher than 1.5%, the explosion strength could be between ME blast curves 5 & 6, predictions with defined explosion strengths of ME curves 5 & 6 are presented for tests of the low congestion rig.

Figure 21 shows the predicted effect contours of 0.05bar overpressure for groups 1-3 with defined explosion strength of ME blast curve 5. Figure 22- Figure 24 compare the predicted overpressure against measurements for groups 1-3 respectively.

Observations of the results are:

- Delayed ignition of hydrogen releases in congested regions seems not always producing meaningful explosion. Tests 1 & 10 with nozzle diameter of 6 and 25.4mm have produced very low peak overpressures which are equivalent to ME blast curve 1 as shown in Figure 22 and Figure 24. Flash fires are the more likely events in these tests. As the result, the predicted explosions with a strength of ME blast curve 5 are very conservative for these cases.
- Low overpressures are also produced by tests 4, 5, 6 & 9. The measured pressures of these cases are just over the predictions for unconfined explosions using MDE blast curve 2 as shown in Figure 23. The PRESLHY report has attributed the low overpressures to relatively low hydrogen inventory in these tests because of low tank pressure of 1 bar and swirling winds on the site which could have diluted the flammable clouds in some tests.
- Predictions using an explosion strength of ME blast curve 5 are conservative at locations outside the congested region, i.e. locations of pressure transducers 1-4 & 8, and largely conservative within the congested region (i.e. locations of transducers 5-7), underpredictions are observed at transducer No 7 in Test No 2 and at transducer No 5 in Test No 7. Predictions with ME blast curve 6 are conservative at all locations, but it may be too conservative for Group 1, i.e. the releases at tank pressure of 1 bar and 6mm nozzle.
- The calculated explosion strength method has produced predictions falling between the predictions with defined strengths of ME curve 5 & 6. This is expected because VBR of the low congestion rig is higher than 1.5%.
- The GAMES correlation seems a suitable method for tests in groups 1-3.

No underprediction is noticed in these tests by assuming wind to be in the same directions in Phast/Safeti.

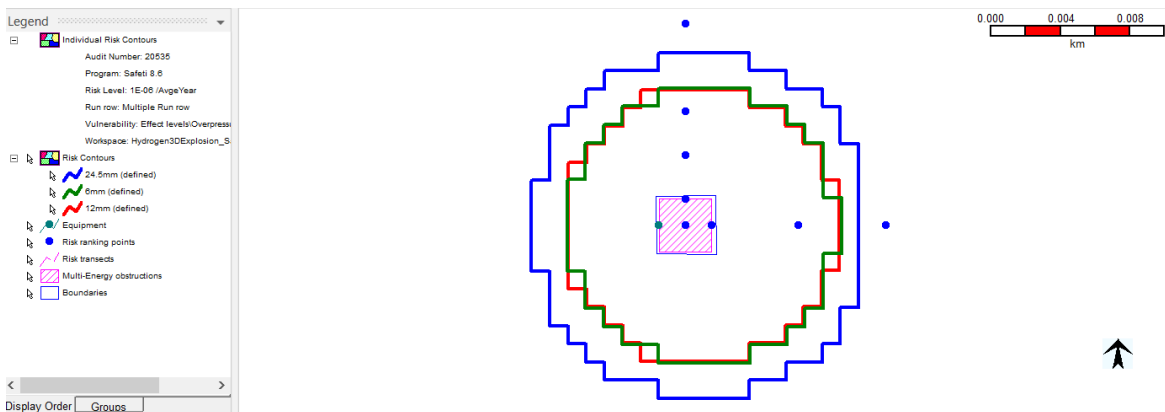


Figure 21 Effect contours of 0.05bar overpressure of the tests with tank pressure of 1bar and low congestion

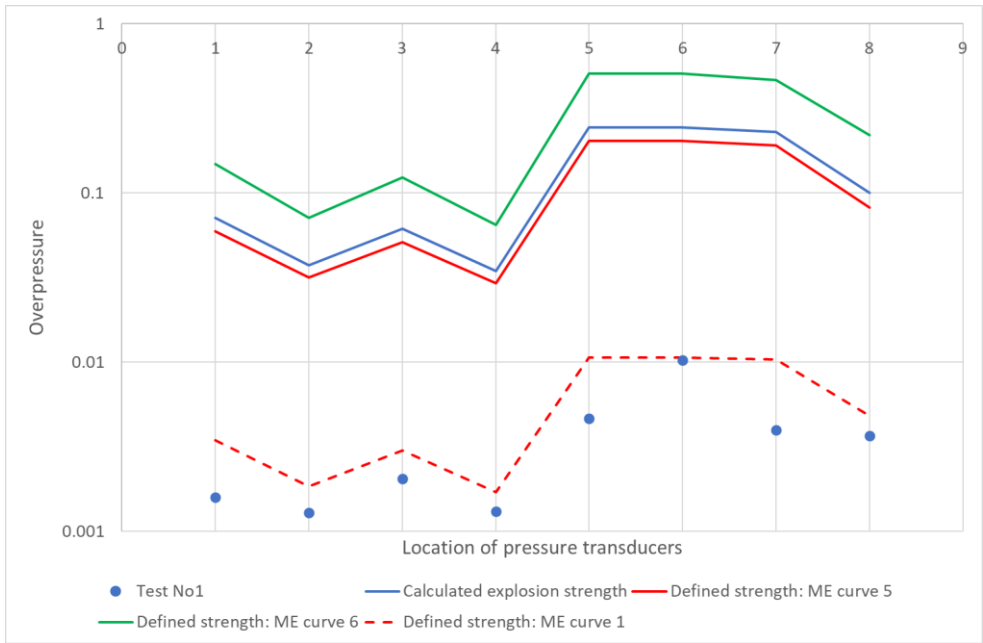


Figure 22 Comparing the measured and predicted overpressures for tests in Group 1 (1bar tank pressure, 6mm nozzle, low congestion)

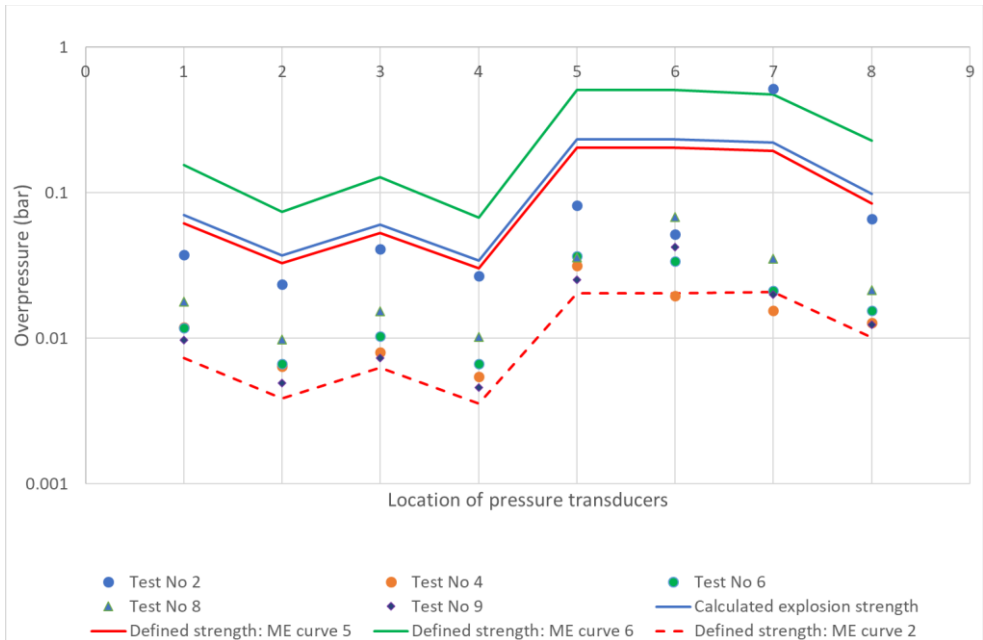


Figure 23 Comparing the measured and predicted overpressures for tests in Group 2 (1 bar tank pressure, 12mm nozzle, low congestion)

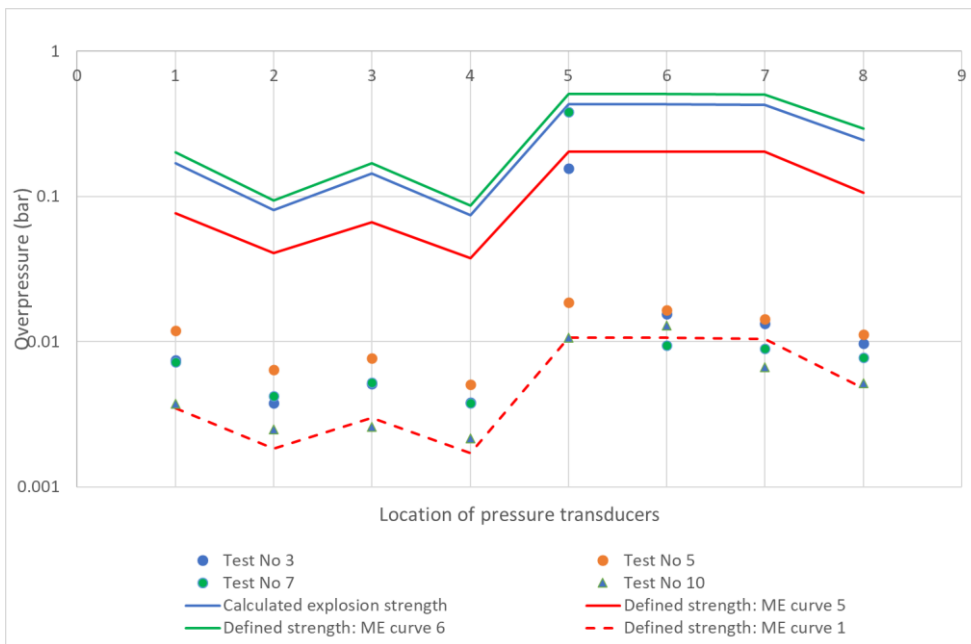


Figure 24 Comparing the measured and predicted overpressures for tests in Group 3 (1 bar tank pressure, 25.4mm nozzle, low congestion)

3.5.3.2 Tests with low congestion and high tank pressure (Groups 4-6)

Figure 25 - Figure 29 shows the predicted explosions for groups 4-5 respectively, i.e. tank pressure of 5 bar and lower congestion, with defined explosion strengths of ME blast curves 5 & 6 and calculated explosion strength using the Games correlations.

Observations of the results are:

- Similar as tests 1 & 10 in the groups with releases at tank pressure 1 bar in previous section, test 18 in Group 6 also produced a very low peak overpressure and flash fire is the more likely event. As the result, explosions predicted with ME blast curve 5 would be very conservative for this case as shown in Figure 27. However, there is a probability of explosion in similar scenarios such as test No 19. When explosion occurs instead of flash fire, Safeti predictions with defined explosion strength of ME curve 5 or calculated explosion strength are satisfactory as shown in Figure 27.
- The results are in similar trends as the results for groups 1-3, even though under-predictions are observed at increased locations while using a defined explosion strength of ME curve 5 as shown in Figure 26 & Figure 27.
- The method of calculated method produces predictions between the results of the defined strengths of ME curve 5 & 6. The GAMES correlation seems a suitable method for tests in groups 4-6.
- Comparing with the explosions in Group 1-3, explosions in Groups 4-6 are generally stronger. The main difference between them is the tank pressure, this seems suggesting that, apart from volume blockage ratio of the congested region, release rate and maybe size of the congested region are also need to be considered in deciding explosion strength for a hydrogen explosion.

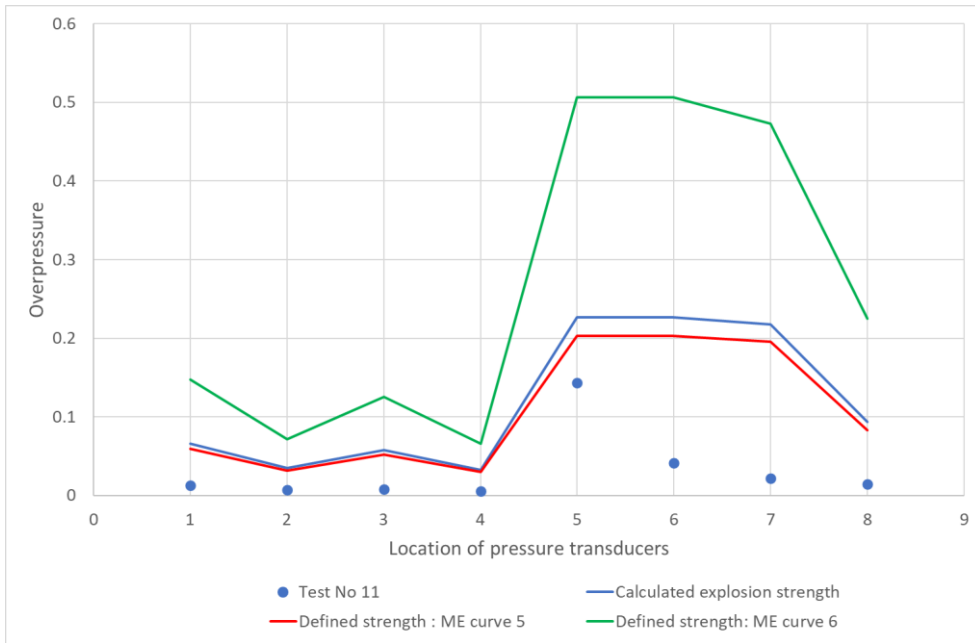


Figure 25 Comparing the measured and predicted overpressures for tests in Group 4 (5 bar tank pressure, 6mm nozzle, low congestion)

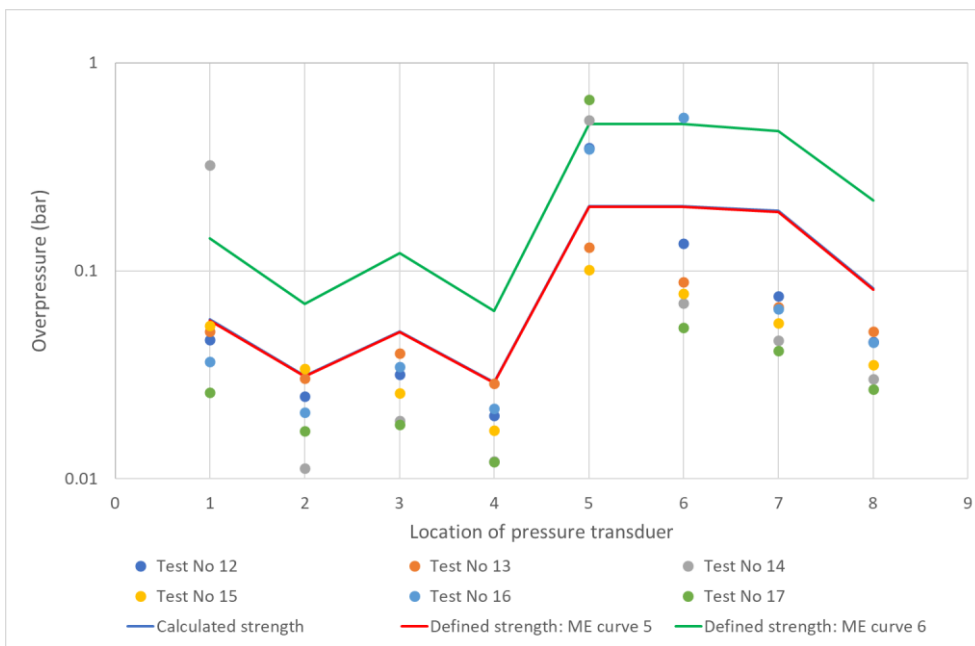


Figure 26 Comparing the measured and predicted overpressures for tests in Group 5 (5 bar tank pressure, 12mm nozzle, low congestion)

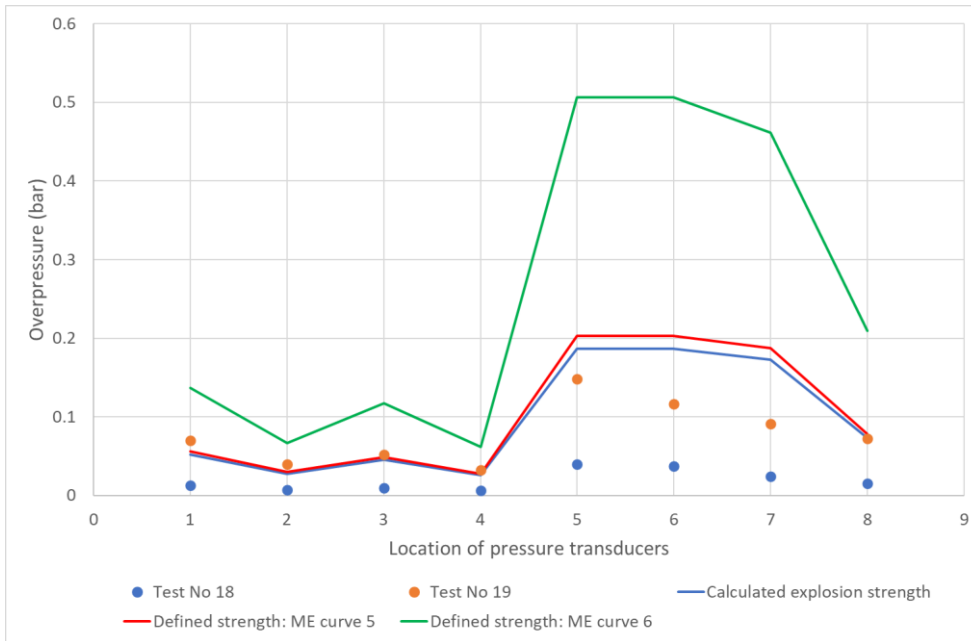


Figure 27 Comparing the measured and predicted overpressures for tests in Group 6 (5 bar tank pressure, 24.5mm nozzle, low congestion)

3.5.3.3 Tests with high congestion (tests in Groups 7 & 8)

Figure 28 & Figure 29 shows the predicted results for tests in groups 7 & 8, i.e. the tests with high congestion as given in Table 12 and shown in Figure 11. No ME blast curve is recommended from the PRESLHY report for explosions of these tests, a defined strength of ME blast curve 7 is used as a reference here. The figures have also included results of three cloud methods, i.e. cloud views predicted by UDM, Cylinder cloud and Fill obstructed region first as explained in section 3.5.1.

Observations of the results are:

- No significant explosion was observed in the test of 6mm nozzle (i.e. test No 20 in Group7), the measured explosion has a strength equivalent to ME blast curve 1 as shown in Figure 28, a flash fire is the more likely event this time. Therefore Safeti predictions with ME blast curve 5 would be very conservative.
- A defined explosion strength of ME blast curve 7 and calculated explosion strength using UDM cloud have produced good predictions for tests 21 & 22.
- Significant underpredictions outside the congested region are produced for test No 23. The PRESLHY has suggested a high order of deflagration or detonation for this test and ME blast curves of 8-10 for it. For Test No 23, the calculated explosion strength using the dispersion methods of either Cylinder cloud or Fill obstructed region first has produced better results at locations outside the congested region. The calculated peak overpressures by these two methods are over 10 bar, which is equivalent to a peak overpressure between ME blast curves 9 & 10 and is consistent as the recommendation by the PRESLHY report of ME blast curves of 8-10.
- As shown in the results for tests in Group 1-6, the Games correlations with UDM clouds produces good predictions, apart from test No 23 which may have DDT. When DDT occurs in an explosion, the flammable mass participating the confined explosion seems higher than that predicted by UDM, cloud method of either Cylinder cloud or Fill obstructed region first seems a good method to use.

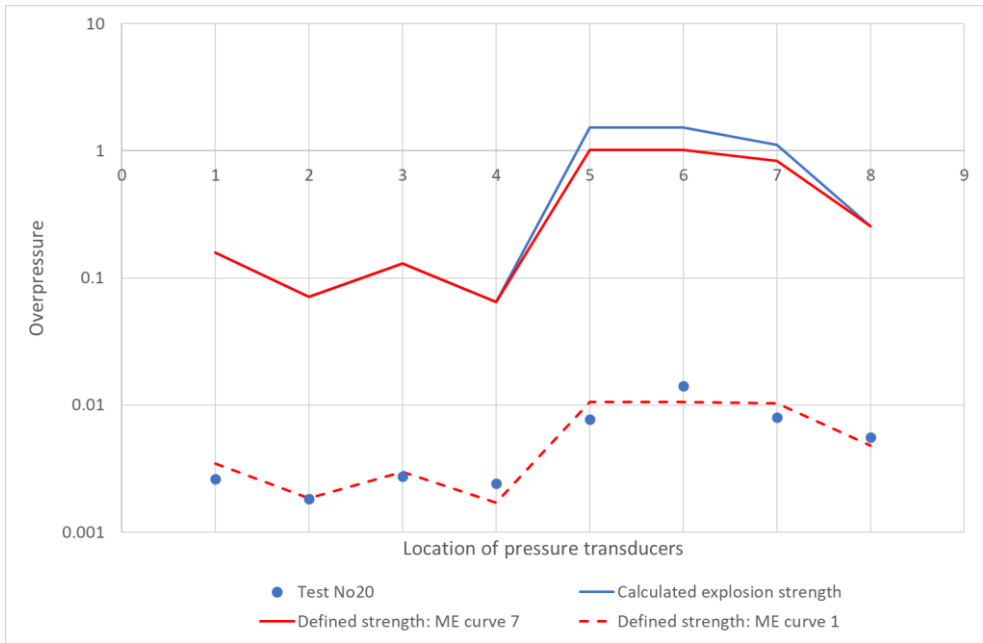


Figure 28 Comparing the measured and predicted overpressures tests in Group 7 (1 bar tank pressure, 6mm nozzle, high congestion)

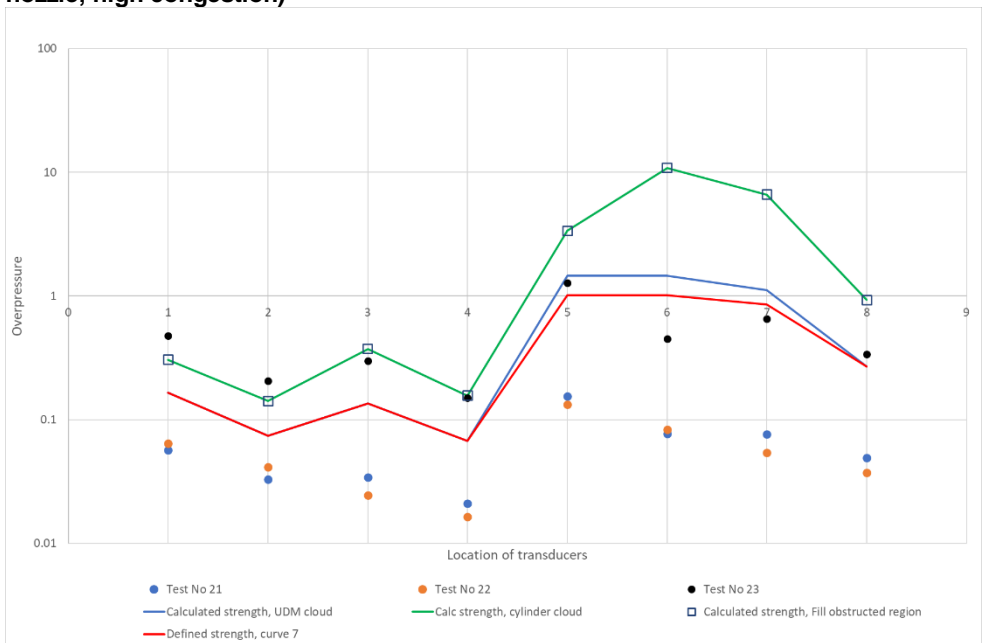


Figure 29 Comparing the measured and predicted overpressures tests in Group 8 (1 bar tank pressure, 12mm nozzle, high congestion)

3.5.4 Predictions by ME model in Phast/Safeti using KFX clouds

UDM is a dispersion method developed for cloud dispersion in open or relative open areas. It has no consideration of interaction between the cloud and obstacles during dispersion and this can produce inaccurate results for releases in highly congested areas. As shown in Figure 15- Figure 17, hydrogen cloud is strongly influenced by the congestions. To address this weakness of using UDM method for explosion calculation, flammable clouds predicted by KFX were imported to Safeti for explosion calculations in this study.

Figure 30 shows the effect contours of 0.05bar overpressure for tests 12,15,15 & 17 in group 6. Figure 31 compares the predicted overpressures using flammable clouds predicted by different methods.

Observations of the results are:

- As expected, effect contours using KFX clouds falls between the contours of UDM (the green contour) and the method of Fill obstructed region first (the blue contour). This indicates that the flammable mass predicted for these tests by KFX are between that estimated by UDM and the method of Fill obstructed region first.
- Explosions predicted using KFX clouds shows good trends for more accurate predictions.

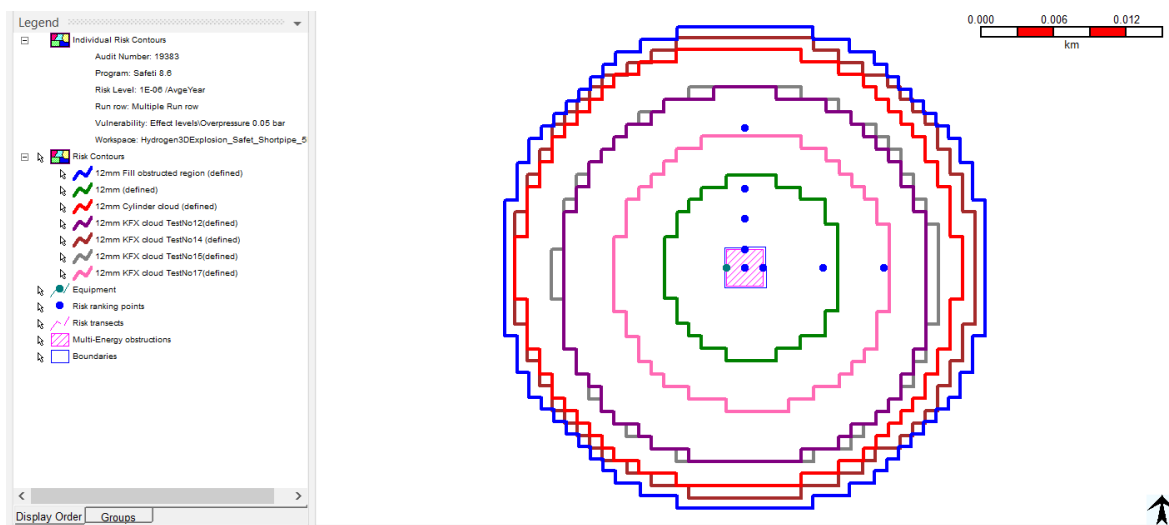


Figure 30 Effect curves of 0.05 bar overpressure predicted by Safeti using UDM and KFX clouds for Tests 12, 14, 15 & 17 (5 bar tank pressure, 12mm nozzle, low congestion)

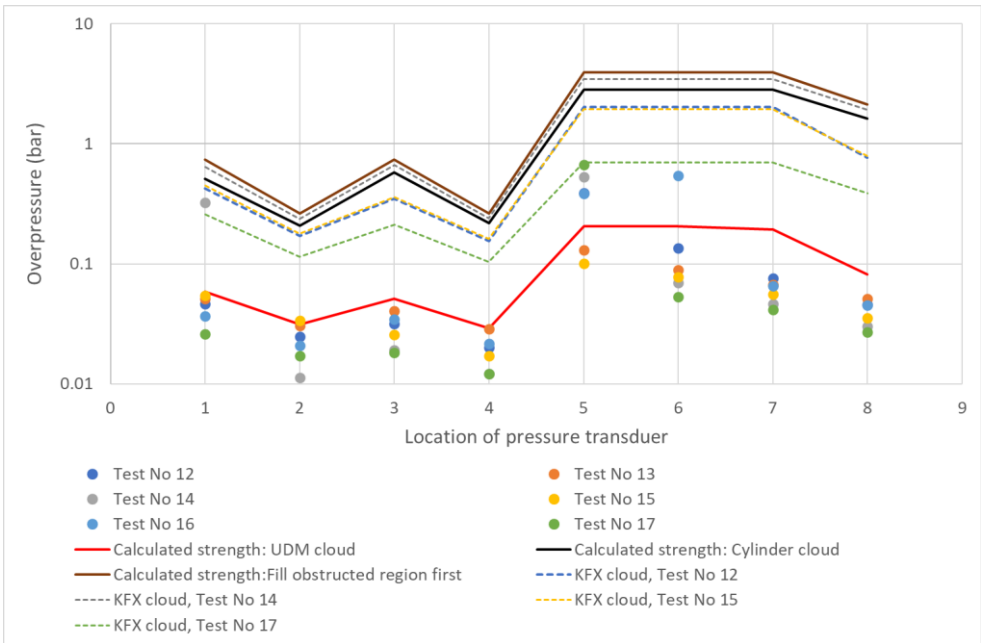


Figure 31 Comparing the measured and predicted overpressures using UDM and KFX clouds with calculated explosion strength using the Games correlations for the Multi-Energy explosion model for tests in Group 5 (5 bar tank pressure, 12mm nozzle, low congestion)

3.6 Predictions of hydrogen explosions by the Baker-Strehlow-Tang (BST) explosion model

3.6.1 Setup of the cases in Safeti

As for the validation of ME model, Safeti is used for the BST model because of its capability in ignition modelling and the convenience of extracting explosion results using risk ranking points. Figure 19 shows setup of the PRESLHY cases in Safeti. The PRESLHY tests are also assessed in 8 groups as explained in section 3.5.2. But there are differences between ME and BST models on methods in defining explosion strength.

Methods for explosion strength, i.e. peak overpressure of an explosion

The peak overpressure of an explosion is the result of accelerated burning of a vapour cloud and it can be determined in two ways in Phast/Safeti for the BST model as:

- **Defined flame speed:** A BST curve is specified for an explosion by specifying flame speed of the explosion in Mach number.
- **Calculated flame speed:** Flame speed of an explosion is determined based on characteristics of congested regions in the cloud and material property using a flame speed table published for the BST methodology, as shown in Table 18. The flame speed can be determined after knowing degree of confinement & congestion of the obstructed regions and material reactivity of the flammable cloud.

Table 18 Flame speed table of the BST explosion model

| Degree of confinement | Material reactivity | Congestion | | |
|-----------------------|---------------------|------------|------------------|------|
| | | Low | Medium | High |
| 2D | High | 0.59 | DDT ³ | DDT |
| | Medium | 0.47 | 0.66 | 1.6 |
| | Low | 0.079 | 0.47 | 0.66 |
| 2.5D | High | 0.47 | DDT | DDT |
| | Medium | 0.29 | 0.55 | 1 |
| | Low | 0.053 | 0.35 | 0.5 |
| 3D | High | 0.36 | DDT | DDT |
| | Medium | 0.11 | 0.44 | 0.5 |
| | Low | 0.026 | 0.23 | 0.34 |

³ For DDT, the flame Mach number is assumed to be 5.2 for conservative predictions.

3.6.2 Flame speed selection for the PRES�HY tests

The PRES�HY study has made following recommendations for modelling hydrogen explosions in congested areas:

- For explosions in low congested regions (volume blockage ratio < 1.5% and area blockage ratio < 1 m²/m³ and congestion length scale between 20-25 mm), it is conservative to use ME blast curve 5 for predicting explosions.
- For explosions in high congestion regions (volume blockage ratio > 4% and congestion length scale between 25-50 mm), high level explosion and possible DDT could occur, the explosion could involve the whole the cloud.

To apply the BST model, a flame speed is required but no recommendation was made on flame speed by the PRES�HY study. So flame speed has to be selected using Table 18 based on characteristics of the explosion, i.e. confinement, congestion and material reactivity.

Confinement

Confinement may also be described as degree of expansion. The flame speed table has three confinement levels, i.e. 2D, 2.5D and 3D. An explosion is considered to be 3D if the flame is free to expand in all directions in the obstructed regions, 2D if the flame can only expand in two dimensions and 2.5D if it is restricted in the third dimension where confinement is made of either frangible panels or by nearly solid confining planes (e.g. pipe rack where pipes are almost touching).

Congestion

Congestion is classified as low, medium and high depending on area blockage ratio (ABR) and pitch (i.e. the distance between successive rows or layers of obstacles) in the flame path as:

- Low congestion level: a few obstacles in the flame's path or ABR less than 10% and a few layers of obstacles
- Medium congestion level: anything falling between the low and high levels.
- High congestion level: closely spaced layers of obstacles with an ABR of 40% or higher.

Reactivity

Material reactivity is rated as low, medium and high as by Zeeuwen & Wiekema¹¹. Methane and carbon monoxide are the materials regarded as low reactivity, whereas hydrogen, acetylene, ethylene, ethylene oxide and propylene oxide are highly reactive, and all other materials have medium reactivity. In general, medium reactivity single component fuels have laminar burning velocities between 0.45-0.75 m/s, low and high reactivity fuels have the velocities lower than 0.45 m/s (inclusive) and higher than 0.75 m/s respectively (Baker et al, 1997¹²).

Applying these criteria, the PRES�HY tests would have the characteristics as:

- Low congestion tests: 2.5D or 3D confinement, medium congestion and high reactivity.
- High congestion test: 2.5D or 3D confinement, medium congestion and high reactivity.

This would imply a flame speed of DDT for all PRES�HY tests according to Table 18, a flame speed of Mach number 5.2 would be used for explosion calculation. A flame speed of Mach number 5.2 is equivalent to ME blast curve 10 for detonation scenarios. Even though DDT is observed in one of the 23 PRES�HY tests, assuming DDT would lead to significant overpredictions for most PRES�HY tests based on the validation results for the ME model. In Table 18, there is a huge jump in flame speed between low and medium congestion for explosions of highly reactive materials with 2.5D or 3D confinement. For hydrogen explosions with 3D confinement, flame speed would jump from Mach number 0.36 to

DDT when congestion changes from low to medium. Such discontinuity in flame speed would produce significant change in explosion results when congestion has just increased a bit.

So, instead of using the flame speed table directly, flame speed used by the BST model for this validation is selected according to peak overpressure of the ME blast curves recommended by the PRESLHY study or the overpressures predicted by the GAMES correlations for explosions in high congestions using Table 19, a conversion table provided by Tang & Baker (1999¹³).

Table 19 Relationship between flame speed and peak overpressure of VCEs (Tang & Baker 1999)

| Flame speed (Mach number) | Peak overpressure (Pmax) |
|------------------------------|--------------------------------|
| 0.07 | 0.010 |
| 0.12 | 0.028 |
| 0.19 | 0.070 |
| 0.35 | 0.218 |
| 0.7 | 0.680 |
| 1 | 1.240 |
| 1.4 | 2.000 |

The PRESLHY study recommends ME blast curve 5 for explosions in low congested regions (volume blockage ratio < 1.5% and area blockage ratio < 1m²/m³ and congestion length scale between 20-25mm). ME blast curve 5 has a peak overpressure just over 0.2bar and this is roughly equivalent to the peak overpressure of BST blast curve for flame speed of Mach number 0.35 as shown in Table 19.

For a hydrogen explosion with high congestions, no ME blast curve is recommended and so the peak overpressure is calculated using the GAMES correlations and it is then converted to flame speed using Table 19.

In the results presented below, the results are marked as converted flame speed for the BST model, this is to differentiate from the options of defined and calculated flame speeds in Phast/Safeti.

3.6.3 Predictions by BST model in Phast/Safeti using UDM clouds

3.6.3.1 Tests with low congestion and low tank pressure (Groups 1-3)

UDM is the default method for cloud dispersion and all results presented in this section are predicted using cloud views predicted by UDM unless a cloud method is specially specified. The PRESLHY report has recommended ME blast curve 5 for hydrogen explosions in low congested regions (volume blockage ratio < 1.5% and area blockage ratio < 1m²/m³ and congestion length scale between 20-25mm). VBR (volume blockage ratio) of the low congestion rig of the PRESLHY tests is 1.74% which is slightly higher than 1.5%, the explosion strength could be between ME blast curves 5 & 6, equivalent flame speeds generating same peak overpressure as ME blast curves 5 & 6 are used in this validation. Figure 22 compare the predicted overpressure against measurements for groups 1-3 respectively.

Observations of the results are:

- Direct applying the BST methodology implies DDT for the PRESLHY tests and would lead to significant overpredictions. So, instead of using the flame speed table directly, flame speeds of the tests are converted from the ME blast curves recommended for the PRESLHY tests.

- Predicted trends by the BST model using converted flame speeds are similar as the trends observed for the ME explosion model. The predicted overpressures are generally conservative using a flame speed with the same peak overpressure as that of ME blast curves 5.
- Explosions with ME blast curve 5 have a peak overpressure just over 0.2 bar and is equivalent to BST explosions of a flame speed at Mach number 0.35. This implies a low congestion level for the tests in groups 1-3 according to the BST flame speed.
- When a calculation method is needed to select flame speed, the GAMES correlations seem suitable for tests in groups 1-3.

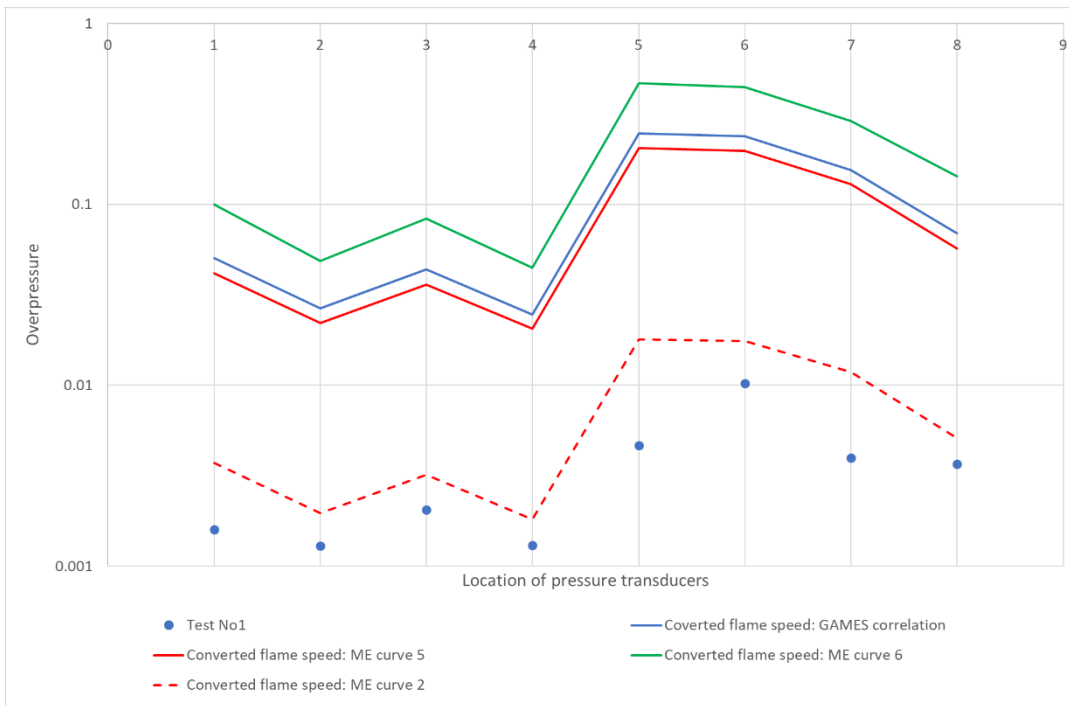


Figure 32 Comparing the measured and predicted overpressures for tests in Group 1 (1bar tank pressure, 6mm nozzle, low congestion)

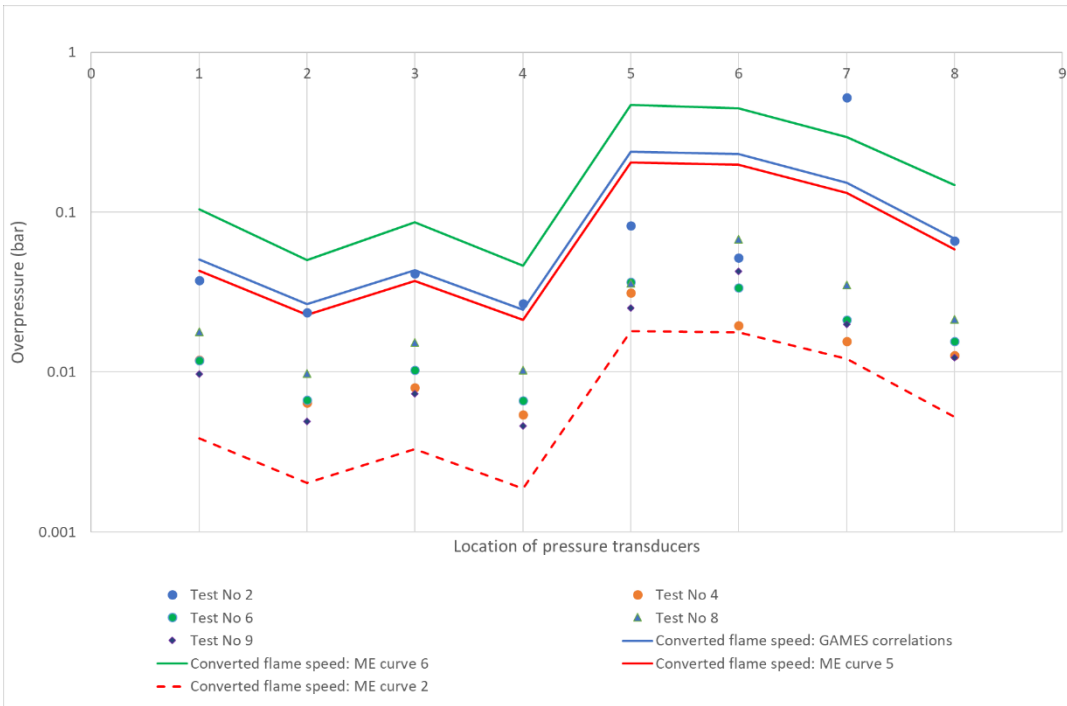


Figure 33 Comparing the measured and predicted overpressures for tests in Group 2 (1 bar tank pressure, 12mm nozzle, low congestion)

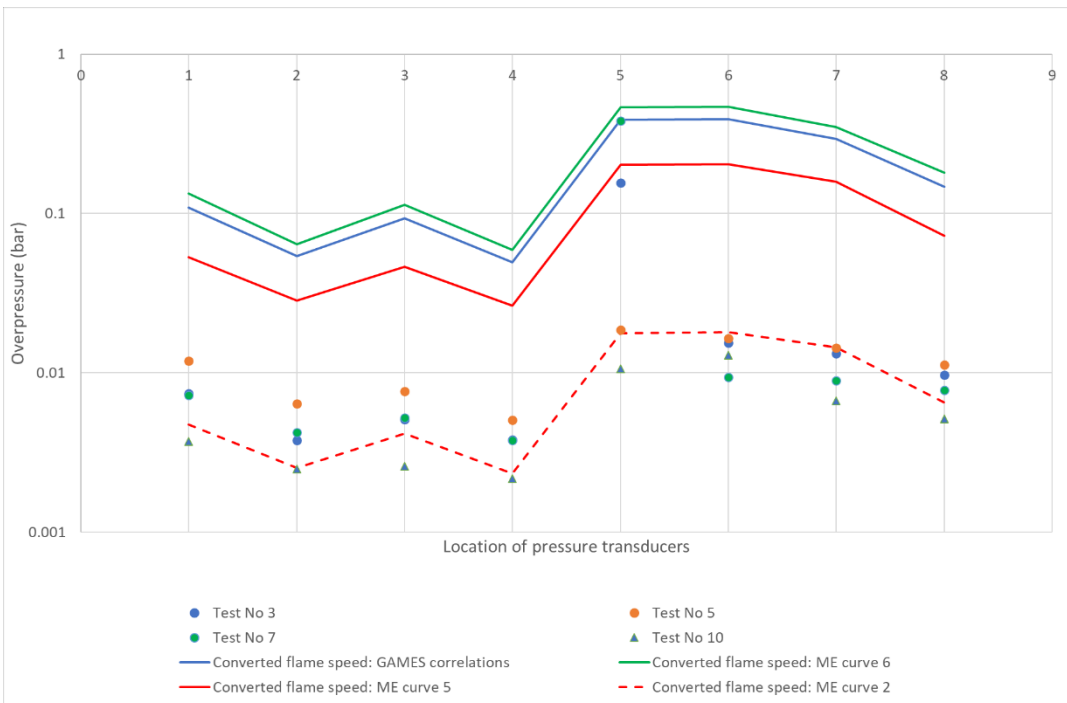


Figure 34 Comparing the measured and predicted overpressures for tests in Group 3 (1 bar tank pressure, 25.4mm nozzle, low congestion)

3.6.3.2 Tests with low congestion and high tank pressure (Groups 4-6)

Figure 35 - Figure 37 show the predicted explosions by the BST model for tests in groups 4-6, i.e. tank pressure of 5 bar and lower congestion, with flame speeds converted from peak overpressures of ME blast curves 5 & 6 or being calculated using the GAMES correlations developed for ME explosion model.

Observations of the results are:

- Test 18 in group 6 produced a very low peak overpressure and flash fire is the more likely event. However, explosion was observed under the same scenarios in test 19. When explosion occurs, predictions with converted flame speeds of ME curve 5 or of the calculated overpressure by the GAMES correlations are satisfactory as shown in Figure 37.
- BST predictions for tests in these groups have similar trends as for groups 1-3, apart from under-predictions at a few locations inside the congested region as shown in Figure 37.
- Flame speeds converted from peak overpressures estimated by the GAMES correlation seems suitable for tests in groups 4-6.

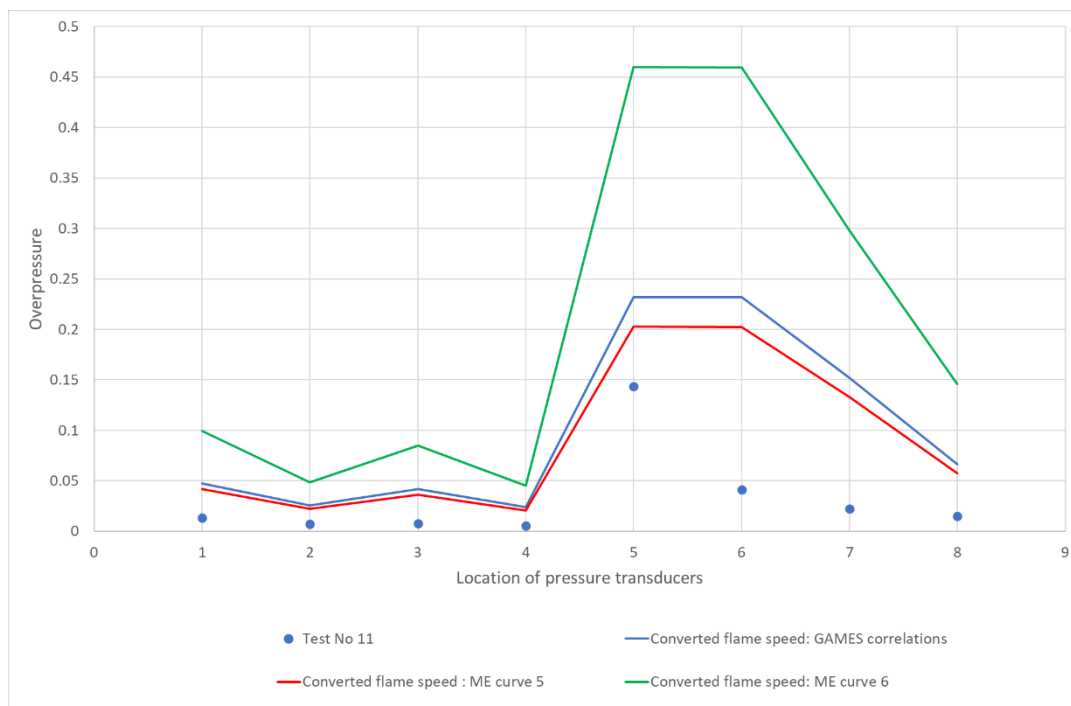


Figure 35 Comparing the measured and predicted overpressures for tests in Group 4 (5 bar tank pressure, 6mm nozzle, low congestion)

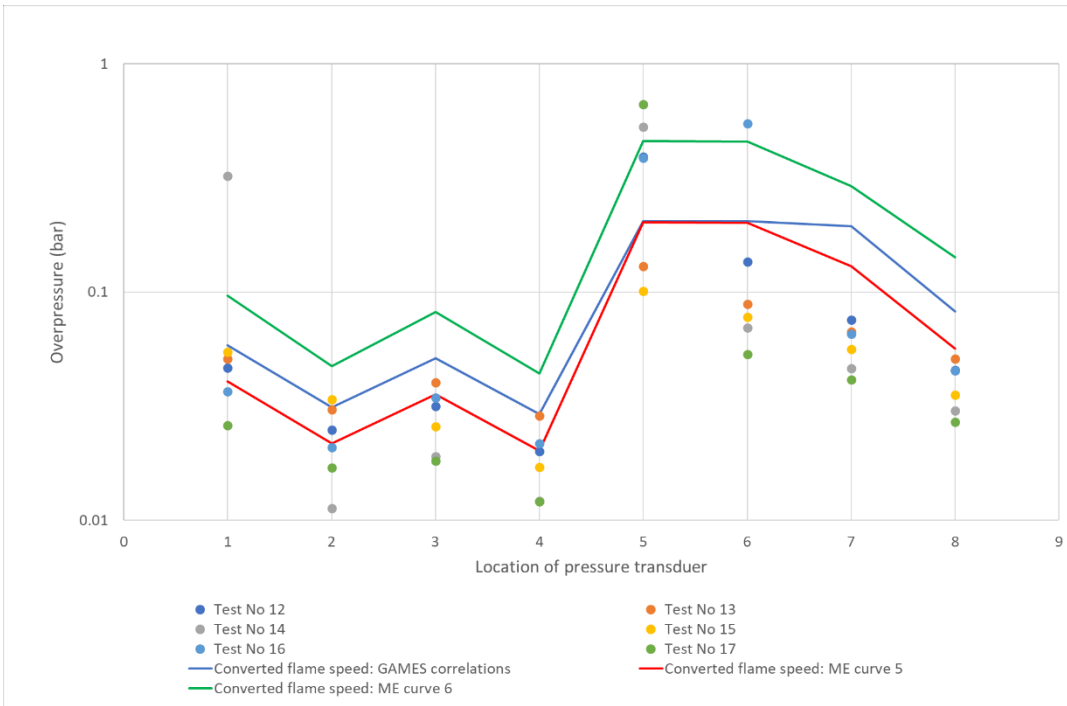


Figure 36 Comparing the measured and predicted overpressures for tests in Group 5 (5 bar tank pressure, 12mm nozzle, low congestion)

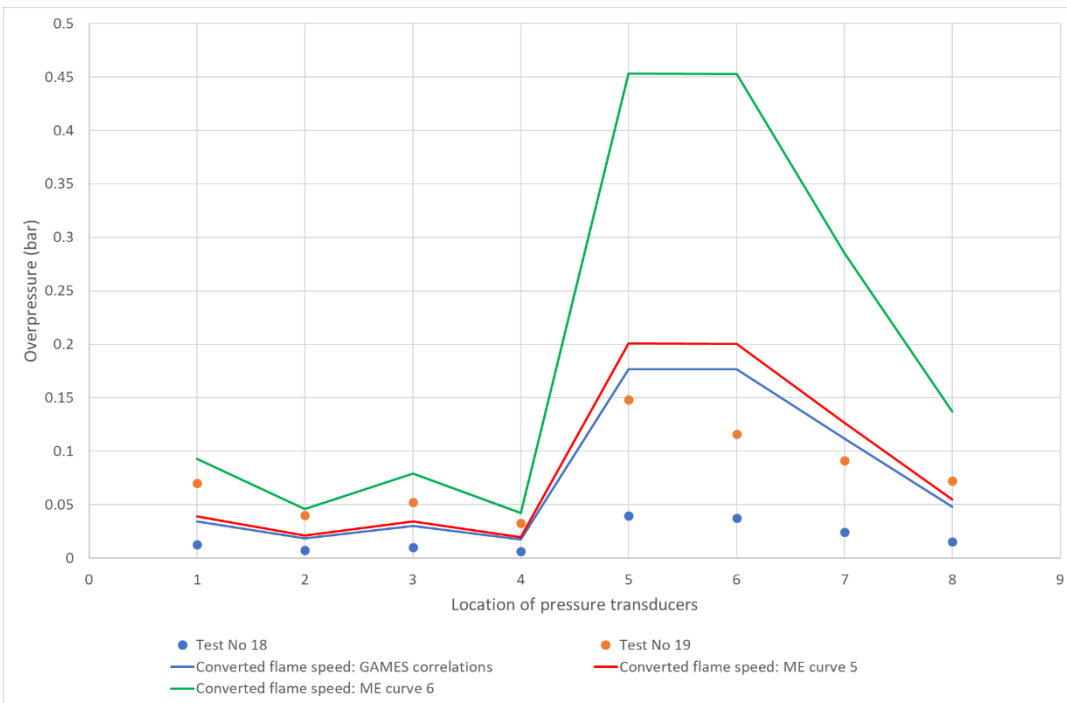


Figure 37 Comparing the measured and predicted overpressures for tests in Group 6 (5 bar tank pressure, 24.5mm nozzle, low congestion)

3.6.3.3 Tests with high congestion (tests in Groups 7 & 8)

Figure 38 and Figure 39 show the predicted results for tests in groups 7 and 8, i.e. the tests with high congestion as given in

| | | Low level of congestion | High level of congestion |
|---|-------------|-------------------------|--------------------------|
| Area blockage ratio (m ² /m ³) | Bottom half | 0.8 | 1.33 |
| | Top half | 1.0 | 1.53 |
| Volume blockage ratio (%) | Bottom half | 1.54 | 4.20 |
| | Top half | 1.93 | 4.60 |

Table 12 and shown in Figure 11. No ME blast curve is recommended from the PRESLHY report for explosions of these tests, a converted flame speed from ME blast curve 7 is used here as a reference here.

Observations of the results are:

- No significant explosion was observed in the test with a 6mm nozzle (i.e. test No 20), the measured explosion has a strength equivalent to converted flame speed of ME blast curve 2 as shown in Figure 38, a flash fire is the more likely event in this test.
- The converted flame speeds of ME blast curve 7 and of the calculated overpressure using the GAMES correlations have produced good predictions for tests 21 & 22. However, the same approach has produced significant under-prediction outside the congested region for test No 23 at transducers 1-4 & 8.
- The PRESLHY has suggested a high order of deflagration or detonation for test No 23, ME blast curves of 8-10 would be suitable for it and the whole cloud could have involved in explosion. So, explosion was also predicted using the DDT scenario of the BST model with the fill obstructed region first cloud method for this test. The fill obstructed region first cloud method has involved more flammable mass for the explosion than using UDM cloud. This approach has accurately predicted overpressures outside the congested region.
- When DDT occurs in an explosion, such as test No 23, flammable mass participating the explosion would be higher than that predicted by UDM in some cases, cloud method of either Cylinder cloud or Fill obstructed region first seems a better method to use.

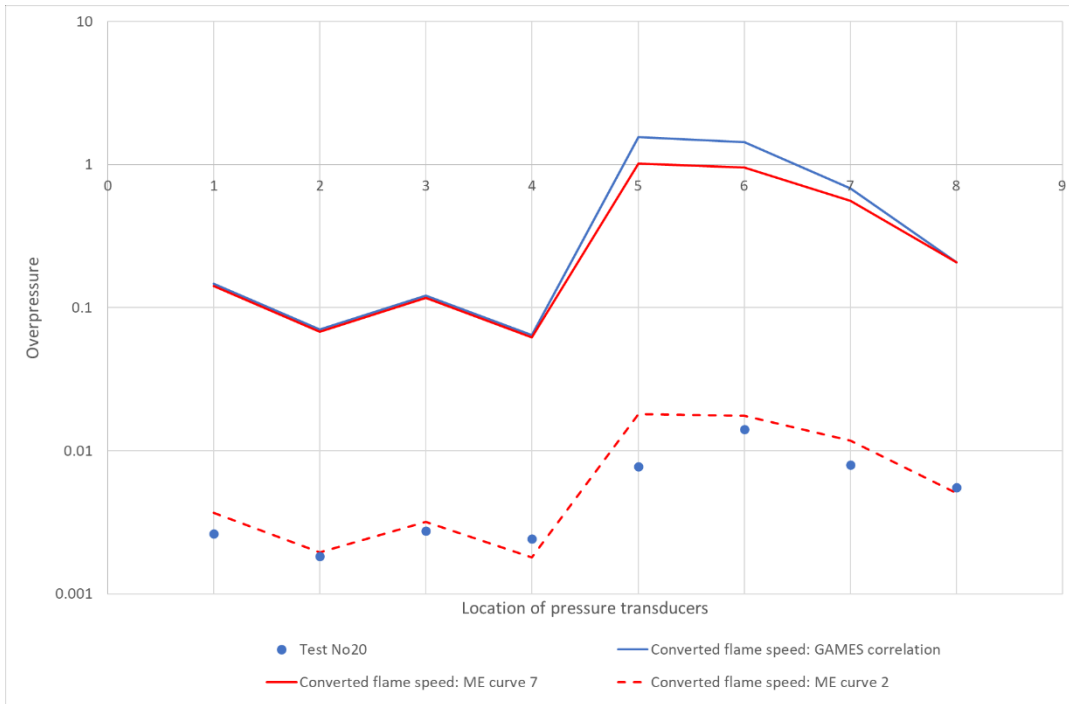


Figure 38 Comparing the measured and predicted overpressures tests in Group 7 (1 bar tank pressure, 6mm nozzle, high congestion)

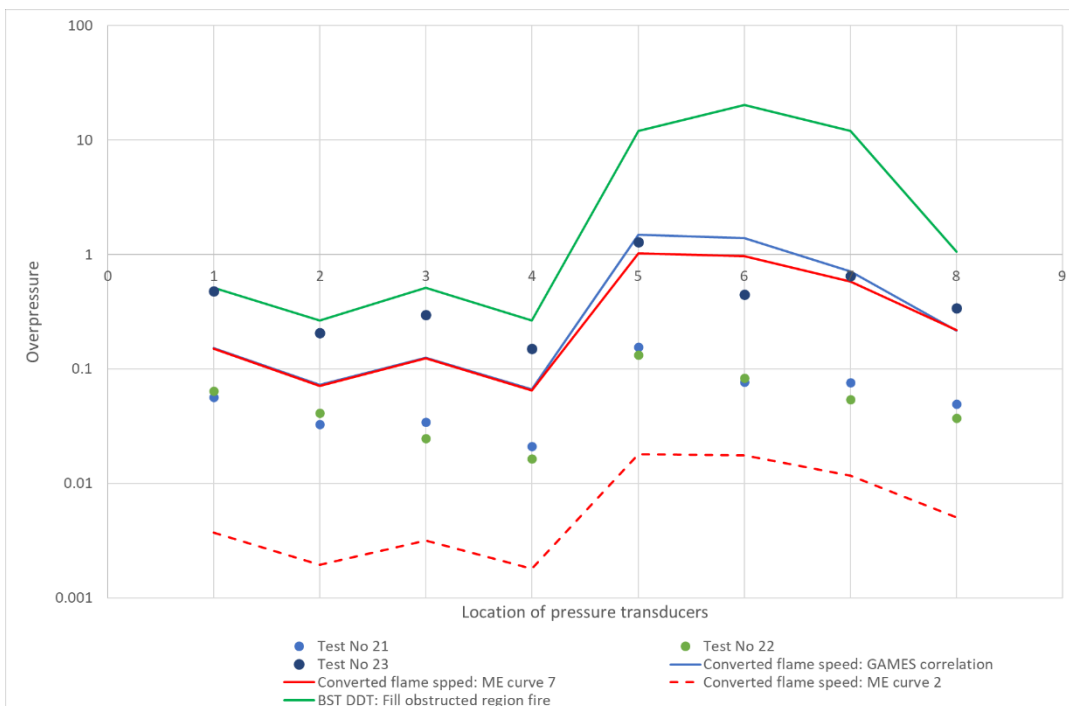


Figure 39 Comparing the measured and predicted overpressures tests in Group 8 (1 bar tank pressure, 12mm nozzle, high congestion)

3.7 Conclusions

PRESLHY, the European sponsored research project on safe use of liquid hydrogen, has carried out 23 tests on explosions from the releases of liquid hydrogen into two congested regions, i.e. low and high congestions. This validation work has assessed the predictions by the Multi-Energy model in Phast/Safeti against test results. Predictions of explosions by the Multi-Energy model are highly dependent on estimations of explosion strength and flammable mass participating the explosions. Modelling methods assessed include:

- Methods for explosion strength: defined explosion strength as recommended by PRESLHY report and calculated explosion strength using the GAMES correlations developed for the Multi-Energy method.
- Methods for predicting flammable cloud of a release: UDM, Cylinder cloud, Fill obstructed region first and KFX.

Delayed ignition of hydrogen releases in congested regions does not always producing meaningful explosion. Tests 1, 10, 18 & 20 have all produced very low peak overpressures and flash fires are the more likely events in these tests. As the result, explosions predicted by the Multi-energy model would be very conservative for these cases. However, when explosion occurs for similar cases instead of flash fire, predicted explosions are satisfactory.

The Multi-Energy model

For hydrogen explosions in congested region of low congestion (i.e. VBR < 1.5%), the recommended ME blast curve 5 by The PRESELHY report produces conservative predictions in general, with a few under-predictions of peak overpressure inside the congested region.

For hydrogen explosions in regions of high congestions (i.e. volume blockage ratio > 4.5%), high level explosion and possible DDT could occur, the explosion could involve all of the cloud. The PRESLHY report has not recommended any ME blast curve to use for these scenarios. The GAMES correlations developed for vapour cloud explosions of hydrocarbon releases have produced reasonable predictions for the tests and they could be used for hydrogen explosions in congested areas.

Explosions predicted using KFX clouds shows good trends for more accurate predictions.

The Baker-Strehlow-Tang model

Direct applying the BST methodology implies DDT for the PRESLHY tests and would lead to significant overpredictions. So, instead of applying the flame speed table directly, flame speeds of the tests are converted from ME blast curves recommended for the PRESLHY tests or from the peak overpressures calculated using the GAMES correlations.

Trends of the BST predictions are similar as the trends observed for the ME explosion model when converted flame speeds are applied.

The approach of using DDT scenario of the BST model and the fill-obstructed-region-first cloud method has accurately predicted overpressures outside the congested region for the test with observed DDT.

4 OBSERVATIONS

The following observations are made based on the validation results above:

- The ME model generally produces more conservative predictions in the near field of explosions compared with the BST model.
- The predictions by ME and BST are comparable in the far field and agree well with the measurements, particularly in the medium- and large-scale cases.
- The BST model with the ground correction method improves the consequence predictions for explosions on or near to the ground.
- Overall, predictions by the Multi-energy model have better agreement with measurements and much improved predictions have been obtained by BST with the ground correction methods.
- When using the GAME correlations to select blast curves for the Multi-energy model, the initial peak overpressure estimated by the correlations is very sensitive to VBR and flame path length of the obstructed regions defining explosions. It is important to create the obstructed regions accurately representing the congested area and to select a flame path length appropriate to the obstructed cloud and ignition.



5 RECOMMENDATIONS FOR FURTHER WORK

The Multi-energy and the Baker-Strehlow-Tang explosion models in OREM are based on published papers and guidance. These models have been implemented in previous releases (prior to v6.60 of Phast and Phast Risk) using a simplified approach which is effective for assessing the worst-case scenarios. OREM has extended these models to model obstructed regions and clouds directly as described in the theory document. The results of OREM are expected to be more realistic and to enable more effective measures to reduce and control plant risk.

Improving the model is an ongoing process determined by the user feedback. The model should be further validated when new data are obtained.

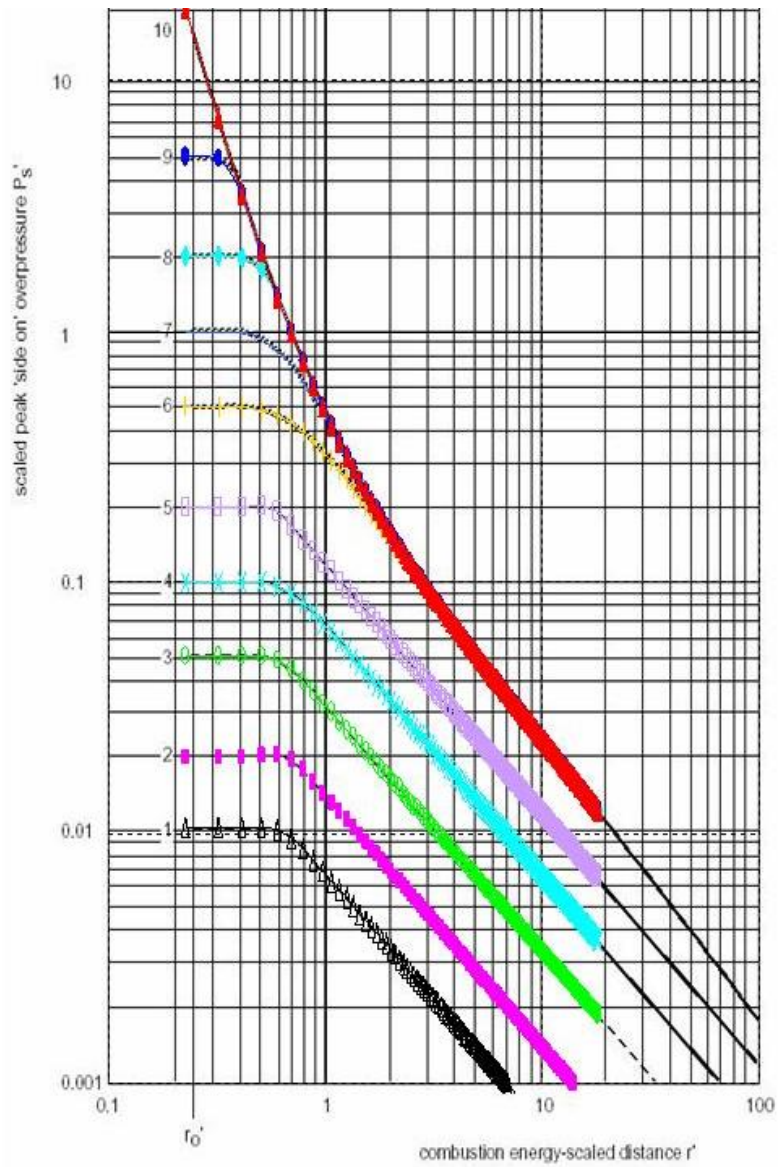


Figure 40 Charts of side-on peak overpressure as reproduced by ME (black lines: original blast curve; symbols: reproduced by ME)

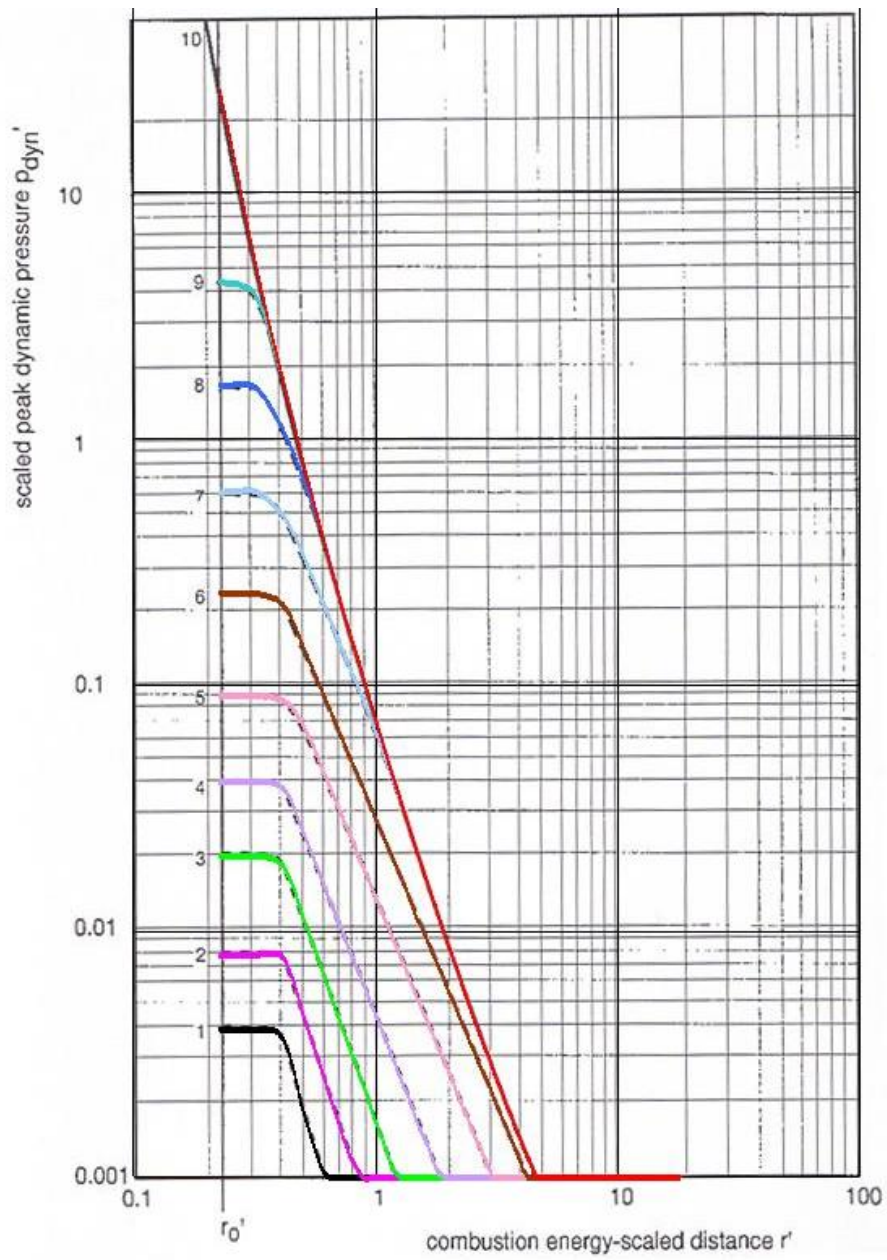


Figure 41 Charts of dynamic peak overpressure as reproduced by ME (black lines: original blast curve; colour lines: reproduced by ME)

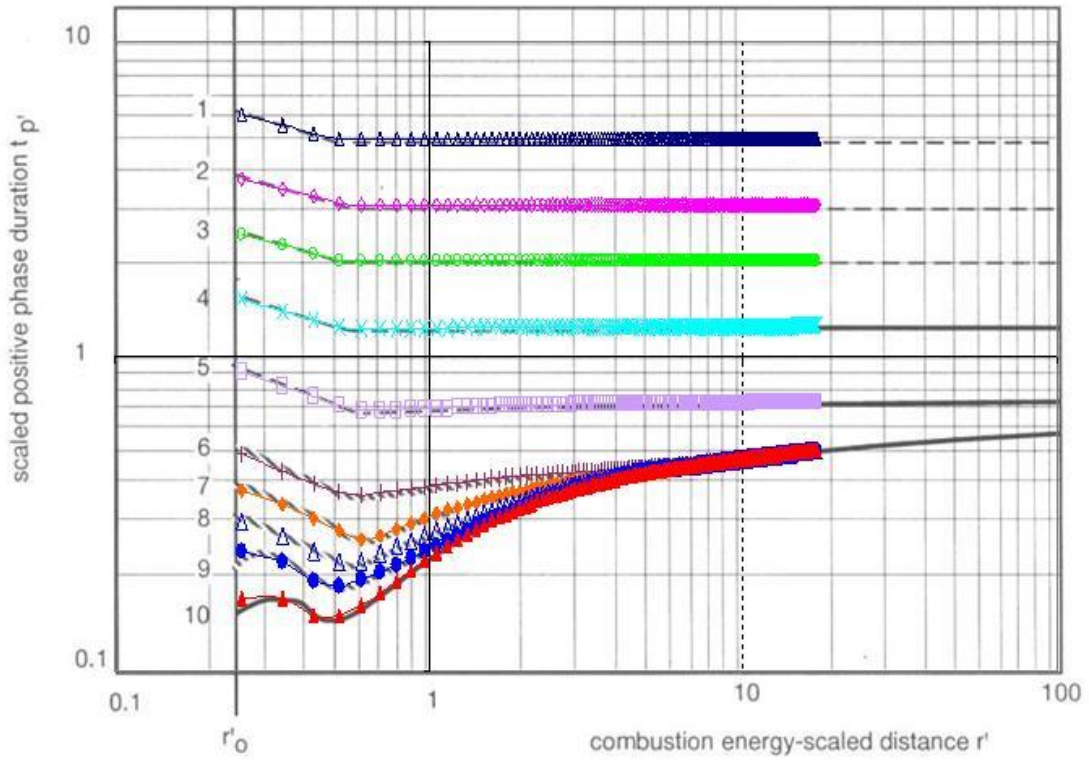


Figure 42 Charts of positive phase duration as reproduced by ME (black lines: original blast curve; symbols: reproduced by ME)

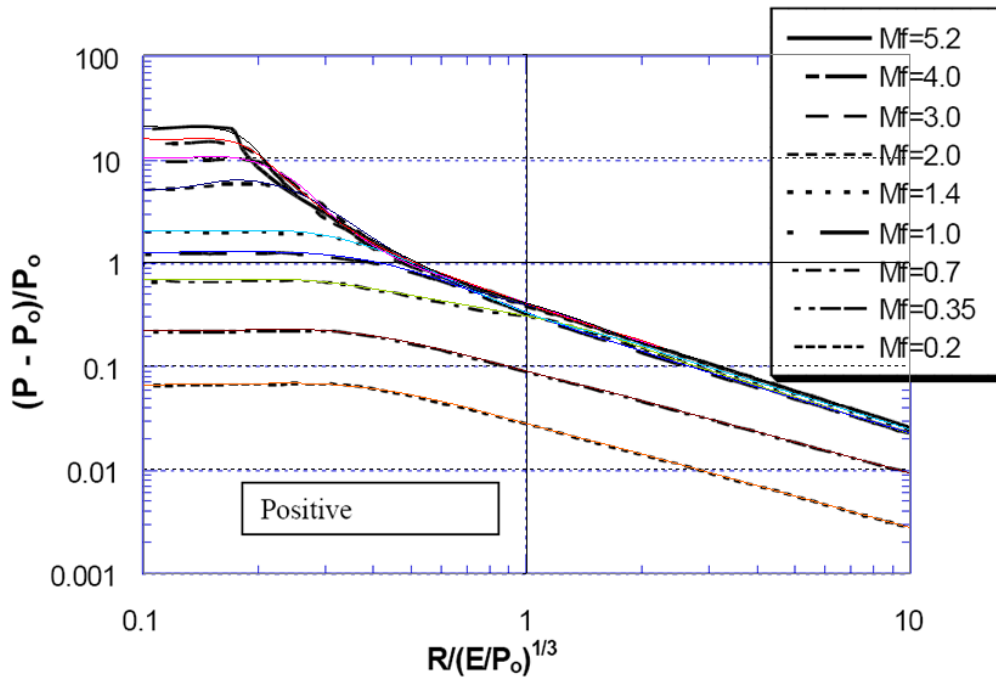


Figure 43 Charts of side-on peak overpressure as reproduced by BST (black lines: original blast curve; colour lines: reproduced by BST)

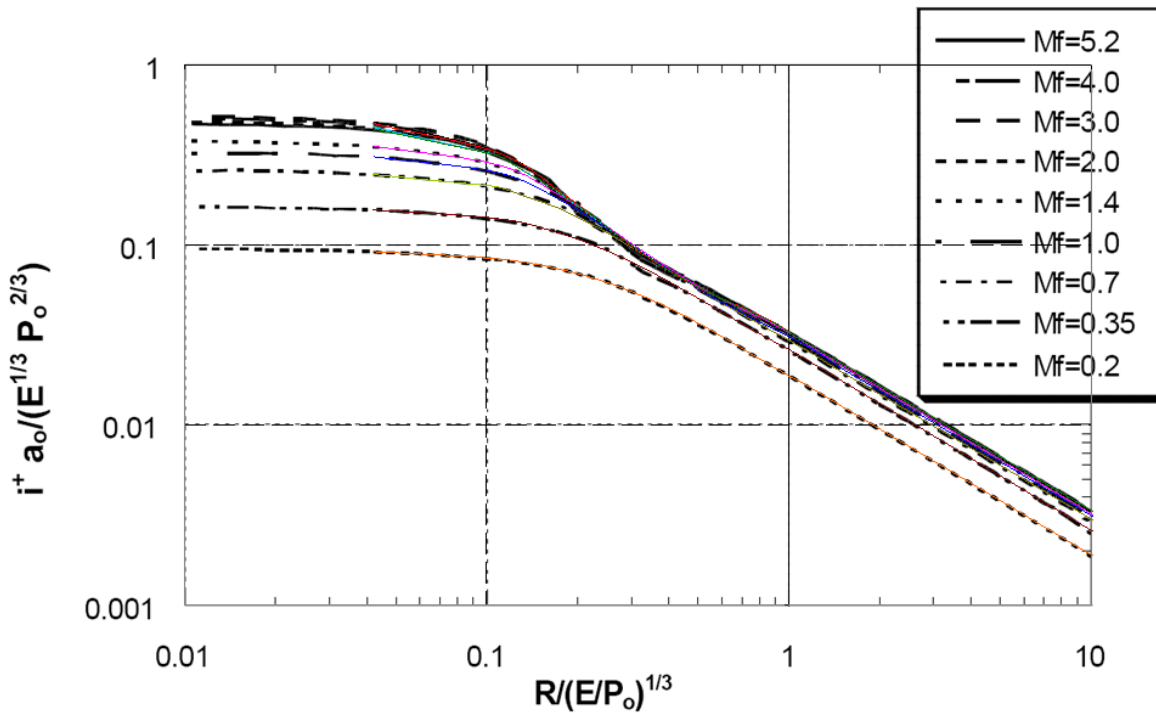


Figure 44 Charts of impulse as reproduced by BT (black lines: original blast curve; colour lines: reproduced by BST)

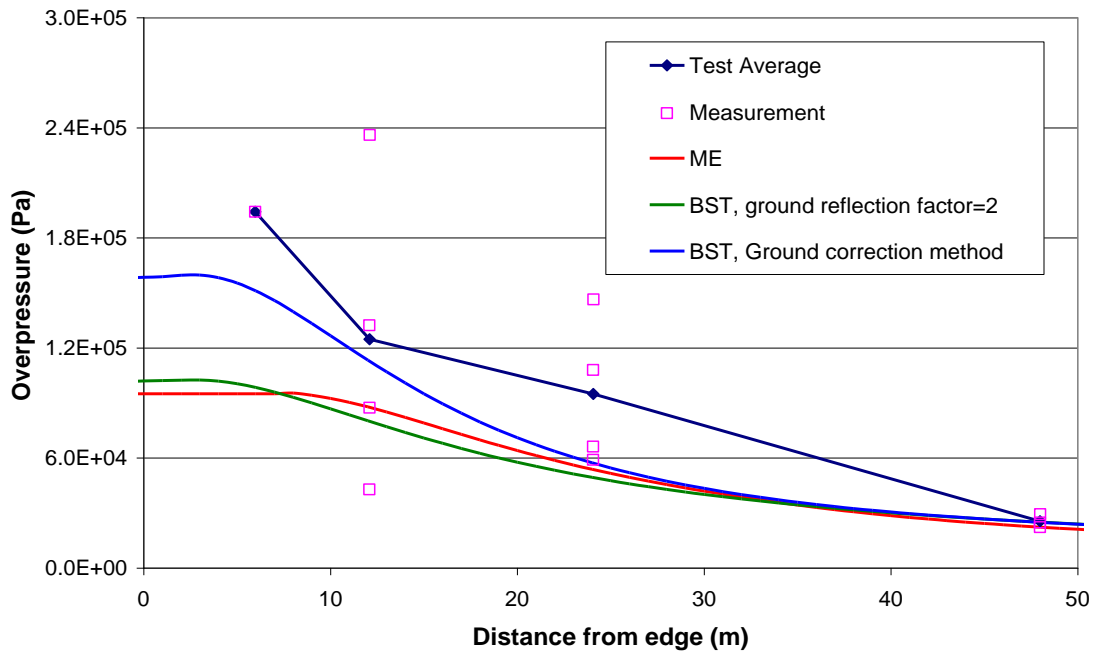


Figure 45 Plot of BFETS3a_A, 2D, high congestion, methane tests: measured, ME and BST predicted overpressures as a function of distance

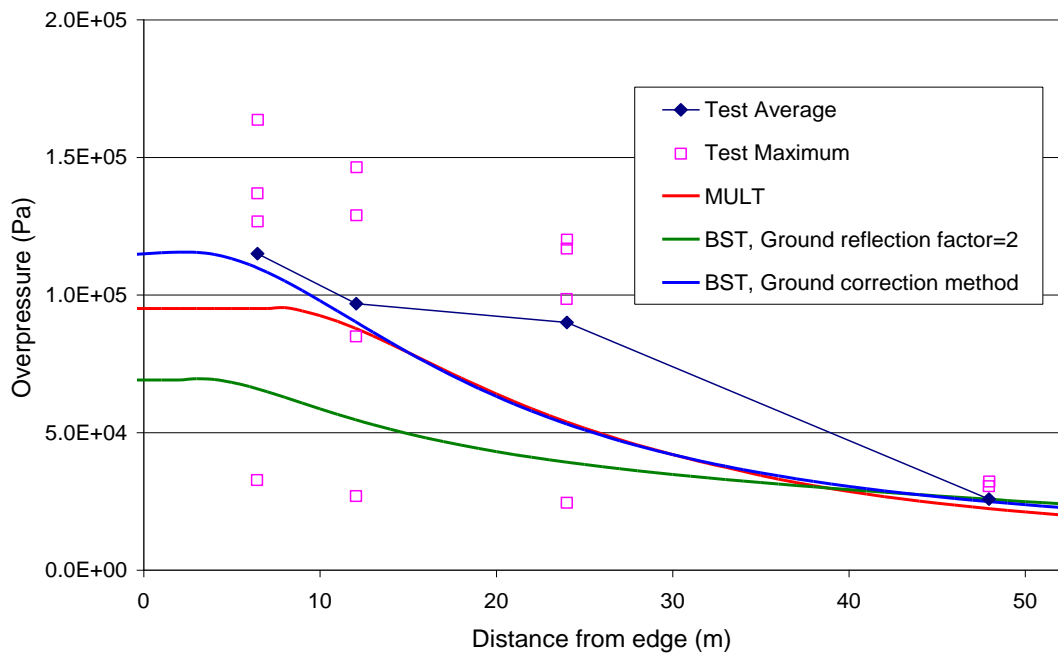


Figure 46 Plot of BFETS3a_B, 2.5D, high congestion, methane tests: measured, ME and BST predicted overpressures as a function of distance

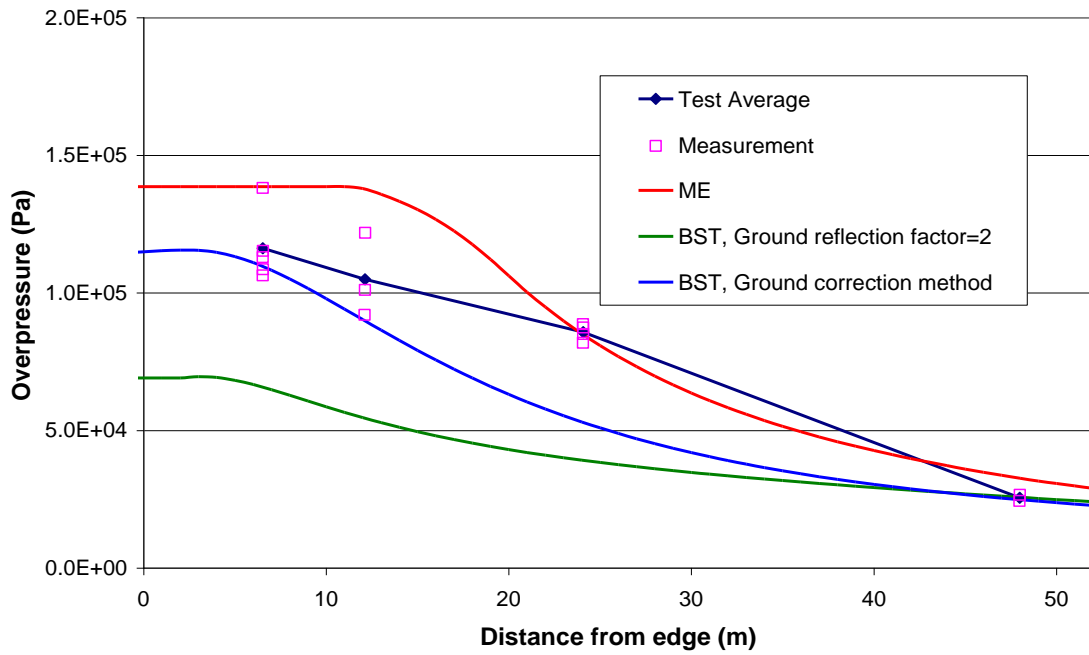


Figure 47 Plot of BFETS3a_C, 2.5D, high congestion, methane tests: measured, ME and BST predicted overpressures as a function of distance

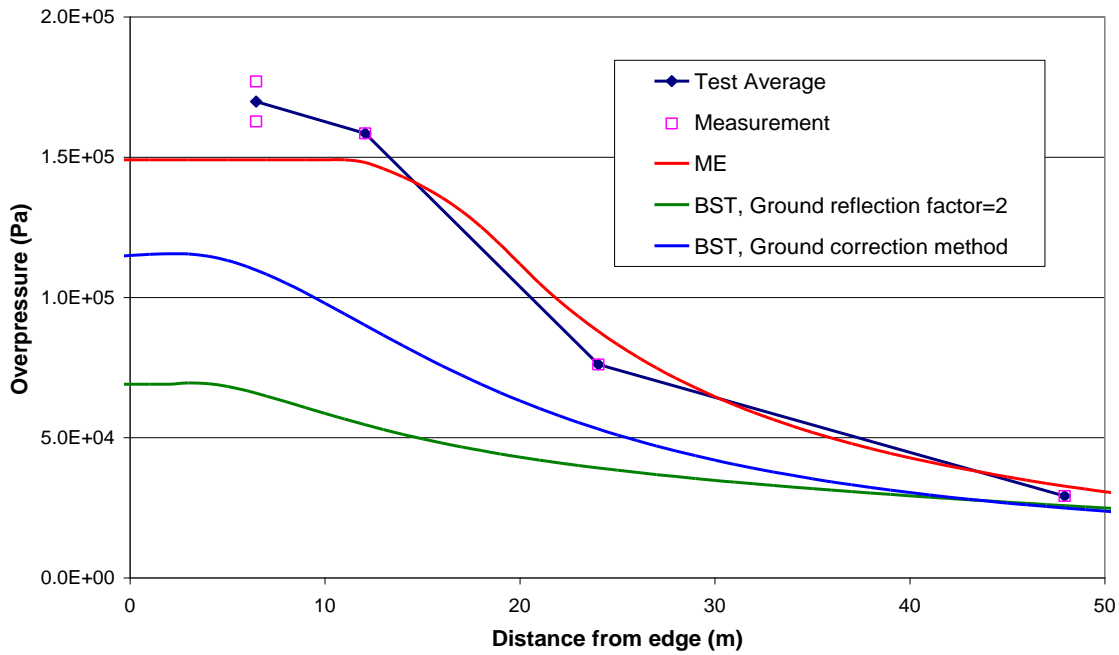


Figure 48 Plot of BFETS3a_D, 2.5D, high congestion, methane tests: measured, ME and BST predicted overpressures as a function of distance

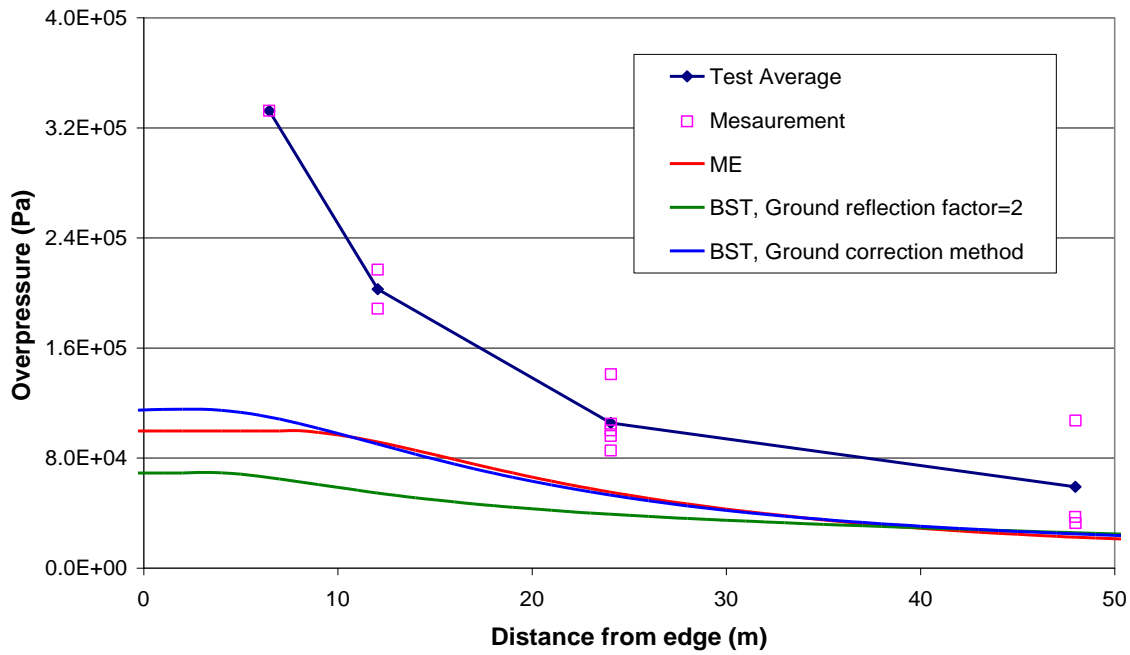


Figure 49 Plot of BFETS3a_E, 2.5D, high congestion, methane tests: measured, ME and BST predicted overpressures as a function of distance

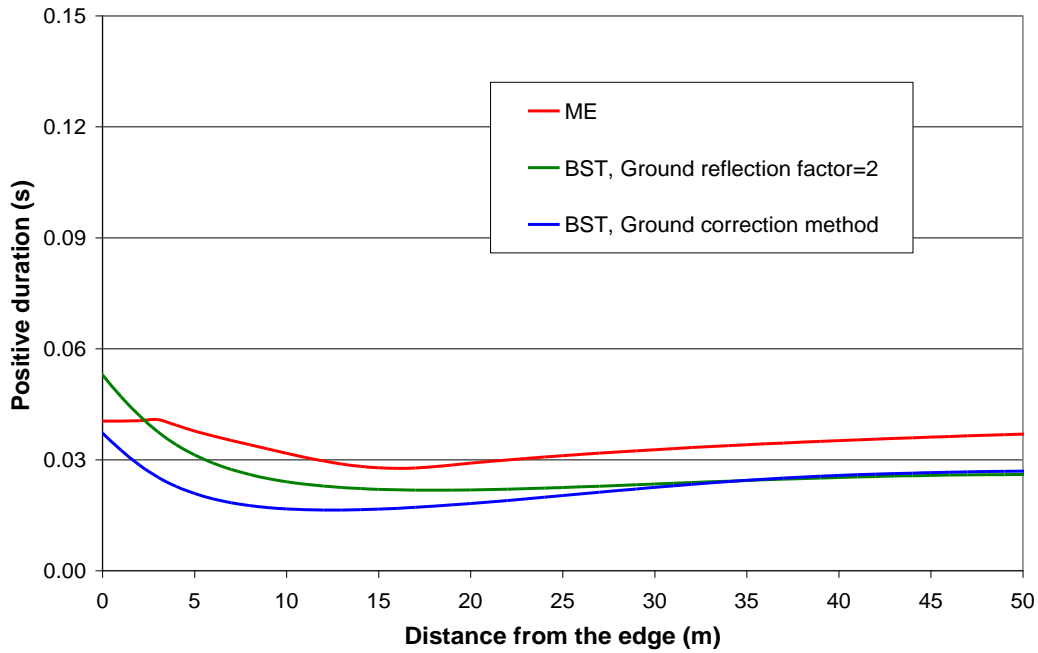


Figure 50 Plot of BFETS3a_A, 2D, high congestion, methane tests: ME and BST predicted positive duration as a function of distance

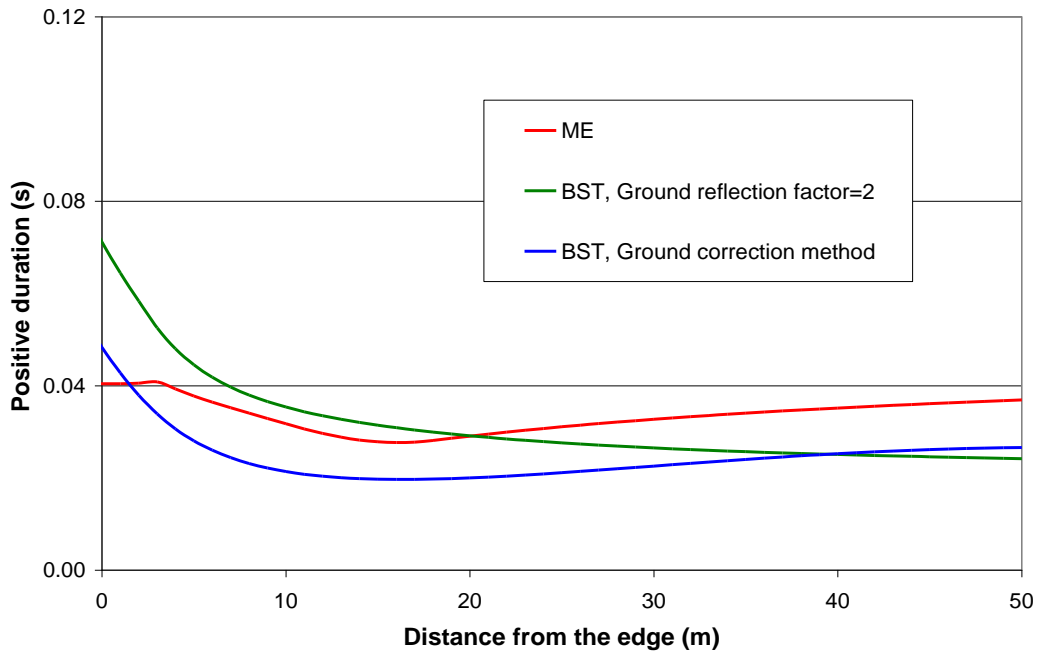


Figure 51 Plot of BFETS3a_B, 2.5D, high congestion, methane tests: ME and BST predicted positive duration as a function of distance

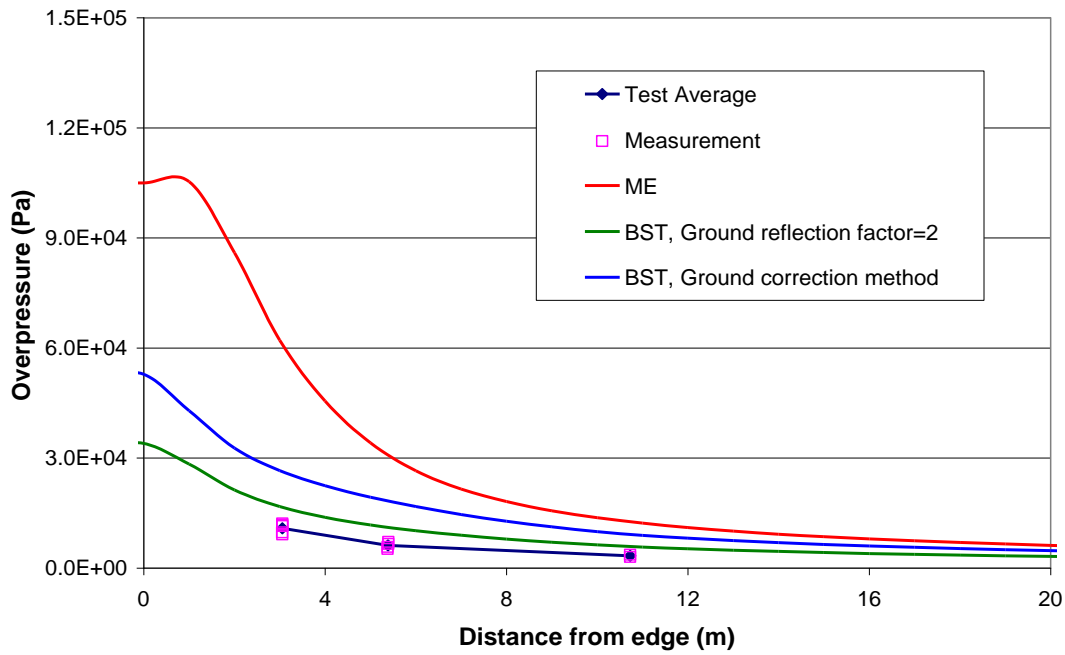


Figure 52 Plot of EMERGE_1, small scale, 3D, high congestion, methane tests: measured, ME and BST predicted overpressures as a function of distance

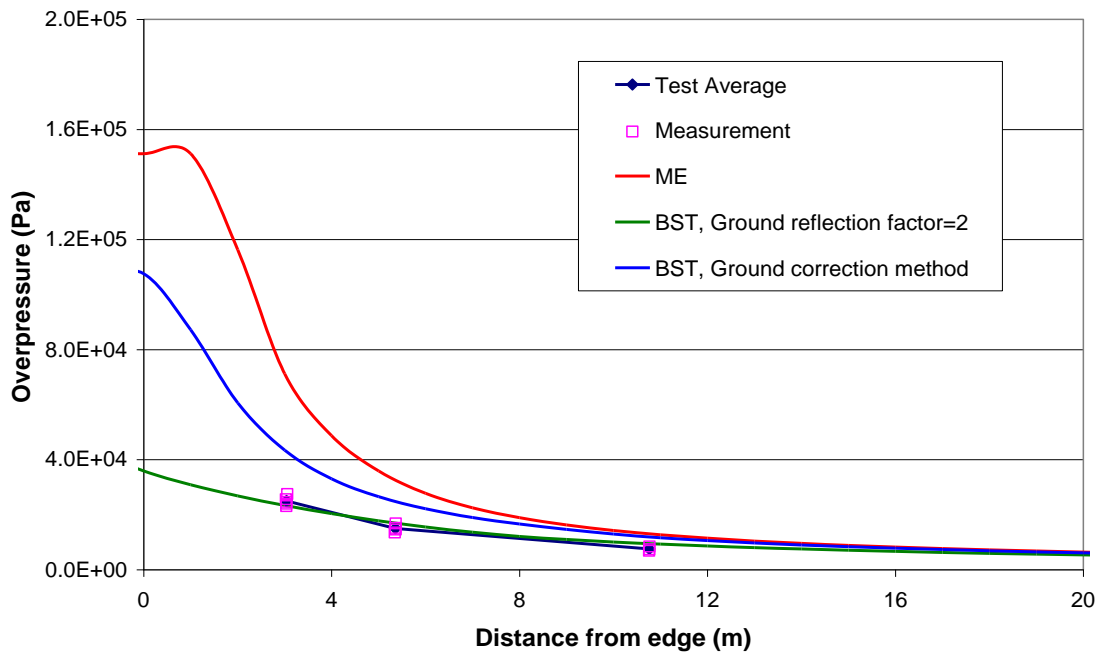


Figure 53 Plot of EMERGE_2, small scale, 3D, high congestion, propane tests: measured, ME and BST predicted overpressures as a function of distance

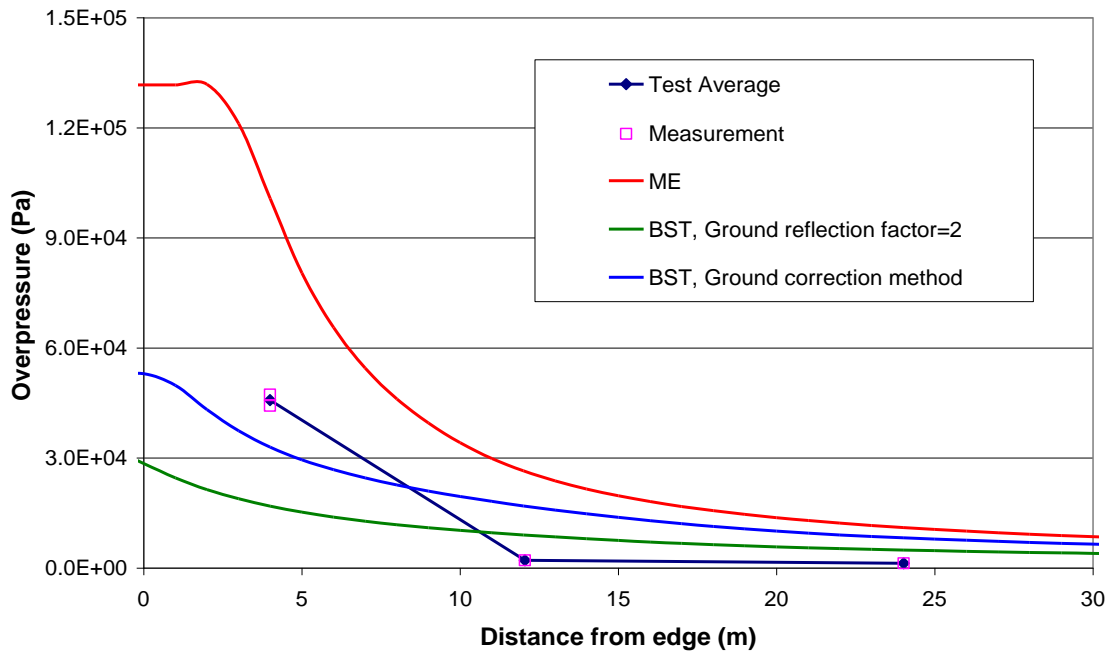


Figure 54 Plot of EMERGE_3, medium scale, 3D, high congestion, methane tests: measured, ME and BST predicted overpressures as a function of distance

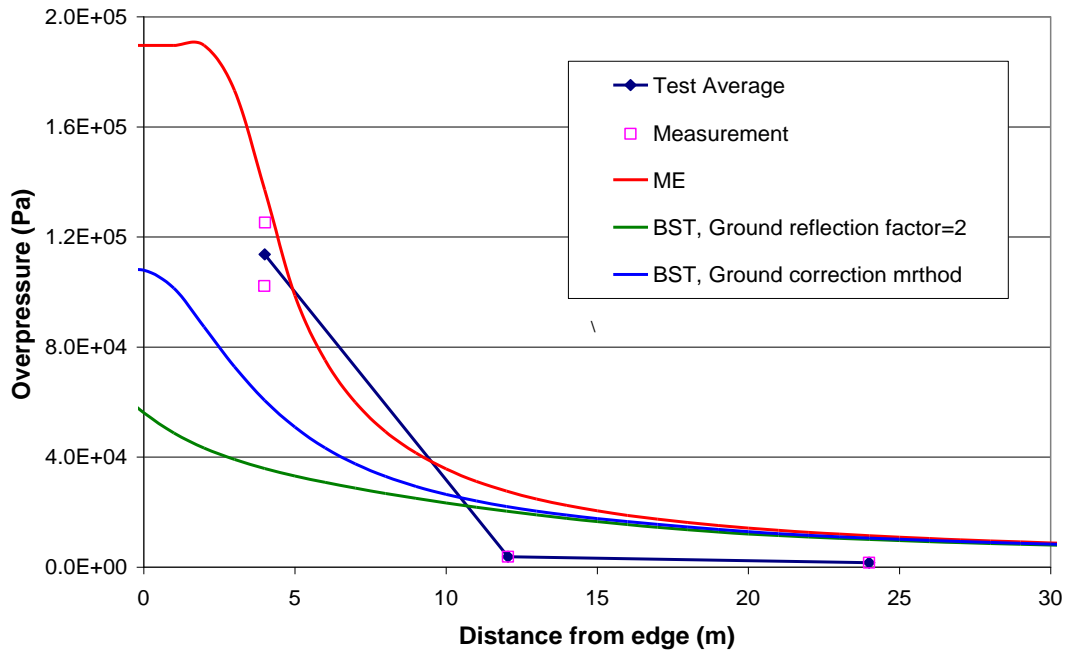


Figure 55 Plot of EMERGE_4, medium scale, 3D, high congestion, propane tests: measured, ME and BST predicted overpressures as a function of distance

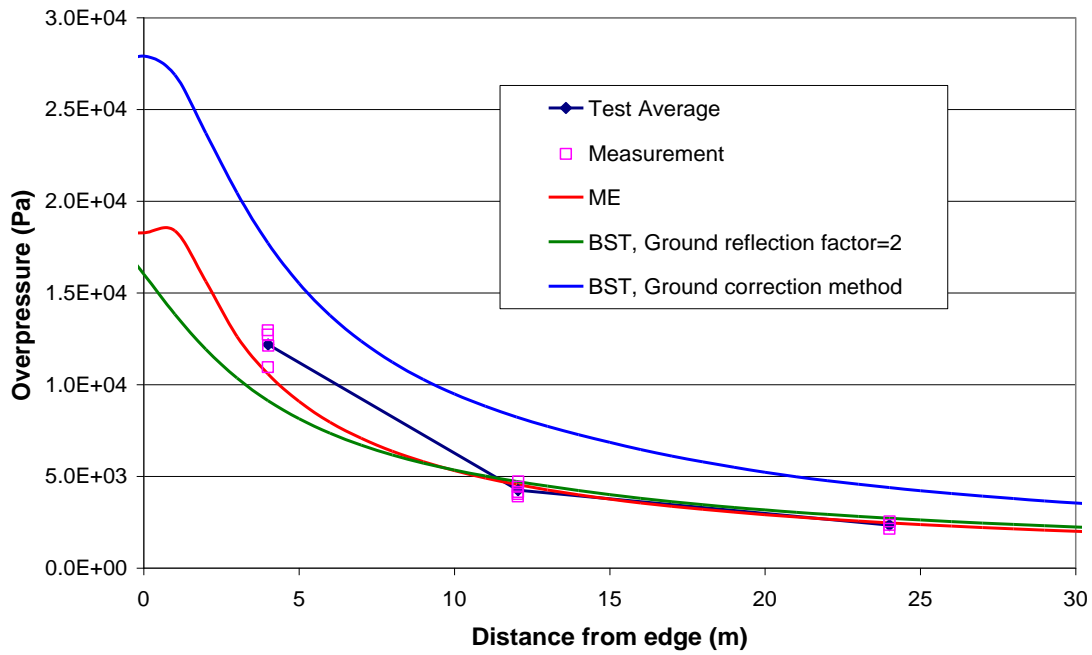


Figure 56 Plot of EMERGE_5, medium scale, 3D, medium congestion, methane tests: measured, ME and BST predicted overpressures as a function of distance

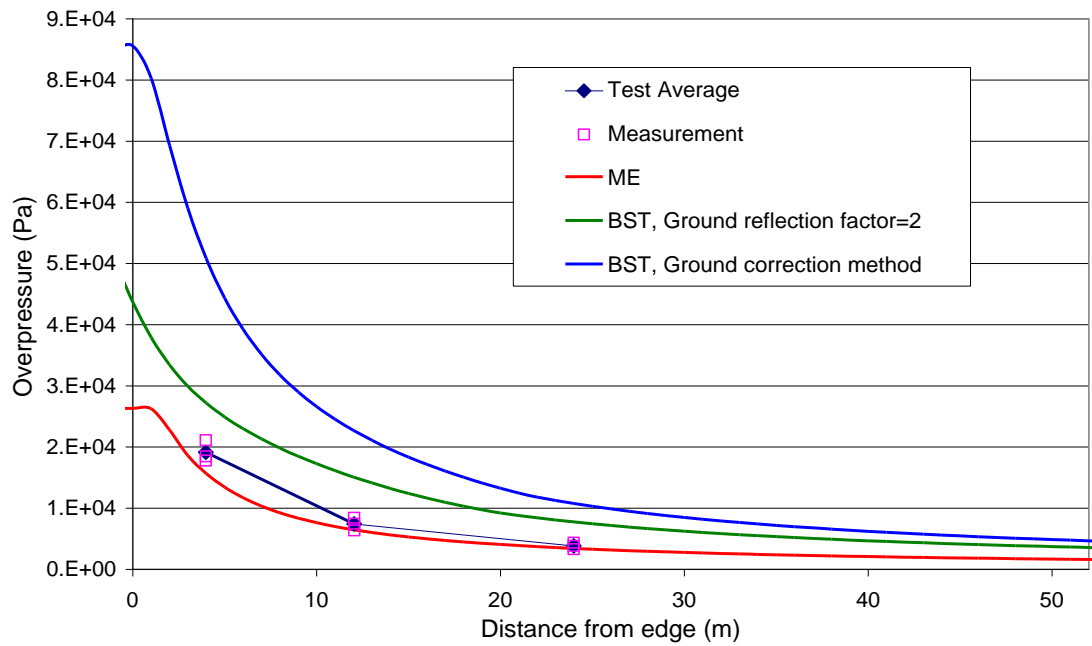


Figure 57 Plot of EMERGE_6, medium scale, 3D, medium congestion, propane tests: measured, ME and BST predicted overpressures as a function of distance

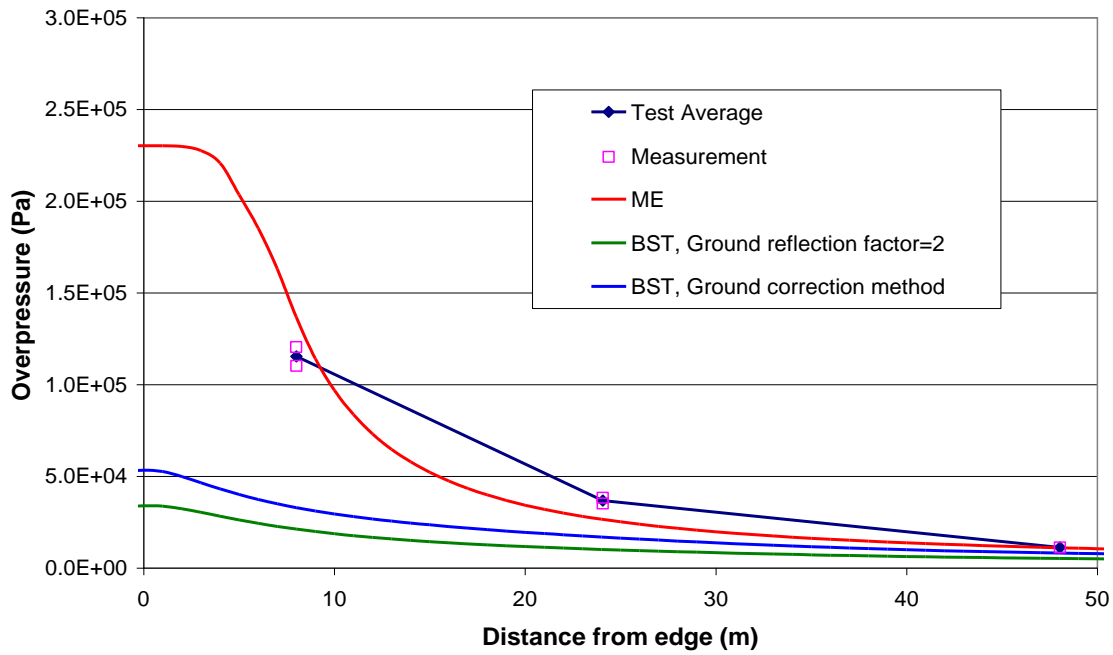


Figure 58 Plot of EMERGE_7, large scale, 3D, medium congestion, methane tests: measured, ME and BST predicted overpressures as a function of distance

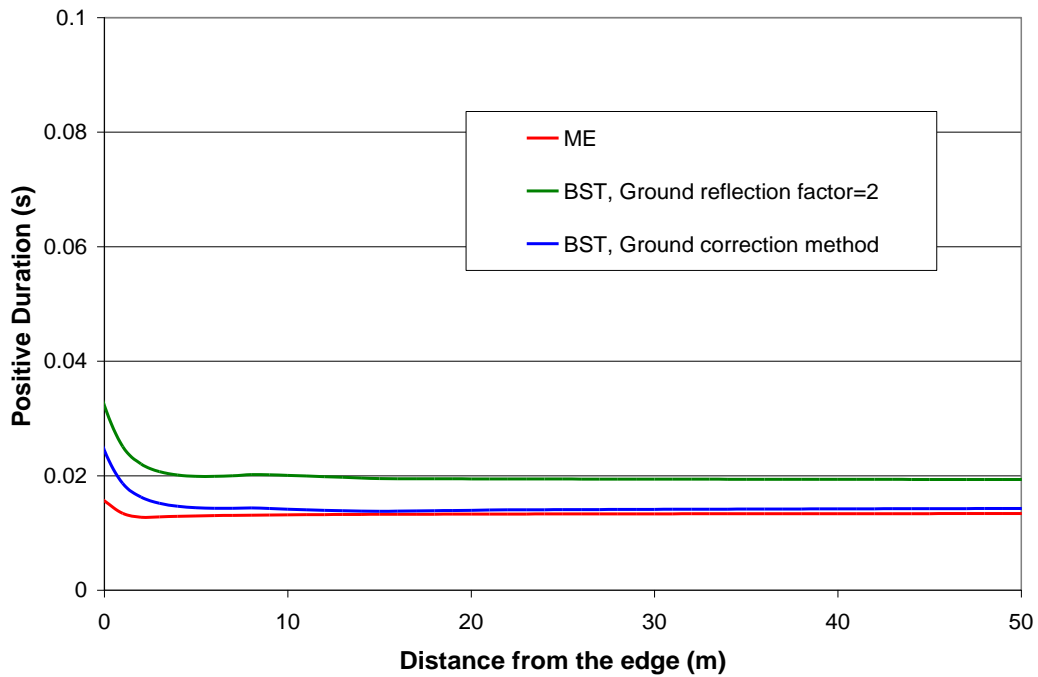


Figure 59 Comparing the predicted positive phase durations by ME and BST as a function of distance: EMERGE_5, medium scale, 3D, medium congestion & methane

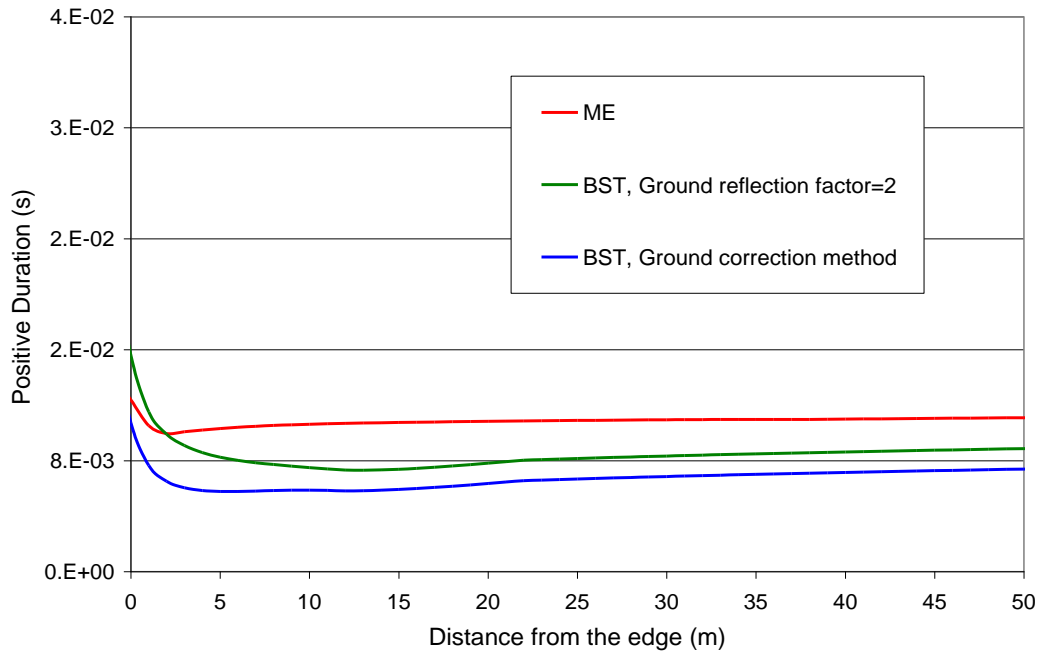


Figure 60 Comparing the predicted positive phase durations by ME and BST as a function of distance: EMERGE_6, medium scale, 3D, medium congestion & propane

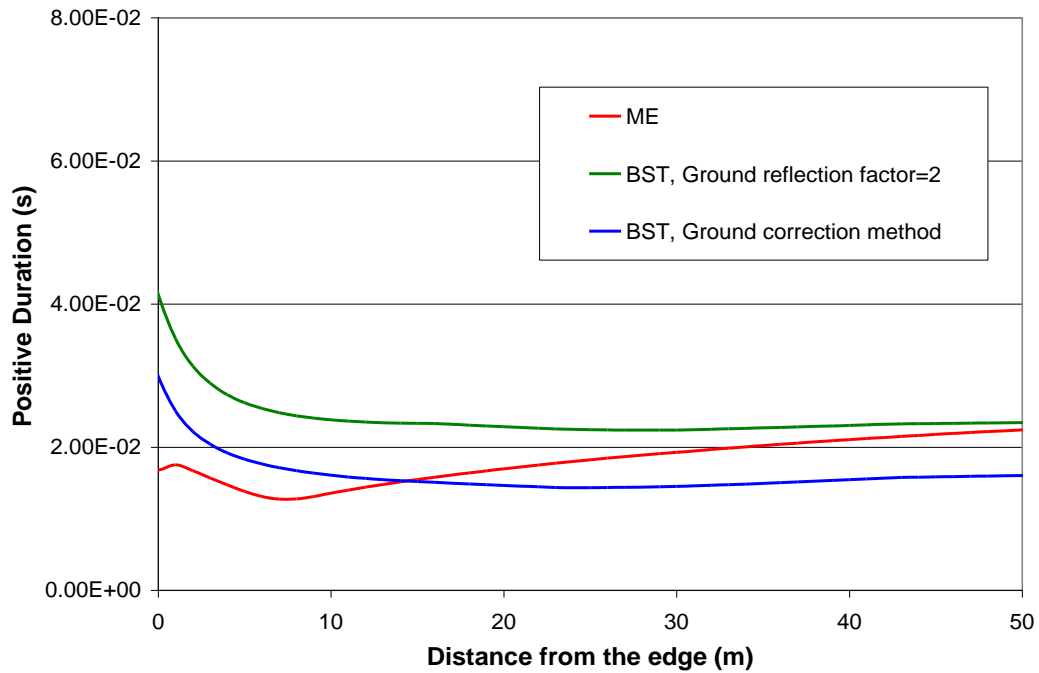


Figure 61 Comparing the predicted positive phase durations by ME and BST as a function of distance: EMERGE_7, large scale, 3D, medium congestion & methane

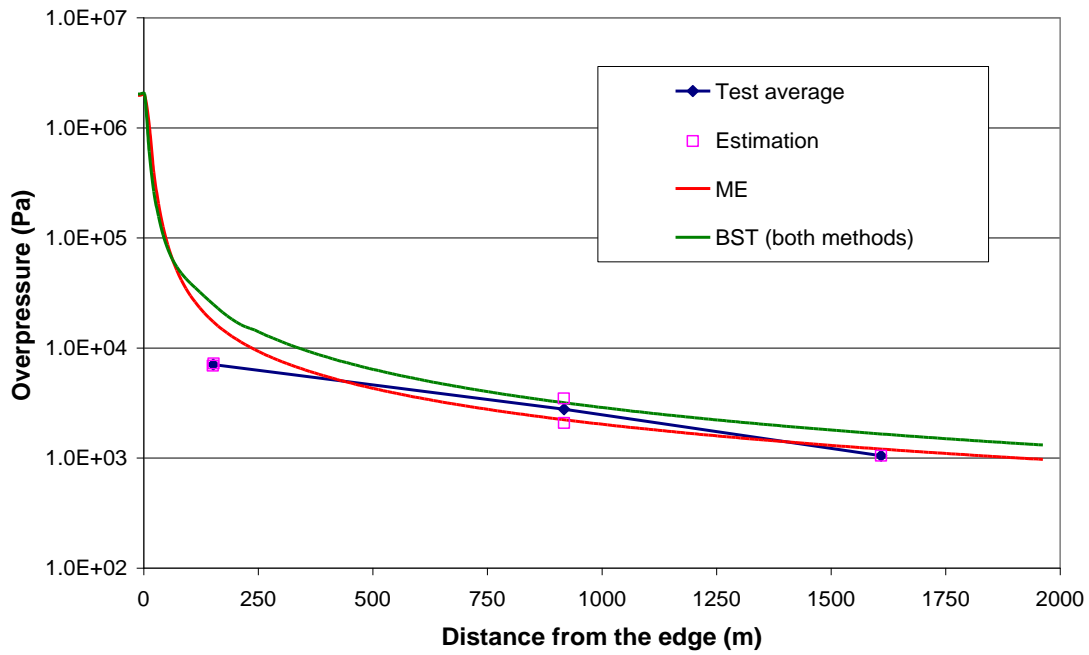


Figure 62 Plot of the Shell Deer Park, large scale, 2.5D, High congestion, ethylene tests: measured, ME and BST predicted overpressures as a function of distance

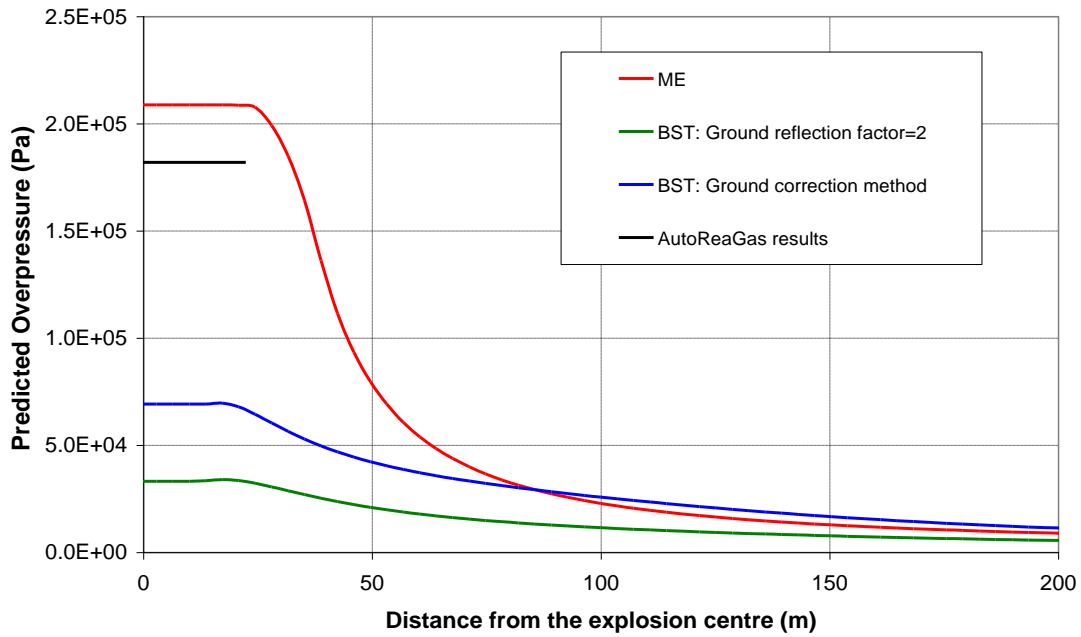


Figure 63 Comparing the predicted overpressures of ME and BST with the predictions by AutoReaGas for the chemical plant case of the GAMES report¹

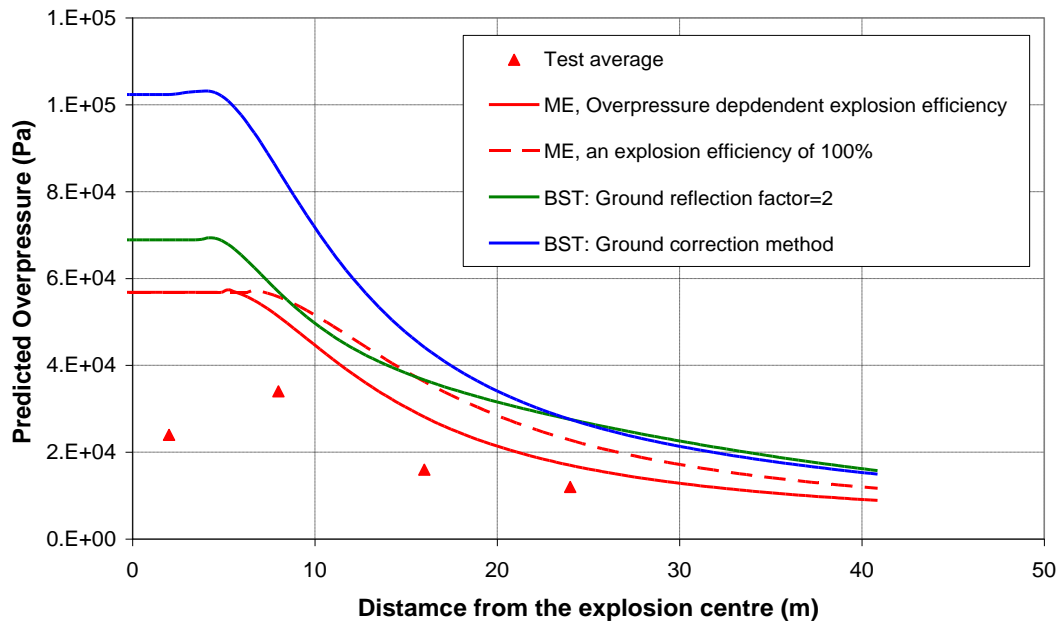


Figure 64 Comparing the predicted overpressures of ME and BST with measurements and predictions by AutoReaGas for the gas processing case of the GAMES report¹

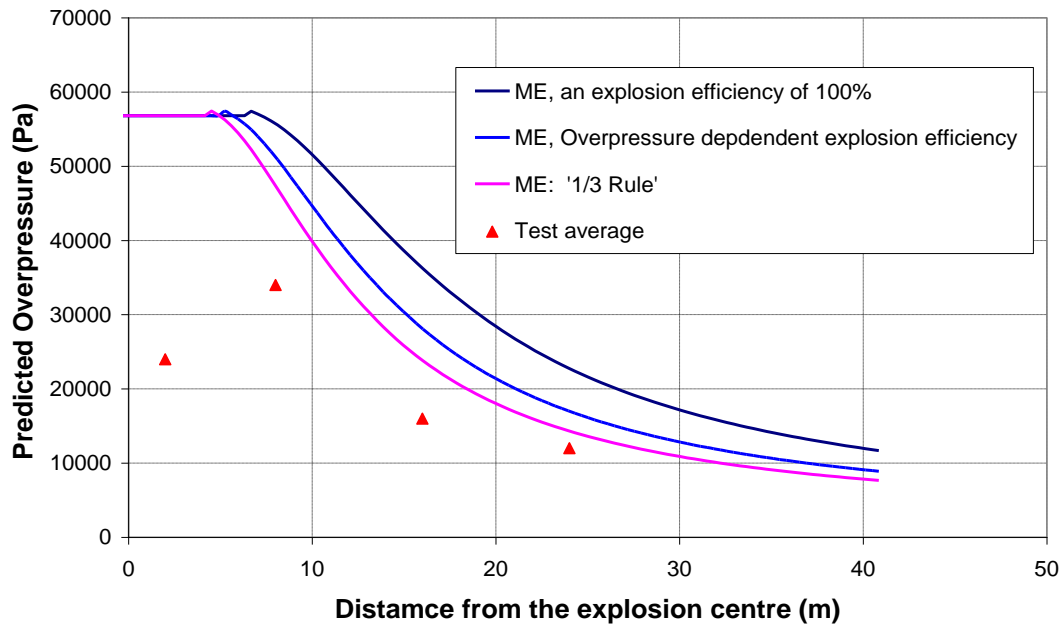


Figure 65 Validating the "1/3 Rule" for the Gas Processing case of the GAMES study: fully filled obstructed regions

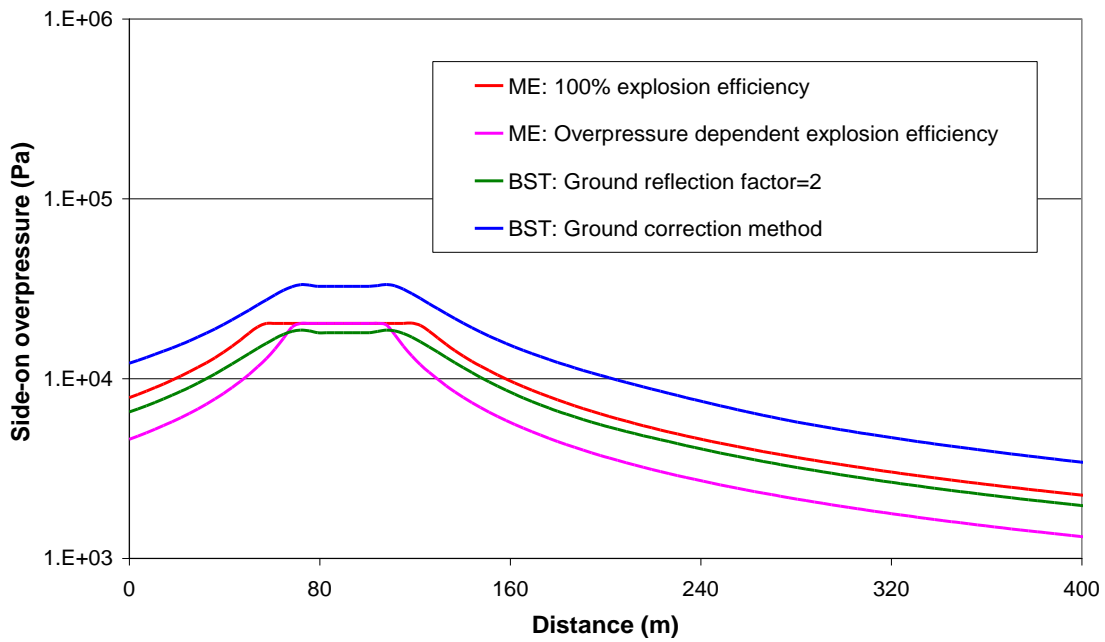


Figure 66 Comparing the predicted overpressures on a transect along OSR1, OSR2 & OSR-5 by ME and BST for Case 3 of the LNG Terminal of the GAMES report¹

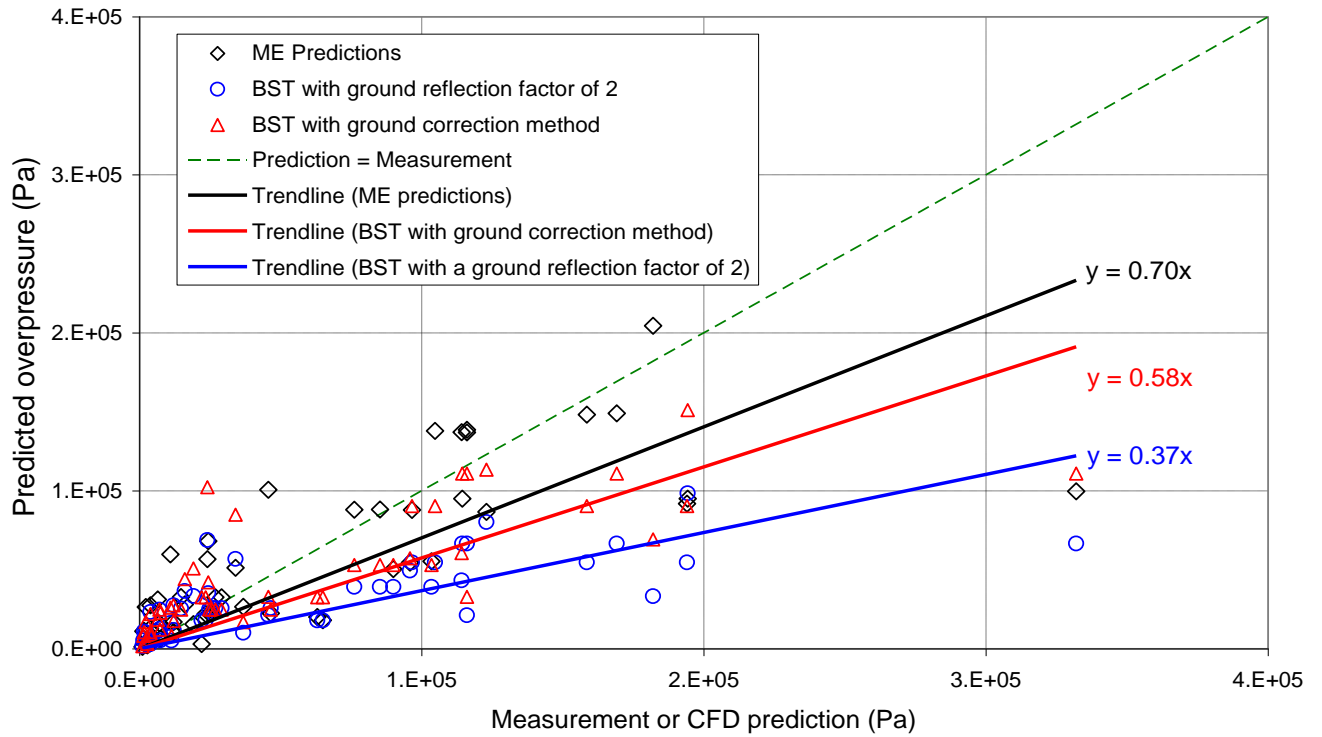


Figure 67 Comparing overpressure predictions of ME and BST models in Phast Risk against measurements and CFD predictions (all cases)

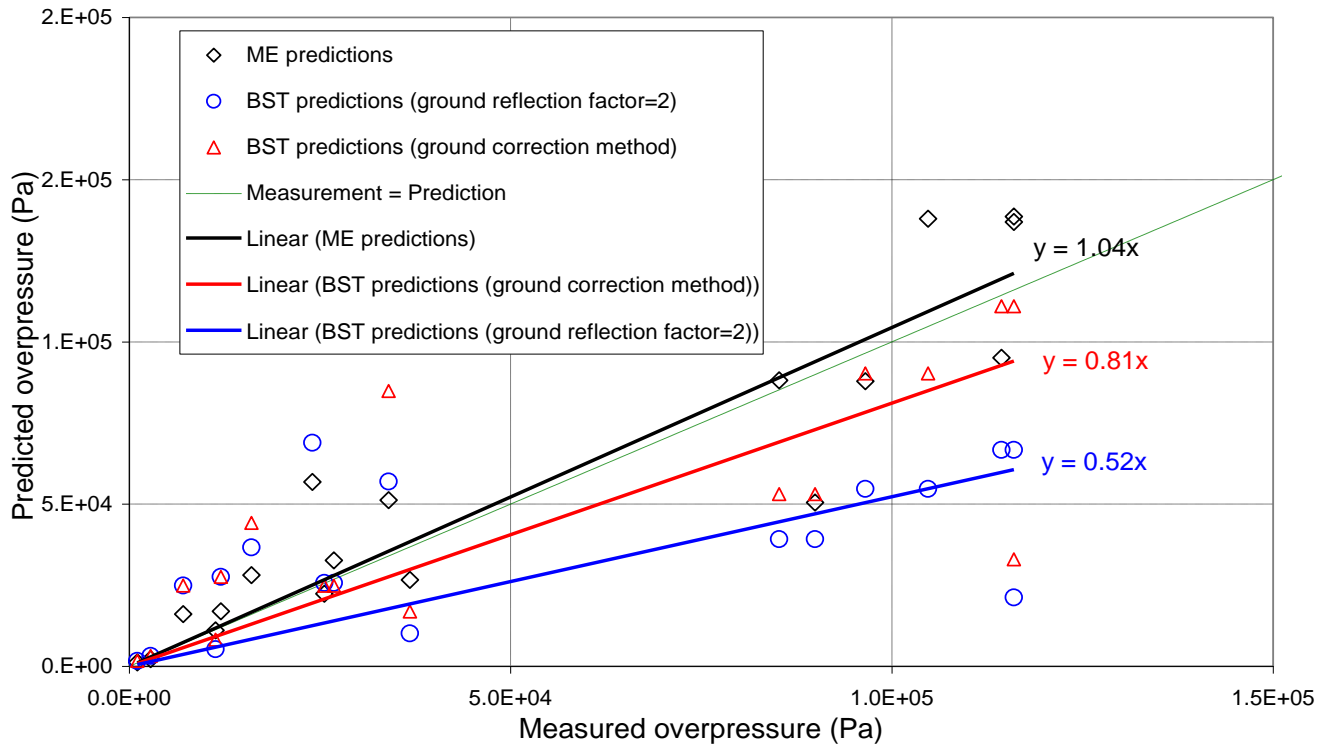


Figure 68 Comparing the overpressure predictions of ME and BST models in Phast Risk against measurements (selected cases)

GLOSSARY

“1/3 Rule”

A simple rule which states that, for explosions from a flammable cloud filling a compartment, the explosion overpressure of a filling ratio 1/3 (i.e. one third of the compartment is filled with flammable cloud) is the same as that when the compartment is fully filled.

ABR

Area blockage ratio in the flame path

AutoReaGas

A CFD model developed by Century Dynamics and TNO for explosion modelling

BFETS

Acronym for a joint industry project on Blast and Fire Engineering for Topside Structures.

Blast curve

The normalised curves describing the change of peak overpressure, duration or impulse against distance for idealised explosion scenarios. The Multi-energy and the BST models each come with a set of blast curves.

BST

The Baker-Strehlow-Tang model implemented in OREM of Phast Risk v6.60. It applies the Baker-Strehlow-Tang methodology with enhanced functionality and GUI for QRA studies

Calculated Flame Speed Obstruction

Obstructed region with a given set of parameters which are used to determine the blast curve for confined explosions formed by it using the flame speed table for the BST model.

Calculated Strength obstruction

Obstructed region with a given set of parameters which are used to determine the blast curve for confined explosions formed in it using the GAME correlations.

CFD

Computational Fluid Dynamics

Cloud View

The geometry of a cloud at a particular time

Confined explosion

Explosion occurring inside obstructed regions

Congestion level

A measure of the congestion affecting flame propagation in an obstructed region in the BST methodology. It is classified as low, medium and high depending on area blockage ratio (ABR) and pitch (i.e. the distance between successive rows of obstacles) in the flame path

Critical separation distance

The maximum separation distance at which the blast waves from donor and acceptor were found to coincide

Cylinder Cloud

A simple model implemented in Phast Risk for flammable clouds released inside obstructed regions. It assumes a cylinder shape for the flammable cloud around the release point for more conservative consequence and risk predictions and is considered suitable for low-momentum releases in densely congested areas

Defined strength obstructed region

Obstructed region with a given blast curve for explosions formed in it.

Degree of confinement

The degree to which the flammable cloud is constrained from expanding in an explosion. It is 3D if the expanding vapour cloud can move in 3 dimensions, 2D if the cloud is constrained to expand in only 2 dimensions as beneath an elevated storage tank or 1 dimension as in a road tunnel.

DDT

Deflagration to Detonation Transition

Defined Flame Speed Obstructed Region

Obstructed region with a given flame Mach number for explosions formed by it. Used by the BST model.

Defined Strength Obstructed Region

Obstructed region with a given blast curve number used to determine the blast curve for explosions formed by it. Used by the Multi-energy model.

Deflagration

A chemical reaction of vapour cloud explosions in which the flame front is propagating at a speed determined by heat conduction and diffusion at the front.

Detonation

A chemical reaction of vapour cloud explosions in which the flame front is propagating as a shock wave which compresses the flammable material immediately ahead of it beyond its auto-ignition temperature

Dynamic overpressure

Blast wave is also accompanied by an air displacement in the same direction as the wave. The dynamic overpressure is the load on a reflective surface by this air displacement.

EMERGE

| | |
|------------------------------|---|
| | <i>Acronym for the joint industry project of Extended Modelling and Extended Research into Gas Explosions</i> |
| Explosion efficiency | <i>A ratio between the energy actually contributing to an explosion and the total combustion energy of an explosion</i> |
| Fill-Obstructed-Region-First | <i>A simple model implemented in Phast Risk for flammable clouds released inside obstructed regions. It redistributes the flammable mass of a cloud view inside the obstructed region for more conservative consequence and risk predictions.</i> |
| Flame Mach number | <i>The ratio between the flame propagating velocity of an explosion and the sonic velocity.</i> |
| Flame path length | <i>Distance travelled by the flame from ignition inside obstructed regions. It depends on the location of ignition and geometry of the obstructed regions.</i> |
| Ground reflection factor | <i>A factor which increases the explosion energy to correct the consequence predictions by the BST model for the ground effect on vapour cloud explosions. It equals one for free air explosions and 2 for ground explosions.</i> |
| Ground correction method | <i>A method developed specially for the BST model in Phast Risk v6.6 which increases both explosion energy and the initial peak overpressure to correct the consequence predictions by the BST model for the ground effect on vapour cloud explosions.</i> |
| GAME | <i>Acronym for a joint research project for Guidance on the Application of the Multi-Energy model.</i> |
| GAMES | <i>Acronym for a joint research project for Guidance on the Application of the Multi-Energy model: Second Phase.</i> |
| Hydraulic diameter | <i>A terminology adopted from Hydrodynamics to estimate the typical diameter of an obstructed region. It is defined as $4V/A$ where V is the volume of an obstacle and A is its surface area</i> |
| IL | <i>Ignition location</i> |
| Impulse | <i>Integration of pressure-time history of a short duration overpressure pulse</i> |
| Initial peak overpressure | <i>The peak overpressure inside the obstructed region of a confined explosion, i.e. $r < r_0$.</i> |
| Laminar burning velocity | <i>The velocity in the region of combustion relative to nonturbulent unburned gas</i> |
| ME | <i>The Multi-energy model implemented in Phast Risk v6.6. It applies the TNO Multi-energy methodology with enhanced functionality and GUI for QRA studies.</i> |
| Obstructed cloud | <i>The part of the flammable cloud which overlaps with obstructed regions to form an explosion source.</i> |
| Obstructed region | <i>Obstructed region is an area where obstacles are present in a configuration which will accelerate a flame if a flammable cloud is ignited inside it</i> |
| OREM | <i>Obstructed region explosion model for Phast Risk v6.60. It includes the TNO Multi-energy model and the Baker_Strehlow-Tang model for vapour cloud explosions in obstructed regions of process plants.</i> |
| Pitch distance | <i>The distance between successive rows of obstacles in obstructed regions</i> |
| Positive phase duration | <i>A blast wave of a vapour cloud explosion is experienced in the surrounding area as a transient change in pressure, density and velocity. The positive phase duration is normally the duration of positive overpressure experienced in the first cycle.</i> |
| Reactivity | <i>A term used to describe the propensity of a flame to accelerate in a vapour cloud explosion for a flammable material. It is rates as low, medium and high in the BST methodology</i> |
| Reflected overpressure | <i>The load exerted on a surface when a blast wave is reflected it</i> |
| RIGOS | <i>Acronym for a joint industry project on Research to improve guidance on separation distance for the multi-energy method (RIGOS)</i> |
| Separation distance | <i>The shortest distance between two obstructed regions</i> |
| Side-on overpressure | <i>Pressure experienced by an object as a blast wave passes by without being disturbed</i> |
| Typical diameter | <i>The average cross-sectional dimension of obstacles in an obstructed region</i> |



Unconfined explosion

An explosion formed by flammable cloud outside obstructed regions

VBR

Volume blockage ratio. VBR of an obstructed region is the ratio between the volume of all obstacles and its total volume.

VCE

Vapour cloud explosion resulting from an ignited flammable cloud



About DNV

We are the independent expert in risk management and quality assurance. Driven by our purpose, to safeguard life, property and the environment, we empower our customers and their stakeholders with facts and reliable insights so that critical decisions can be made with confidence. As a trusted voice for many of the world's most successful organizations, we use our knowledge to advance safety and performance, set industry benchmarks, and inspire and invent solutions to tackle global transformations.

Digital Solutions

DNV is a world-leading provider of digital solutions and software applications with focus on the energy, maritime and healthcare markets. Our solutions are used worldwide to manage risk and performance for wind turbines, electric grids, pipelines, processing plants, offshore structures, ships, and more. Supported by our domain knowledge and Veracity assurance platform, we enable companies to digitize and manage business critical activities in a sustainable, cost-efficient, safe and secure way.

REFERENCES

- ¹ TNO, "Methods for the calculation of physical effects, (The Yellow Book), CPR14E", Parts 1-2, 3rd Ed., Sdu Uitgevers, The Hague, 1997
- ² Eggen, J.B.M.M., "GAME: development of guidance for the application of the Multi-Energy Method". TNO Report PML 1995-C44, August 1995
- ³ Mercx, W.P.M., van den Berg, A.C. and van Leeuwen, D., "Application of correlations to quantify the source strength of vapour cloud explosions in realistic situations. Final report for the project: 'GAMES'", TNO Report PML 1998-C53, October 1998, NL
- ⁴ Pierorazio, A.J., Thomas, J.K, Baker, Q.A. and Ketchum, D.E, 2005, An update to the Baker-Strehlow-Tang vapour cloud explosion prediction methodology flame speed table, *Process Safety Progress*, 24, 59-65.
- ⁵ Tang, M.J. and Baker, Q.A., 1999, A new set of blast curves from Vapour Cloud Explosions, *Process Safety Progress*, 18, 235-240.
- ⁶ Baker, Q.A., Doolittle, C.M., Fitzgerald, G.A. and Tang, M.J., 1997, Recent development in the Baker-Strehlow VCE analysis Methodology, 31st Loss Prevention Symposium, American Institute of Chemical Engineers, Houston, TX.
- ⁷ Xu, Y. and Worthington, D., "Obstructed Region Explosion Model Theory", DNV, 2010
- ⁸ Fitzgerald, G., A Comparison of Simple Vapor Cloud Explosion Prediction methodologies. Second Annual Symposium, Mary Kay O'Connor Process Safety Center, Texas A&M University, October, 2001.
- ⁹ Lyons, Kieran, Summary of experiment series E5.5 (Congestion) results, PRESLHY, 2020
- ¹⁰ DNV, Obstructed region explosion model, Theory manual for Phast/Safeti, 2021.
- ¹¹ Zeeuwen, J.P. & Wiekema, B.J., The measurement of relative reactivities of combustible gases, Conference on mechanisms of explosions in dispersed energetic material, 1978.
- ¹² Baker, Q.A., Doolittle, C.M., Fitzgerald, G.A. and Tang, M.J., 1997, Recent development in the Baker-Strehlow VCE analysis Methodology, 31st Loss Prevention Symposium, American Institute of Chemical Engineers, Houston, TX.
- ¹³ Tang, M.J. and Baker, Q.A., 1999, A new set of blast curves from vapour cloud explosion, *Process Safety Progress*, Vol.18, No.3.